




AUTOMATED COASTAL ENGINEERING SYSTEM

TECHNICAL REFERENCE

by

David A. Leenknecht, Andre Szuwalski
and Ann R. Sherlock



Coastal Engineering Research Center

DEPARTMENT OF THE ARMY

Waterways Experiment Station, Corps of Engineers
3909 Halls Ferry Road, Vicksburg, Mississippi 39180-6199

Version 1.07
September 1992



HECSA TECHNICAL LIBRARY

Report Documentation Page				Form Approved OMB No. 0704-0188	
Public reporting burden for the collection of information is estimated to average 1 hour per response, including the time for reviewing instructions, searching existing data sources, gathering and maintaining the data needed, and completing and reviewing the collection of information. Send comments regarding this burden estimate or any other aspect of this collection of information, including suggestions for reducing this burden, to Washington Headquarters Services, Directorate for Information Operations and Reports, 1215 Jefferson Davis Highway, Suite 1204, Arlington VA 22202-4302. Respondents should be aware that notwithstanding any other provision of law, no person shall be subject to a penalty for failing to comply with a collection of information if it does not display a currently valid OMB control number.					
1. REPORT DATE SEP 1992		2. REPORT TYPE		3. DATES COVERED 00-00-1992 to 00-00-1992	
4. TITLE AND SUBTITLE Automated Coastal Engineering System: Technical Reference				5a. CONTRACT NUMBER	
				5b. GRANT NUMBER	
				5c. PROGRAM ELEMENT NUMBER	
6. AUTHOR(S)				5d. PROJECT NUMBER	
				5e. TASK NUMBER	
				5f. WORK UNIT NUMBER	
7. PERFORMING ORGANIZATION NAME(S) AND ADDRESS(ES) U.S. Army Corps of Engineers, Waterway Experiment Station, 3903 Halls Ferry Road, Vicksburg, MS, 39180				8. PERFORMING ORGANIZATION REPORT NUMBER	
9. SPONSORING/MONITORING AGENCY NAME(S) AND ADDRESS(ES)				10. SPONSOR/MONITOR'S ACRONYM(S)	
				11. SPONSOR/MONITOR'S REPORT NUMBER(S)	
12. DISTRIBUTION/AVAILABILITY STATEMENT Approved for public release; distribution unlimited					
13. SUPPLEMENTARY NOTES					
14. ABSTRACT					
15. SUBJECT TERMS					
16. SECURITY CLASSIFICATION OF:			17. LIMITATION OF ABSTRACT Same as Report (SAR)	18. NUMBER OF PAGES 213	19a. NAME OF RESPONSIBLE PERSON
a REPORT unclassified	b ABSTRACT unclassified	c THIS PAGE unclassified			

Destroy this report when no longer needed.
Do not return it to the originator.

The findings in this report are not to be construed as an official Department of the Army position unless so designated by other authorized documents.

The computer program and supporting technical data provided by the US Army Corps of Engineers in this package are received and accepted by the user with the express understanding that the Government makes no warranties, expressed or implied, regarding functionality, accuracy, or utility of the package or of the information generated by the package. **THE IMPLIED WARRANTIES OF MERCHANTABILITY AND OF FITNESS OR SUITABILITY FOR A PARTICULAR PURPOSE ARE SPECIFICALLY DISCLAIMED.** The Government also makes no representations that this package will meet the user's needs or requirements, will properly operate in the systems selected by the user, or will be uninterrupted or error free in the user's applications. Accordingly, it is recommended that each person or entity using or relying on this package undertake an independent assessment and thorough evaluation of his own requirements and needs before proceeding.

Further, this package is provided to and accepted by the user "as is" with any accompanying faults and defects. Any person or entity that relies upon information generated or obtained by this package does so at his own risk. The Government does not and cannot warrant the performance or results of this package under any and all circumstances. Therefore, no representations or claims are made about the completeness, accuracy, reliability, usability, or suitability of this package for any particular purpose or of any results derived by the use of this package.

Finally, the Government also disclaims all liability to users and third parties for damages including, but not limited to, direct, indirect, incidental, special, consequential, or any other damages whatsoever arising from, or in connection with, the use and results of this package. These disclaimers extend to any and all advice, interpretations, or other information given by Government personnel about the use or modification of the package.

Any references to products, tradenames, or trademarks herein are made for the purpose of illustration or clarification and do not constitute an official endorsement or approval of such items by the Government.

This program is the work of the United States Government and is in the public domain. It is approved for public release with unlimited distribution. It is improper and against Army policy to assist or encourage any advertisement, commercial product, or promotional activity which might imply Army endorsement for private benefit. Permission to use the Corps' name, materials, and activities can be obtained only under Army Regulation 360-5, dated 31 May 1989.

Copies of this software may be obtained from the Federal Software Exchange Center, National Technical Information Service, 5285 Port Royal Road, Springfield, VA 22161 or 703-487-4650.

PREFACE

The Automated Coastal Engineering System (ACES) is being developed by the Automated Coastal Engineering (ACE) Group, Research Division (RD), Coastal Engineering Research Center (CERC), US Army Engineer Waterways Experiment Station (WES). Funding for the effort is part of the Coastal Structures Evaluation and Design Research and Development Program. Messrs. John H. Lockhart, Jr., John G. Housley, Barry W. Holiday, and David Roellig are the Technical Monitors, Headquarters, US Army Corps of Engineers, for this program.

Development of the system was performed by Mr. David A. Leenknecht, Principal Investigator of the ACES, assisted by Mrs. Ann R. Sherlock, ACE Group. Contributors in the development were Miss Willie A. Brandon, Dr. Robert E. Jensen, Mr. Doyle L. Jones, Dr. Edward F. Thompson, CERC, Mr. Michael E. George, Information Technology Laboratory (ITL), and Mr. David W. Hyde, Structures Laboratory, WES; former CERC employees who also made contributions include Mr. John Ahrens, National Oceanic and Atmospheric Administration Sea Grant, Silver Spring, MD; Dr. Mark R. Byrnes, Louisiana State University, Baton Rouge, LA; Mr. Peter L. Crawford, US Army Engineer (USAE) District, Buffalo (NCB); Miss Leslie M. Fields, Aubrey Consultants Incorporated, Falmouth, MA; Mr. James M. Kaihatu, University of Delaware, Newark, DE; and Mr. Kent A. Turner, USAE Division, Lower Mississippi Valley. This report was edited by Mrs. Janean Shirley, ITL, WES.

The work was performed under the general supervision of Dr. James R. Houston, Director, CERC; Mr. Charles C. Calhoun, Jr., Assistant Director, CERC; Ms. Carolyn M. Holmes, CERC Coastal Program Manager; Mr. H. Lee Butler, Chief, RD; and under the direct supervision of Mr. Andre Szuwalski, Chief, ACE Group. Commander and Deputy Director of WES during publication of this guide was COL Leonard G. Hassell, EN. Dr. Robert W. Whalin was the Director of WES.

A Corps-wide Pilot Committee of coastal specialists guides the direction of the ACES effort. Members of the ACES Pilot Committee during this period were Mr. George Domurat, (Chairman), USAE Division, South Pacific (SPD); Mr. Dave Timpy, (Vice-Chairman), USAE District, Wilmington; Mr. John Oliver, USAE Division, North Pacific; Mr. Doug Pirie, SPD; Mr. Peter Crawford, NCB; Mr. Doug Gaffney, USAE District, Philadelphia; Ms. Cheryl Ulrich, USAE District, Mobile; Mr. Housley; and Dr. C. Linwood Vincent (CERC).

TABLE OF CONTENTS

Preface	i
Introduction	v
General Goals of the ACES	v
ACES Contents	v
Target Hardware Environment	v
Document Overview	v
Reference	vi
Descriptions of Individual Applications	
Wave Prediction Functional Area	
Windspeed Adjustment and Wave Growth	1-1
Beta-Rayleigh Distribution	1-2
Extremal Significant Wave Height Analysis	1-3
Constituent Tide Record Generation	1-4
Wave Theory Functional Area	
Linear Wave Theory	2-1
Cnoidal Wave Theory	2-2
Fourier Series Wave Theory	2-3
Wave Transformation Functional Area	
Linear Wave Theory with Snell's Law	3-1
Irregular Wave Transformation (Goda's Method)	3-2
Combined Diffraction and Reflection by a Vertical Wedge	3-3
Structural Design Functional Area	
Breakwater Design Using Hudson and Related Equations	4-1
Toe Protection Design	4-2
Nonbreaking Wave Forces at Vertical Walls	4-3
Rubble-Mound Revetment Design	4-4
Wave Runup, Transmission, and Overtopping Functional Area	
Irregular Wave Runup on Beaches	5-1
Wave Runup and Overtopping on Impermeable Structures	5-2
Wave Transmission on Impermeable Structures	5-3

Wave Transmission Through Permeable Structures	5-4
Littoral Processes Functional Area	
Longshore Sediment Transport	6-1
Numerical Simulation of Time-Dependent Beach and Dune Erosion	6-2
Calculation of Composite Grain-Size Distributions	6-3
Beach Nourishment Overfill Ratio and Volume	6-4
Inlet Processes Functional Area	
A Spatially Integrated Numerical Model for Inlet Hydraulics	7-1
Miscellaneous Routines	8-1
Appendix A: Tables	
Table A-1: K_D Values for Use in Determining Armor Unit Weight	A-1
Table A-2: Layer Coefficient and Porosity for Various Armor Units	A-2
Table A-3: Rough Slope Run-up Coefficients	A-2
Table A-4: Grain-Size Scales (Soil Classification)	A-3
Table A-5: Major Tidal Constituents	A-4
References and Bibliography	A-5

INTRODUCTION

GENERAL GOALS OF THE ACES

The Automated Coastal Engineering System (ACES) is an interactive computer-based design and analysis system in the field of coastal engineering. In response to a charge by the Chief of Engineers, LTG E. R. Heiberg III, to the Coastal Engineering Research Board (US Army Engineer Waterways Experiment Station, 1985) to provide improved design capabilities to Corps coastal specialists, the Coastal Engineering Research Center (CERC) conducted a series of six regional workshops in July 1986 to gather input from Corps field offices concerning various aspects of an ACES. Subsequent to the workshops, the ACES Pilot Committee and various working committees were formed from coastal experts throughout the Corps, and the Automated Coastal Engineering (ACE) Group was formed at CERC. The general goal of the ACES is to provide state-of-the-art computer-based tools that will increase the accuracy, reliability, and cost-effectiveness of Corps coastal engineering endeavors.

ACES CONTENTS

Reflecting the nature of coastal engineering, methodologies contained in this release of the ACES are richly diverse in sophistication and origin. The contents range from simple algebraic expressions, both theoretical and empirical in origin, to numerically intense algorithms spawned by the increasing power and affordability of computers. Historically, the methods range from classical theory describing wave motion, to expressions resulting from tests of structures in wave flumes, and to recent numerical models describing the exchange of energy from the atmosphere to the sea surface. In a general procedural sense, much has been taken from previous individual programs on both mainframes and microcomputers.

The various methodologies included in ACES are called **applications** and are organized into categories called **functional areas** differentiated according to general relevant physical processes and design or analysis activities. A list of the applications currently resident in the ACES is given in the table on the next page.

TARGET HARDWARE ENVIRONMENT

A strong preference expressed in the workshops and subsequent meetings was for the system to reside in a desktop hardware environment. To meet this preference, the ACES is designed to reside on the current base of PC-AT class of personal computers resident at many Corps coastal offices. While expected to migrate to more powerful hardware technologies, this current generation of ACES is designed for the above environment and is written in FORTRAN 77.

DOCUMENT OVERVIEW

The documentation set for the ACES comprises two manuals: *Technical Reference* and *User's Guide*.

- * The *Technical Reference* contains theory and discussion of the various methodologies contained in the ACES. The material included in the *Technical Reference* is relatively brief. For essential features of derivations and mathematical manipulations of equations presented in each section of this manual, the reader is strongly directed to references presented at the end of each application description.
- * The *User's Guide* contains instructions for using individual applications within the ACES software package.

Current ACES Applications	
Functional Area	Application Name
Wave Prediction	Windspeed Adjustment and Wave Growth Beta-Rayleigh Distribution Extremal Significant Wave Height Analysis Constituent Tide Record
Wave Theory	Linear Wave Theory Cnoidal Wave Theory Fourier Series Wave Theory
Wave Transformation	Linear Wave Theory with Snell's Law Irregular Wave Transformation (Goda's method) Combined Diffraction and Reflection by a Vertical Wedge
Structural Design	Breakwater Design Using Hudson and Related Equations Toe Protection Design Nonbreaking Wave Forces on Vertical Walls Rubble-Mound Revetment Design
Wave Runup, Transmission, and Overtopping	Irregular Wave Runup on Beaches Wave Runup and Overtopping on Impermeable Structures Wave Transmission on Impermeable Structures Wave Transmission Through Permeable Structures
Littoral Processes	Longshore Sediment Transport Numerical Simulation of Time-Dependent Beach and Dune Erosion Calculation of Composite Grain-Size Distribution Beach Nourishment Overfill Ratio and Volume
Inlet Processes	A Spatially Integrated Numerical Model for Inlet Hydraulics

REFERENCE

US Army Engineer Waterways Experiment Station. 1985. *Proceedings of the 44th Meeting of the Coastal Engineering Research Board*, 4-6 November 1985, Sausalito, California, James R. Houston, Editor, Vicksburg, MS, pp. 11-21.

WINDSPEED ADJUSTMENT AND WAVE GROWTH

TABLE OF CONTENTS

Description	1-1-1
Introduction	1-1-1
General Assumptions and Limitations	1-1-1
Wind Adjustment	1-1-2
Initial Adjustments and Estimates	1-1-3
Constant Stress Region	1-1-4
Full Boundary Layer	1-1-5
Final Adjustments	1-1-6
Wave Growth	1-1-6
Fetch Considerations	1-1-7
Open-Water Fetches	1-1-8
Restricted Fetches	1-1-8
Deepwater Wave Growth	1-1-9
Shallow-Water Wave Growth	1-1-11
References and Bibliography	1-1-12

WINDSPEED ADJUSTMENT AND WAVE GROWTH

DESCRIPTION

The methodologies represented in this ACES application provide quick and simple estimates for wave growth over open-water and restricted fetches in deep and shallow water. Also, improved methods (over those given in the *Shore Protection Manual* (SPM), 1984) are included for adjusting the observed winds to those required by wave growth formulas.

INTRODUCTION

Wind-generated wave growth is a complex process of considerable practical interest. Although the process is only partially understood, substantial demand remains for quick estimates required for design and analysis procedures. The most accurate estimates available are those provided by sophisticated numerical models such as those presented in Cardone et al. (1976), Hasselmann et al. (1976), Resio (1981), and Resio (1987). Yet many studies, especially at the preliminary level, attempt to describe wind-generated wave growth without the benefit of intensive large-scale modeling efforts. The prediction methods that follow present a first-order estimate for the process, but their simplification of the more complex physics should always be considered.

Methods are included for adjusting observed winds of varying character and location to the conditions required by wave growth formulas. A model depicting an idealized atmospheric boundary layer over the water surface is employed to estimate the low-level winds above the water surface. Stability effects (air-sea temperature gradient) are included, but barotropic effects (horizontal temperature gradient) are ignored. The numerical descriptions of the planetary boundary layer model are based upon similitude theory. Additional corrections are provided for the observed bias of ship-based wind observations as well as short fetches. Formulas for estimating winds of alternate durations are also included. The methodology for this portion of the application is largely taken from Resio, Vincent, and Corson (1982).

The simplified wave growth formulas predict deepwater wave growth according to fetch- and duration-limited criteria and are bounded (at the upper limit) by the estimates for a fully developed spectrum. The shallow-water formulations are based partly upon the fetch-limited deepwater forms and do not encompass duration effects. The methods described are essentially those in Vincent (1984), the SPM (1984), and Smith (1991).

Unless otherwise annotated, metric units are assumed for the following discussion.

GENERAL ASSUMPTIONS AND LIMITATIONS

The deep- and shallow-water wave growth curves are based on limited field data that have been generalized and extended on the basis of dimensionless analysis. The wind estimation procedures are based on a combination of boundary layer theory and limited field data largely from the Great Lakes. Wind transformation from land to water tends to be highly site and condition specific. The derivation of an individual site from these generalized conditions can create significant errors. Collection of site-specific field data to calibrate the techniques is suggested.

WIND ADJUSTMENT

The methodology for preparing wind observations for use in the wave growth formulas is based upon an idealized model of the planetary boundary layer depicted in Figure 1-1-1. For typical mid-latitude conditions, this planetary boundary layer exists in the lowest kilometer of the atmosphere and contains about 10 percent of the atmospheric mass (Holton, 1979).

Low-level winds directly over the water surface are considered to exist in a region characterized as having relatively constant stress at the air-sea interface. This surface layer will be designated the constant stress region for the remainder of this discussion.

Above the constant stress region is the Ekman layer, where the additional forces of Coriolis force, pressure gradient force, viscous stress, and convectively driven mixing are considered important.

Finally, above the Ekman region, geostrophic winds are considered to exist which result from considering the balance between pressure gradient forces and Coriolis force for synoptic scale systems.

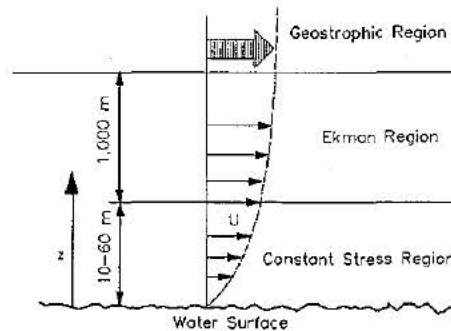


Figure 1-1-1. Idealized Atmospheric Boundary Layer over Water

Observed winds for use in the wave growth equations are considered to be characterized by six categories summarized in Table 1-1-1.

Table 1-1-1 Character and Action for Wind Observations		
Observation type	Initial Action	Solution Domain
Over water (non-ship obs)	-----	Constant stress layer
Over water (ship obs)	Adjusted	Constant stress layer
At shoreline (onshore winds)	-----	Constant stress layer
At shoreline (offshore winds)	Geostrophic wind estimated	Full PBL* model
Over land	Geostrophic wind estimated	Full PBL model
Geostrophic wind	-----	Full PBL model

* PBL = Planetary Boundary Layer

Although the above six wind observation categories are presented for user convenience, only two separate cases are ultimately considered by the methodology: low-level winds observed within the constant stress region and known or estimated geostrophic winds. In the ACES application, adjustments for ship-based observations are made before proceeding with a solution in the constant stress region, and geostrophic winds are estimated for cases where low-level observed winds are predominantly over land masses. The case of observed winds blowing onshore and measured at the shoreline is considered to be effectively identical to the case of winds observed over water. Similarly, winds observed at the shoreline but blowing from the land mass in an offshore direction are considered effectively equivalent to winds observed at a more inland location. Complex wind patterns caused by local frictional characteristics or topography are obviously not considered by these simplifications.

Initial Adjustments and Estimates

Wind observations over water are typically the most desirable choice of available data sources for wave prediction. Observers on ships at sea frequently record such data and make qualitative estimates. Cardone (1969) reviewed the bias of ship-based observations and suggested the following adjustment:

$$U = 1.864 U_{obs}^{\frac{7}{9}} \quad (mps) \quad (1)$$

where

U = adjusted ship-based wind speed

U_{obs} = ship-based observations

For cases where the observed winds are predominantly over land surfaces, similar models of the boundary layer are sometimes employed for other prediction purposes. However, in this application, the following simple estimate for geostrophic winds is made from low-level wind observations (cgs units):

$$V_g = \frac{U_*}{\sqrt{C_{D land}}} \quad (2)$$

where

U_* = friction velocity

$$= \frac{k U_{obs}}{\ln \left(\frac{z_{obs}}{z_0} \right)} \quad (3)$$

k = von Karman constant ($k \sim 0.4$)

z_{obs} = elevation of wind observation

z_0 = surface roughness length (assumed = 30 cm)

$C_{D land}$ = drag coefficient over land

$$C_{D land} \sim 0.00255 z_0^{0.1639} \quad (4)$$

Constant Stress Region

The major features of the constant stress region can be summarized as follows:

- The constant stress region is confined to the lowest few meters of the boundary layer.
- Wind flow is assumed parallel to the water surface.
- The wind velocity is adjusted so that the horizontal frictional stress is nearly independent of height.
- The stress remains constant within the layer and is characterized by the friction velocity U_* .

Stability (air-sea temperature gradient) has an important effect on wave growth. The wind profile within this region is described by the following modified logarithmic form:

$$U_z = \frac{U_*}{k} \left[\ln \left(\frac{z}{z_0} \right) - \Psi \left(\frac{z}{L} \right) \right] \quad (5)$$

where

U_z = wind velocity at elevation z

z_0 = surface roughness length

$$= \frac{C_1}{U_*} + C_2 U_*^2 + C_3 \quad (6)$$

$$\left(C_1 = 0.1525 \quad , \quad C_2 = \frac{0.019}{980} \quad , \quad C_3 = -0.00371 \right) \quad (7)$$

Ψ = universal similarity function

KEYPS formula (Lumley and Panofsky, 1964)

L = Obukov stability length

$$= 1.79 \frac{U_*^2}{\Delta T} \left[\ln \left(\frac{z}{z_0} \right) - \Psi \left(\frac{z}{L} \right) \right] \quad (8)$$

ΔT = air-sea temperature gradient

$$\left. \begin{array}{l} \Psi = 0 \\ \Psi = C \frac{z}{L} \end{array} \right\} \begin{array}{l} \Delta T = 0 \\ \frac{z}{L} > 0 \end{array} \quad (9)$$

$$\Psi = 1 - \phi_u - 3 \ln \phi_u + 2 \ln \left(\frac{1 + \phi_u}{2} \right) + 2 \tan^{-1} \phi_u - \frac{\pi}{2} + \ln \left(\frac{1 + \phi_u^2}{2} \right) \quad \left| \frac{z}{L} \leq 0 \right.$$

$$\phi_u = \frac{1}{1 - 18 R_i^{1/4}} \quad (10)$$

$$R_i = \frac{z}{L} (1 - 18 R_i)^{1/4} \quad (11)$$

The solution of the above equations is an iterative process that converges very rapidly. The convergence criterion (ϵ) for U_* and L are given below:

$$\epsilon_{U_*} \rightarrow 0.1 (cm/sec) \quad \text{and} \quad \epsilon_L \rightarrow 1 (cm) \quad (12)$$

The wave growth equations discussed later require the equivalent wind speed at a 10-m elevation under conditions of neutral stability ($\Delta T = 0$). Having solved the equations in the constant stress region for U_* , the required equivalent neutral wind speed U_{e1000} may be easily obtained from Equation 5 using (U_* , $z = 10 m$, $\Delta T = 0$):

$$U_{e1000} = \frac{U_*}{k} \left[\ln \left(\frac{1000}{z_0} \right) - 0 \right] \quad (13)$$

Full Boundary Layer

For cases where the geostrophic winds are known or have been estimated, the similitude equations describing the entire planetary boundary layer are solved. In addition to the relations described above for the constant stress region, the following relationships describe the model from water surface level to the geostrophic level:

$$\ln \frac{|\vec{V}_g|}{f z_0} = A - \ln \frac{U_*}{|\vec{V}_g|} + \sqrt{\frac{k^2 |\vec{V}_g|^2}{U_*^2} - B^2} \quad (14)$$

$$\sin \theta = \frac{B U_*}{k |\vec{V}_g|} \quad (15)$$

where

\vec{V}_g = geostrophic wind

f = Coriolis acceleration

A, B = nondimensional functions of stability

$$\left. \begin{aligned} A &= A_0 [1 - e^{(0.015\mu)}] \\ B &= B_0 - B_1 [1 - e^{(0.03\mu)}] \end{aligned} \right| \mu \leq 0 \quad (16)$$

$$\left. \begin{aligned} A &= A_0 - 0.96\sqrt{\mu} + \ln(\mu + 1) \\ B &= B_0 + 0.7\sqrt{\mu} \end{aligned} \right| \mu > 0 \quad (17)$$

μ = dimensionless stability parameter

$$= \frac{k U_*}{f L} \quad (18)$$

A_0, B_0, B_1 = constants

θ = angle between \vec{V}_g and the surface stress

Equations 14-18 are solved simultaneously together with Equations 5-11 until the convergence of U_* , L , and A is obtained. A slightly different value of ($C_2 = 0.0144/980$) in Equation 7 is used (Dr. C. Linwood Vincent, CERC, personal communication, September 1989). The convergence criteria for the iterative solution to the equations are as follows:

$$\epsilon_{U_*} \rightarrow 0.1 (cm/sec) \quad \text{and} \quad \epsilon_L \rightarrow 1 (cm) \quad \text{and} \quad \epsilon_A \rightarrow 0.1 \quad (19)$$

The solution procedure converges very rapidly. As before, Equation 13 is then used to determine the equivalent neutral wind speed at the 10-m elevation using (U_* , $z = 10 \text{ m}$, $\Delta t = 0$).

Final Adjustments

An additional adjustment is made for situations having relatively short fetch lengths before application of the wave growth equations. For fetch lengths shorter than 16 km, the following reduction is applied:

$$U_e = 0.9 U_* \quad (20)$$

Finally, it is necessary to evaluate the effects of winds of varying duration, t_i , on the wave growth equations. The following expressions are used to adjust the wind speed to a duration of interest:

$$\frac{U_i}{U_{3600}} = 1.277 + 0.296 \tanh\left(0.9 \log \frac{45}{t_i}\right) \quad \left| \quad (1 < t_i < 3600 \text{ sec}) \quad (21)\right.$$

$$\frac{U_i}{U_{3600}} = -0.15 \log t_i + 1.5334 \quad \left| \quad (3600 < t_i < 36000 \text{ sec}) \quad (22)\right.$$

The 1-hr wind speed U_{3600} is first determined (using $t_i = t_{obs}$). The wind speed U_i at the desired duration of interest is then determined by selecting the desired t_i and using the appropriate equation.

WAVE GROWTH

Having estimated the winds above the water surface at a duration of interest, the objective is to provide an estimate of the wave growth caused by the winds. The simple wave growth formulas that follow provide quick estimates for wind-wave growth in deep and shallow water. The open-water expressions correspond to those listed in the SPM (1984) and Vincent (1984). The

restricted fetch deepwater expressions can be found in Smith (1991). It should be noted that the drag law (Garratt, 1977) employed differs from that in the SPM. The major assumptions regarding the use of the simplified wave growth expressions include:

- Energy from the presence of other existing wave trains is neglected.
- Relatively short fetch geometries ($F \leq 75 \text{ mi}$).
- Relatively constant wind speed ($\Delta U \leq 5 \text{ kts}$) and direction ($\Delta \alpha \leq 15^\circ$).
- Winds prescribed at the 10-m elevation ($z = 10 \text{ m}$).
- Neutral stability conditions.
- Fixed value of drag coefficient ($C_D = 0.001$).

The wind adjustment methodology described earlier in this report adjusts the observed wind, U_{obs} , to the 10-m elevation under neutrally stable conditions U_e . Vincent (1984) maintains the wind speed should be adjusted to consider the nonlinear effect on the wind stress creating the waves. The drag law reported by Garratt (1977) is used:

$$\tau = \rho_a C_D U^2 \quad (23)$$

where

ρ = air density

$$C_D = 0.001(0.75 + 0.067 U) \quad (24)$$

The equivalent neutral wind speed, then, is adjusted (or linearized) to a constant drag coefficient ($C_D = 0.001$) before application in the wave growth formulas:

$$U_a = U_e \sqrt{\frac{C_D}{0.001}} \quad (25)$$

Fetch Considerations

The wave growth formulations which follow are segregated into four categories: deep and shallow-water forms for both simple open-water fetches and for more complex, limiting geometries (designated "restricted fetch"). A brief discussion of fetch delineation is useful.

Open-Water Fetches

In open water, wave generation is limited by the dimensions of the subject meteorological event, and fetch widths are of the same order of magnitude as the fetch length. The simplified estimates for wave growth in open water attribute significance to the fetch length (but not width or shape). The wave growth is assumed to occur along the fetch in the direction of the wind.

Restricted Fetches

The more limiting or complex geometries of water bodies such as lakes, rivers, bays, and reservoirs have an impact on wind-wave generation. This restricted fetch methodology applies the concept of wave development in off-wind directions and considers the shape of the basin. The details of the method are reported by Smith (1991), and are based upon a concept reported by Donelan (1980) whereby the wave period (as a function of fetch lengths at off-wind directions) is maximized. For this approach, the radial fetch lengths (as measured from various points along the shoreline of the basin to the point of interest) are used to describe the geometry of the basin. In addition, the wind direction must be specified. Figure 1-1-2 illustrates the relevant geometric data required for the restricted fetch approach.

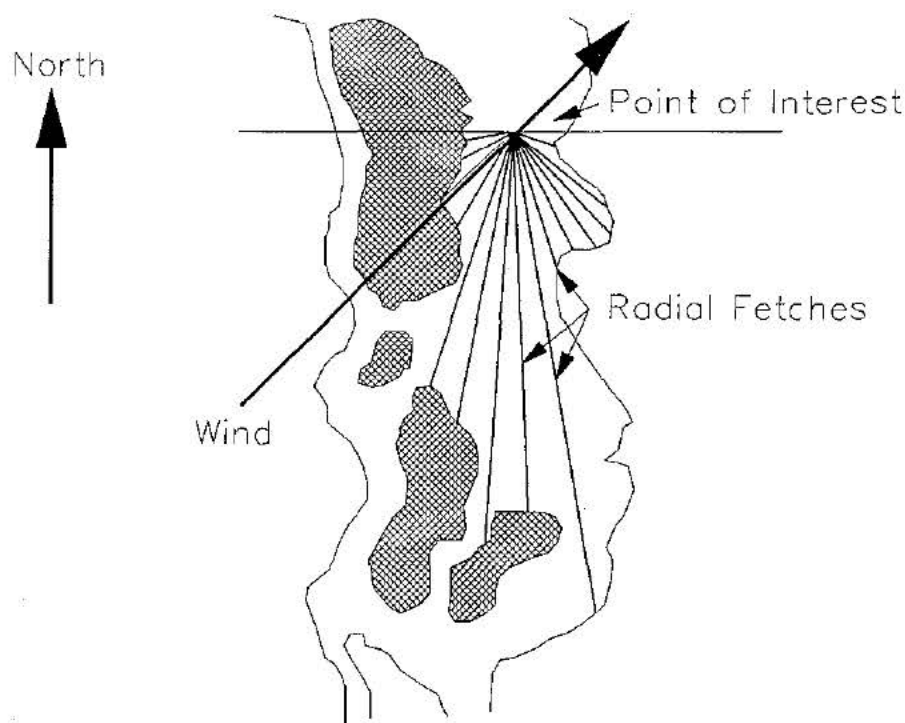


Figure 1-1-2. Restricted Fetch Geometry Data

The conventions used for specifying wind direction and fetch geometry are illustrated in Figure 1-1-3. The approach wind direction (α) as well as the radial fetch angles (β_1), and ($\Delta\beta$) should be specified in a clockwise direction from north from the point of interest where wave growth prediction is required.

From the specified radial fetch data, intermediate values are interpolated at 1-deg increments around the entire 360-deg compass. These interpolated fetches are subsequently averaged over 15-deg arcs centered at each whole 1-deg value.

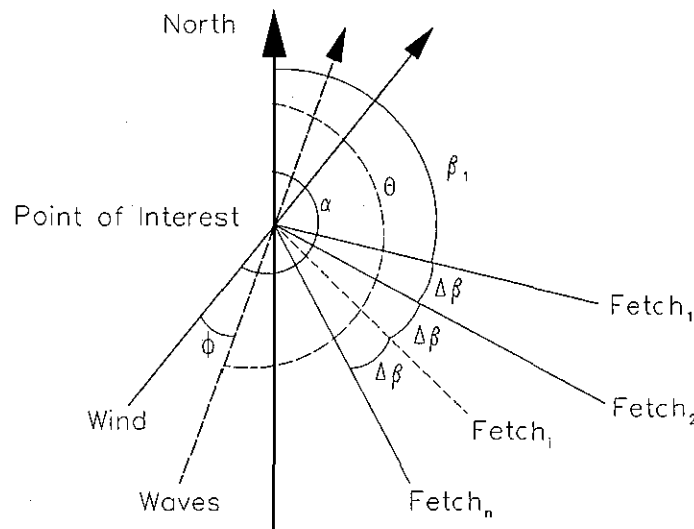


Figure 1-1-3. Restricted Fetch Conventions

The direction of wave development (θ) is solved by maximizing the product

$$F_{\phi}^{0.28} \cdot (\cos \phi)^{0.44} \quad (26)$$

This procedure maximizes the relevant terms in the expression for wave period (T_p) (Equation 36). The angle (ϕ) is defined as the off-wind direction angle associated with the interpolated averaged fetch length value (F_{ϕ}). Product results (Equation 26) are evaluated from ($\phi = 0 \pm 90^\circ$) at 1-deg increments. When the product (Equation 26) is maximized, (ϕ) represents the angle between the wind and waves, and (θ) represents the compass direction from which wave development occurs along (F_{ϕ}). For a specified wind direction, there will be a corresponding wave development direction where (T_p) is maximized by Equation 26.

Deepwater Wave Growth

The formulas for wave growth in deep water encompass the effects of fetch and duration. The open-water formulas for fetch- and duration-limited wave growth are taken from Vincent (1984) and are based upon the spectrally based results given in Hasselmann et al. (1973, 1976). The fetch-limited and fully developed forms are also tabulated in the SPM (1984). The expressions for restricted fetch wave growth in deep water are from Smith (1991). In all cases, the wave growth estimates are bounded by the expressions for a fully developed equilibrium spectrum. The procedure is outlined as follows:

- ° Determine the minimum duration, t_{fetch} , required for a wave field to become fetch-limited:

Open Water

$$t_{fetch} = 68.8 \frac{F^{2/3}}{g^{1/3} U_a^{1/3}} \quad (27)$$

Restricted Fetch

$$t_{fetch} = 51.09 \frac{F^{0.72}}{g^{0.28} \hat{U}_a^{0.44}} \quad (28)$$

- ° Determine the character of the wave growth (duration-limited or fetch-limited):

Open Water

$$H = 0.0000851 \left(\frac{U_a^2}{g} \right) \left(\frac{gt_i}{U_a} \right)^{5/7} \quad (29)$$

$$T = 0.0702 \left(\frac{U_a}{g} \right) \left(\frac{gt_i}{U_a} \right)^{0.411} \quad (31)$$

**Duration
Limited**

$$(t_i < t_{fetch})$$

Restricted Fetch

$$H = 0.000103 \left(\frac{\hat{U}_a^2}{g} \right) \left(\frac{gt_i}{\hat{U}_a} \right)^{0.69} \quad (30)$$

$$T = 0.082 \left(\frac{\hat{U}_a}{g} \right) \left(\frac{gt_i}{\hat{U}_a} \right)^{0.39} \quad (32)$$

--- or ---

$$H = 0.0016 \left(\frac{U_a^2}{g} \right) \left(\frac{gF}{U_a^2} \right)^{1/2} \quad (33)$$

$$T = 0.2857 \left(\frac{U_a}{g} \right) \left(\frac{gF}{U_a^2} \right)^{1/3} \quad (35)$$

**Fetch
Limited**

$$(t_i \geq t_{fetch})$$

$$H = 0.0015 \left(\frac{\hat{U}_a^2}{g} \right) \left(\frac{gF}{\hat{U}_a^2} \right)^{1/2} \quad (34)$$

$$T = 0.3704 \left(\frac{\hat{U}_a}{g} \right) \left(\frac{gF}{\hat{U}_a^2} \right)^{0.28} \quad (36)$$

- ° Determine the "fully developed" condition:

Open Water

$$H_{fd} = 0.2433 \left(\frac{U_e^2}{g} \right) \quad (37)$$

$$T_{fd} = 8.134 \left(\frac{U_e}{g} \right) \quad (39)$$

**Fully
Developed****Restricted Fetch**

$$H_{fd} = 0.2433 \left(\frac{\hat{U}_e^2}{g} \right) \quad (38)$$

$$T_{fd} = 8.134 \left(\frac{\hat{U}_e}{g} \right) \quad (40)$$

- ° Ensure that the "fully developed" condition is not exceeded:

$$H_{m0} = \min(H, H_{fd}) \quad (41)$$

$$T_p = \min(T, T_{fd}) \quad (42)$$

where

g = acceleration due to gravity

t_i = wind duration used in duration-limited expressions

F = fetch length used in fetch-limited expressions

$\bar{U}_a = U_a \cos(\phi)$ = fetch-parallel component of U_a for restricted fetch approach

$\bar{U}_e = U_e \cos(\phi)$ = fetch-parallel component of U_e for restricted fetch approach

H = wave height determined by duration-limited or fetch-limited expressions

T = wave period determined by duration-limited or fetch-limited expressions

H_{fd} = wave height limited by fully developed spectrum criteria

T_{fd} = wave period limited by fully developed spectrum criteria

H_{m0} = final wave height determined from spectrally based methods

T_p = final wave period determined from spectrally based methods

Shallow-Water Wave Growth

Estimates for wave growth in shallow water are based upon the fetch-limited deepwater formulas, but modified to include the effects of bottom friction and percolation (Bretschneider and Reid, 1954). Water depth is assumed to be constant over the fetch. Duration-limited effects are not embodied by these formulas. The relationships have not been verified and may (or may not) be appropriate for the conditions and assumptions of the original Bretschneider-Reid work. **The expressions represent an interim method pending results of further research.** The open-water forms are also presented in the SPM (1984).

Open-Water Forms:

$$H_{m0} = \frac{U_a^2}{g} 0.283 \tanh \left[0.530 \left(\frac{gd}{U_a^2} \right)^{0.75} \right] \tanh \left\{ \frac{\frac{0.0016 \left(\frac{gF}{U_a^2} \right)^{0.5}}{0.283}}{\tanh \left[0.530 \left(\frac{gd}{U_a^2} \right)^{0.75} \right]} \right\} \quad (43)$$

$$T_p = \frac{U_a}{g} 7.54 \tanh \left[0.833 \left(\frac{gd}{U_a^2} \right)^{0.375} \right] \tanh \left\{ \frac{\frac{0.2857 \left(\frac{gF}{U_a^2} \right)^{0.333}}{7.54}}{\tanh \left[0.833 \left(\frac{gd}{U_a^2} \right)^{0.375} \right]} \right\} \quad (44)$$

Restricted Fetch Forms:

$$H_{m0} = \frac{U_a^2}{g} 0.283 \tanh \left[0.530 \left(\frac{gd}{\bar{U}_a^2} \right)^{0.75} \right] \tanh \left\{ \frac{\frac{0.0015 \left(\frac{gF}{\bar{U}_a^2} \right)^{0.5}}{0.283}}{\tanh \left[0.530 \left(\frac{gd}{\bar{U}_a^2} \right)^{0.75} \right]} \right\} \quad (45)$$

$$T_p = \frac{U_a}{g} 7.54 \tanh \left[0.833 \left(\frac{gd}{\bar{U}_a^2} \right)^{0.375} \right] \tanh \left\{ \frac{\frac{0.3704 \left(\frac{gF}{\bar{U}_a^2} \right)^{0.28}}{7.54}}{\tanh \left[0.833 \left(\frac{gd}{\bar{U}_a^2} \right)^{0.375} \right]} \right\} \quad (46)$$

REFERENCES AND BIBLIOGRAPHY

- Bretschneider, C. L., and Reid, R. O. 1954. "Modification of Wave Height Due to Bottom Friction, Perlocation and Refraction," Technical Report 50-1, The Agricultural and Mechanical College of Texas, College Station, TX.
- Cardone, V. J. 1969. "Specification of the Wind Distribution in the Marine Boundary Layer for Wave Forecasting," TR-69-1, Geophysical Sciences Laboratory, Department of Meteorology and Oceanography, School of Engineering and Science, New York University, New York.
- Cardone, V. J., et al. 1976 "Hindcasting the Directional Spectra of Hurricane-Generated Waves," *Journal of Petroleum Technology*, American Institute of Mining and Metallurgical Engineers, No. 261, pp. 385-394.
- Donelan, M.A. 1980. "Similarity Theory Applied to the Forecasting of Wave Heights, Periods, and Directions," *Proceedings of the Canadian Coastal Conference*, National Research Council, Canada, pp. 46-61.
- Garratt, J. R., Jr. 1977. "Review of Drag Coefficients over Oceans and Continents," *Monthly Weather Review*, Vol. 105, pp. 915-929.
- Hasselmann, K., Barnett, T. P., Bonws, E., Carlson H., Cartwright, D. C., Enke, K., Ewing, J., Gienapp, H., Hasselmann, D. E., Kruseman, P., Meerburg, A., Muller, P., Olbers, D. J., Richter, K., Sell, W., and Walden, H. 1973. "Measurements of Wind-Wave Growth and Swell Decay During the Joint North Sea Wave Project (JONSWAP)," Deutsches Hydrographisches Institut, Hamburg, 95 pp.
- Hasselmann, K., Ross, D. B., Muller, P., and Sell, W. 1976. "A Parametric Prediction Model," *Journal of Physical Oceanography*, Vol. 6, pp. 200-228.
- Holton, J. R. 1979. *An Introduction to Dynamic Meteorology*, Academic Press, Inc., New York, pp. 102-118.
- Lumley, J. L., and Panofsky, H. A. 1964. *The Structure of Atmospheric Turbulence*, Wiley, New York.

- Mitsuyasu, H. 1968. "On the Growth of the Spectrum of Wind-Generated Waves (I)," Reports of the Research Institute of Applied Mechanics, Kyushu University, Fukuoka, Japan, Vol. 16, No. 55, pp. 459-482.
- Resio, D. T. 1981. "The Estimation of Wind Wave Generation in a Discrete Model," *Journal of Physical Oceanography*, Vol. 11, pp. 510-525.
- Resio, D. T. 1987. "Shallow Water Waves. I: Theory," *Journal of Waterway, Port, Coastal and Ocean Engineering*, American Society of Civil Engineers, Vol. 113, No. 3, pp. 264-281.
- Resio, D. T., Vincent, C. L., and Corson, W. D. 1982. "Objective Specification of Atlantic Ocean Wind Fields from Historical Data," Wave Information Study Report No. 4, US Army Engineer Waterways Experiment Station, Vicksburg, MS.
- Shore Protection Manual*. 1984. 4th ed., 2 Vols., US Army Engineer Waterways Experiment Station, Coastal Engineering Research Center, US Government Printing Office, Washington, DC, Chapter 3, pp. 24-66.
- Smith, J.M. 1991. "Wind-Wave Generation on Restricted Fetches," Miscellaneous Paper CERC-91-2, US Army Engineer Waterways Experiment Station, Vicksburg, MS.
- Vincent, C. L. 1984. "Deepwater Wind Wave Growth with Fetch and Duration," Miscellaneous Paper CERC-84-13, US Army Engineer Waterways Experiment Station, Vicksburg, MS.

BETA-RAYLEIGH DISTRIBUTION

TABLE OF CONTENTS

Description	1-2-1
Introduction	1-2-1
General Assumptions and Limitations	1-2-1
Rayleigh Distribution	1-2-2
Shallow-Water Distributions	1-2-4
Beta-Rayleigh Distribution	1-2-4
Parameterization	1-2-6
Root-Mean-Square Wave Height	1-2-6
Root-Mean-Quad Wave Height	1-2-7
Breaking Wave Height	1-2-8
Application	1-2-8
References and Bibliography	1-2-9

BETA-RAYLEIGH DISTRIBUTION

DESCRIPTION

This application provides a statistical representation for a shallow-water wave height distribution. The Beta-Rayleigh distribution is expressed in familiar wave parameters: H_{mo} (energy-based wave height), T_p (peak spectral wave period), and d (water depth). After constructing the distribution, other statistically based wave height estimates such as H_{rms} , H_{mean} , $H_{1/10}$ can be easily computed. The Beta-Rayleigh distribution features a finite upper bound corresponding to the breaking wave height, and the expression collapses to the Rayleigh distribution in the deepwater limit. The methodology for this portion of the application is taken exclusively from Hughes and Borgman (1987).

INTRODUCTION

Economic coastal engineering design requires accurate specification of the characteristics of the irregular wave field in nearshore waters. In the absence of a fully deterministic understanding of irregular water waves, coastal engineers often describe the sea surface in terms of meaningful wave field parameters which appear to vary in a consistent and predictable manner.

An important and useful statistical descriptor of irregular waves is the wave height distribution. It provides knowledge of the range of wave heights under a given sea condition, as well as the probability of occurrence of a particular wave height within the range. This knowledge can be used to better represent the effects of irregular waves in coastal engineering calculations.

The Rayleigh distribution has proven to be a reliable measure of the wave height distribution for waves in deep water. It is theoretically valid for a wave field composed of a very large number of superimposed deepwater, small-amplitude sinusoidal waves with random phasing and with frequencies very narrowly spread about a single value. For deepwater waves, only the tail in the region of the highest waves exhibits any noticeable deviation from the theory (SPM, 1984, Figure 3-4), and this tendency occurs primarily in the most energetic conditions such as hurricanes (Earle, 1975; Forristall, 1978). Nevertheless, application of the Rayleigh distribution to field wave data has shown repeatedly that the distribution does a remarkable job of predicting the wave height distribution in cases well outside its strict theoretical limits.

GENERAL ASSUMPTIONS AND LIMITATIONS

All wave parameters derived from the Beta-Rayleigh distribution are limited by the data used to derive this parametric formulation. This derivation was based on preliminary examination of surf zone wave height distributions which indicated that the Beta-Rayleigh distribution can provide a reasonable fit to the data. If the input information H_{mo} , T_p , and d do not fall within the range of data used to derive the parametric formulation, inaccuracies may result. Also, the assumption that the maximum individual wave condition can equal the water depth (upper limit of the Beta-Rayleigh distribution) was suggested by Hughes and Borgman (1987), but they concluded

it was only a recommendation until further research is conducted. Because the Beta-Rayleigh distribution reverts to the Rayleigh distribution as depth increases, parameters given by this application when $d/gT^2 \geq 0.01$ are calculated from the Rayleigh distribution.

RAYLEIGH DISTRIBUTION

One of the most significant contributions to the parameterization of ocean waves was the demonstration that the wave height distribution of a narrowly banded Gaussian sea state is described by the Rayleigh distribution (Longuet-Higgins, 1952) as

$$p(H) = \frac{2H}{H_{rms}^2} \exp \left[- \left(\frac{H}{H_{rms}} \right)^2 \right] \quad (1)$$

where:

$p(H)$ = probability density function of wave heights

H = wave height (vertical distance between wave trough and peak)

H_{rms} = root-mean-squared wave height

$$= \left[\frac{1}{N} \sum_{i=1}^N H_i^2 \right]^{\frac{1}{2}}$$

The Rayleigh probability distribution also can be written as

$$p(H) = \frac{2H}{8\sigma^2} \exp \left[\frac{-H^2}{8\sigma^2} \right] \quad (2)$$

where:

σ^2 = variance of the sea surface elevations

Equating Equations 1 and 2 gives

$$H_{rms} = 2\sqrt{2} \sigma \quad (3)$$

The frequently used definition of significant wave height is given by

$$H_{mo} = 4\sigma \quad (4)$$

The Rayleigh distribution also has been used to describe wave heights in finite depth water with reasonable success if the assumption of a Gaussian sea state is not violated to a great extent. However, as waves approach depth-limited breaking, they become highly nonsinusoidal in shape, they interact with other nonlinear waves (Scheffner, 1986), and the larger waves in the sea state start breaking. Hence, the process becomes very non-Gaussian, and the wave height distributions deviate from the Rayleigh theory. This deviation can become significant during high-energy wave conditions as evidenced in the Atlantic Ocean Remote Sensing Land-Ocean Experiment (ARSLOE) data set (Ochi, Malakar, and Wang, 1982), in data collected during the monsoonal season in India (Dattatri, 1973), and in data from the US coastline (Thompson, 1974). The Rayleigh distribution of wave heights shows a definite weighting toward the higher end of the distribution. For example, Figure 1-2-1 presents two wave height distribution functions measured in shallow water during the DUCK 85 experiment (Ebersole and Hughes, 1987).

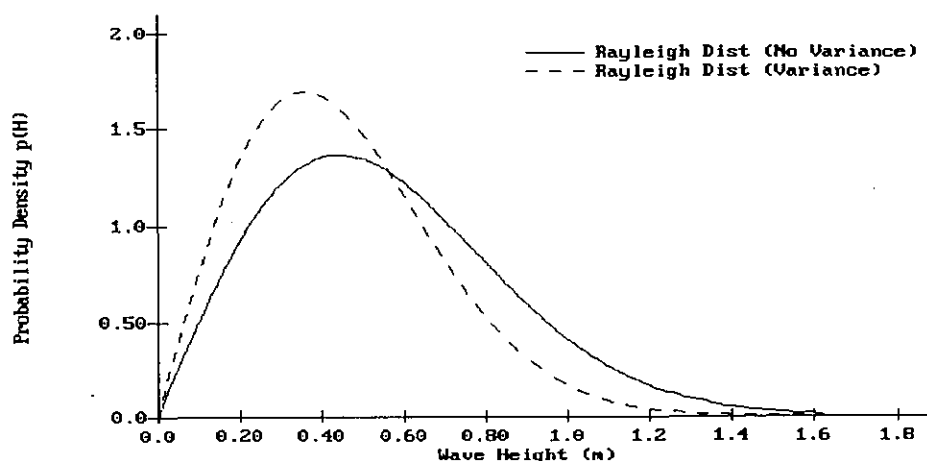


Figure 1-2-1. Rayleigh Distribution Comparison ($H_{mo} = 0.72\text{m}$; $T_p = 10.9\text{sec}$; $d = 1.63\text{m}$)

The solid curve in Figure 1-2-1 is the Rayleigh prediction using the measured H_{rms} (root mean square) and the dashed curve is the Rayleigh distribution using the variance as the governing parameter. Theoretically, the two curves should coincide, but in shallow water the nonlinear shape of the waves causes the statistical measure of the wave heights H_{rms} to be larger than that predicted by Equation 3. This difference becomes pronounced as the waves approach breaking. From Figure 1-2-1, it is seen that the shallow-water wave height distribution shows a tendency to skew toward the high-wave side of the Rayleigh distribution; that is, there are more of the higher waves than predicted by the Rayleigh theory. Also, using the statistical parameter, H_{rms} , in the Rayleigh distribution provides a better (though still not good) estimation of the observed wave height distributions.

SHALLOW-WATER DISTRIBUTIONS

Previous investigators have suggested improved wave height distributions for shallow water and for the surf zone that are either modified Rayleigh distributions or mathematical forms that have the Rayleigh distribution as a deepwater asymptote. Collins (1970) and Battjes (1972) assumed that the Rayleigh distribution was valid up until the point that depth-limited breaking begins to occur. They then truncated the Rayleigh distribution at the breaking wave height and assumed that all broken waves have a height equal to the local breaking wave height. Hence, the truncated probability density is represented by a delta function located at the breaking wave height. This modification becomes pronounced within the surf zone. Kuo and Kuo (1974) truncated the Rayleigh distribution at the breaking wave height and redistributed the truncated probability density over the remaining wave heights. Goda (1975) assumed wave breaking occurs over a small range of wave heights together with a redistribution of the truncated probability density over the smaller wave heights.

The three examples of modified Rayleigh distributions discussed above result in probability density functions (*pdf*) which have a maximum in about the same location as the original Rayleigh distribution; thus, these distributions do not adequately model the characteristic skewing of the shallow-water wave height distribution toward the higher waves as observed in energetic sea conditions.

BETA-RAYLEIGH DISTRIBUTION

To better characterize the wave height distribution for shallow-water waves, a *pdf* with the following attributes is desirable:

- The *pdf* should be bounded by a maximum wave height.
- The *pdf* should have the capability to skew toward higher wave heights than predicted by the Rayleigh distribution, as the sea becomes increasingly non-Gaussian.
- The *pdf* should transform into the Rayleigh distribution as the maximum wave height approaches infinity (i.e., deep water).
- The *pdf* should be mathematically tractable and not too complicated.
- The *pdf* should have some physical justification, either from a deterministic or stochastic viewpoint.

In Hughes and Borgman (1987), a plausible candidate for a shallow-water wave height *pdf* that satisfies these five criteria is derived. The resulting shallow-water *pdf* is referred to as the *Beta-Rayleigh distribution*, and it is expressed as a variation of the beta distribution as

$$P_{BR}(H) = \frac{2\Gamma(\alpha + \beta)}{\Gamma(\alpha)\Gamma(\beta)} \frac{H^{2\alpha-1}}{H_b^{2\alpha}} \left(1 - \frac{H^2}{H_b^2}\right)^{\beta-1} \quad (5)$$

valid in the range $0 < H < H_b$. In Equation 5, H_b denotes the maximum (or breaking) wave height, and α and β are related to the rms wave height by the expression

$$\overline{H^2} = H_{rms}^2 = \int_0^{H_b} H^2 p_{BR}(H) dH = \frac{\alpha H_b^2}{\alpha + \beta} \quad (6)$$

or

$$\beta = \alpha \left(\frac{H_b^2}{H_{rms}^2} - 1 \right) \quad (7)$$

Other moments of the *pdf* given in Equation 5 also yield relationships between α and β . The first and third moments are complicated by gamma functions, but the fourth moment provides a simple relationship given by

$$\overline{H^4} = H_{rmq}^2 = \int_0^{H_b} H^4 p_{BR}(H) dH = \frac{\alpha(\alpha + 1)H_b^4}{(\alpha + \beta)(\alpha + \beta + 1)} \quad (8)$$

where:

H_{rmq} = root-mean-quad wave height

$$= \left[\frac{1}{N} \sum_{i=1}^N H_i^4 \right]^{\frac{1}{2}} \quad (9)$$

Solving Equations 6 and 8 provides expressions for α and β in terms of physical parameters of the wave height distribution.

$$\alpha = \frac{K_1(K_2 - K_1)}{K_1^2 - K_2} \quad (10)$$

$$\beta = \frac{(1 - K_1)(K_2 - K_1)}{K_1^2 - K_2} \quad (11)$$

where:

$$K_1 = \frac{H_{rms}^2}{H_b^2}$$

$$K_2 = \frac{H_{rmq}^2}{H_b^4}$$

Thus, the *pdf* of Equation 5 can be expressed in terms of three parameters, H_b , H_{rmq} , and H_{rms} . Since this is a three-parameter distribution, Equation 5 will provide a better realization than the Rayleigh *pdf* for shallow-water wave heights, provided the three parameters can be correlated to the sea state.

The transition of Equation 5 to the Rayleigh distribution can be seen by taking the limit, as H_b approaches infinity, of the *pdf* given by Equations 5, 10, and 11. This procedure yields (Hughes and Borgman, 1987) a *generalized Rayleigh distribution* given by

$$p_{GR}(H) = \frac{2H^{2\alpha_0-1}}{b_0^{\alpha_0} \Gamma(\alpha_0)} \exp\left(\frac{-H^2}{b_0}\right) \quad (12)$$

where:

$$\alpha_0 = \frac{H_{rms}^4}{H_{rmq}^2 - H_{rms}^4} \quad (13)$$

$$b_0 = \frac{H_{rmq}^2 - H_{rms}^4}{H_{rms}^2} \quad (14)$$

By noting that $H_{rmq} = \sqrt{2} H_{rms}$ for the Rayleigh distribution, Equation 12 reverts to the Rayleigh form given by Equation 1.

PARAMETERIZATION

The most often used parameters for describing sea states in shallow water are the energy-based significant wave height H_{mo} , the peak spectral period T_p , and the water depth d . Less often used parameters include the width of the spectral peak, some indicators of wave groupiness, and the skewness and kurtosis of sea surface elevations.

Root-Mean-Square Wave Height

Following Thompson and Vincent (1985), the deviation of the ratio H_{rms}/H_{mo} as a function of relative depth, d/gT_p^2 , was examined. For the deepwater Rayleigh case, Equations 3 and 4 can be combined to give

$$\frac{H_{rms}}{H_{mo}} = \frac{1}{\sqrt{2}} = 0.707 \quad (15)$$

However, data obtained from the field (Hughes and Ebersole, 1987) and from laboratory tests indicate that this ratio increases as relative depth decreases. A fit to the data is suggested by the following equation:

$$\frac{H_{rms}}{H_{mo}} = \frac{1}{\sqrt{2}} \exp \left[\alpha \left(\frac{d}{gT_p^2} \right)^{-b} \right] \quad (16)$$

where:

α, b = fitting parameters

g = gravitational acceleration

Linear regression of Equation 16 to laboratory and field data yields values of:

$$\alpha = 0.00089 \quad \text{and} \quad b = 0.834$$

with a correlation coefficient of $r = 0.848$. Applying linear regression to Equation 16 weights the lower values of H_{rms}/H_{mo} more than the higher values. This procedure tends to force the fit through the data at the larger values of relative depth, which serves as a good control in view of the observed scatter at smaller values of relative depth. A reasonable upper envelope to the data is given by Equation 16 when $\alpha = 0.00136$ and b remains as before.

Root-Mean-Quad Wave Height

As previously mentioned, the Rayleigh distribution has a theoretical value of

$$H_{rmq} = \sqrt{2} H_{rms}^2 \quad (17)$$

Combining Equations 15 and 17 provides a deepwater Rayleigh limit for the ratio of H_{rmq} to H_{rms}^2 ,

$$\frac{H_{rmq}}{H_{mo}^2} = \frac{1}{\sqrt{2}} = 0.707 \quad (18)$$

Plotting this ratio based on laboratory and field data showed a strong deviation from its theoretical value of 0.707 as relative depth decreased. This deviation was most likely caused by the increasing nonlinearity of the waves as they move into shallow water. As the wave crests peak up and the troughs flatten out, individual wave heights increase without a corresponding increase in sea surface variance, as represented by H_{mo} .

The quantity H_{rmq} is sensitive to the accurate determination of wave height because it is calculated from wave heights raised to the fourth power. This sensitivity might account for some of the scatter found in the data; however, it is entirely possible that H_{rmq} depends on more than the three parameters investigated here. Surprisingly, the scatter was not reduced by including skewness of sea surface elevations in the parameterization.

Linear regression of the curve

$$\frac{H_{rmq}}{H_{mo}^2} = \frac{1}{\sqrt{2}} \exp \left[\alpha \left(\frac{d}{gT_p^2} \right)^{-b} \right] \quad (19)$$

resulted in a fit to the data with

$$\alpha = 0.000098 \quad \text{and} \quad b = 1.208$$

and a correlation coefficient of $r = 0.7863$. Here, the weighting has resulted in a fit that will tend to underpredict H_{rmq} at lower values of relative depth. A reasonable upper envelope to the data is given by Equation 19 when $\alpha = 0.00023$ and b remains as before.

Breaking Wave Height

There are numerous methods for determining a breaking wave height for use in the Beta-Rayleigh distribution. Because the standard predictive expression of

$$H_b = 0.78d \quad (20)$$

appears to underestimate the breaking wave height, as observed in the photopole data (Ebersole and Hughes, 1987), a representative breaking wave height is suggested of simply

$$H_b = 0.9d \quad (21)$$

To investigate the effect of the choice for breaking wave height on the Beta-Rayleigh distribution, comparisons were made graphically (Hughes and Borgman, 1987), using Equations 20 and 21. The differences between Equations 20 and 21 were minimal at the lower values of H_{mo}/d , but a distinct deviation occurred at the higher values of H_{mo}/d . Until further research is conducted, it is recommended that H_b be taken as equal to the depth, based on the field data obtained from Ebersole and Hughes (1987) and as expressed by Equation 21.

APPLICATION

Application of the Beta-Rayleigh distribution requires specification of the water depth, d ; the energy-based significant wave height, H_{mo} ; and the peak spectral period, T_p . These parameters

are used in Equations 16 and 19 to determine H_{rms} and H_{rmq} , respectively. Next, α and β can be computed by Equations 10 and 11 using a value of H_b equal to the depth (Equation 21). Finally, the Beta-Rayleigh *pdf* is determined from Equation 5.

The relative improvement of this method over the Rayleigh distribution is illustrated in Figure 1-2-2, where a prebreaking wave height distribution histogram from the photopole experiment is plotted together with the Rayleigh prediction based on H_{m0} (dashed line) and the Beta-Rayleigh prediction (solid line). In this example (typical of the other cases studied), the Beta-Rayleigh *pdf* provides a better estimate, as somewhat expected since these data are part of the set used in the parameterization. The Rayleigh prediction to the data based on H_{rms} has already been presented in Figure 1-2-1.

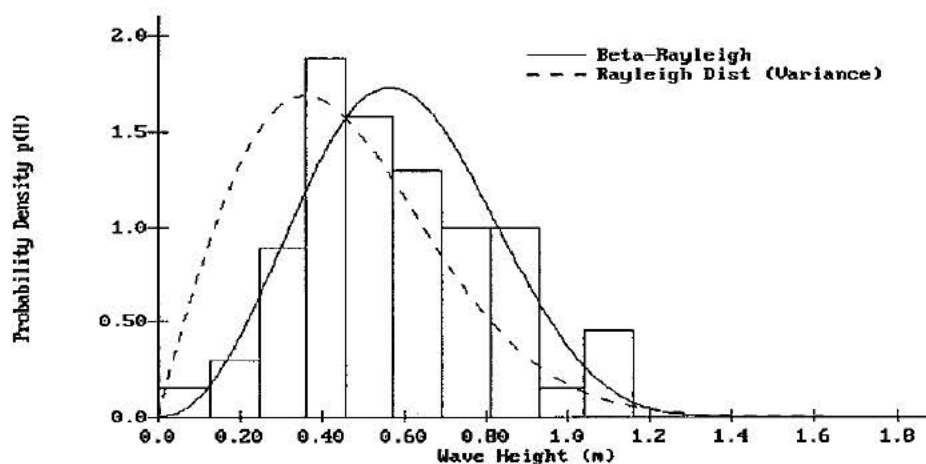


Figure 1-2-2. Beta-Rayleigh Predictions ($H_{m0} = 0.72\text{m}$; $T_p = 10.9\text{sec}$; $d = 1.63\text{m}$)

REFERENCES AND BIBLIOGRAPHY

- Battjes, J. A. 1972. "Set-Up Due to Irregular Waves," *Proceedings of the 13th International Conference on Coastal Engineering*, American Society of Civil Engineers, pp. 1993-2004.
- Collins, J. I. 1970. "Probabilities of Breaking Wave Characteristics," *Proceedings of the 12th International Conference on Coastal Engineering*, American Society of Civil Engineers, pp. 399-412.
- Dattatri, J. 1973. "Waves off Mangalore Harbor - West Coast of India," *Journal of the Waterway, Port, Coastal, and Ocean Engineering Division*, American Society of Civil Engineers, Vol. 99, No. 1, pp. 39-58.

- Earle, M. D. 1975. "Extreme Wave Conditions During Hurricane Camille," *Journal of Geophysical Research*, Vol. 80, No. 3, pp. 377-379.
- Ebersole, B. A., and Hughes, S. A. 1987. "DUCK85 Photopole Experiment," Miscellaneous Paper CERC-87-18, US Army Engineer Waterways Experiment Station, Vicksburg, MS.
- Forristall, G. Z. 1978. "On the Statistical Distribution of Wave Heights in a Storm," *Journal of Geophysical Research*, Vol. 83, No. C5, pp. 2353-2358.
- Goda, Y. 1975. "Irregular Wave Deformation in the Surf Zone," *Coastal Engineering in Japan*, Vol. 18, pp. 13-26.
- Hughes, S. A., and Borgman, L. E. 1987. "Beta-Rayleigh Distribution for Shallow Water Wave Heights," *Proceedings of the American Society of Civil Engineers Specialty Conference on Coastal Hydrodynamics*, American Society of Civil Engineers, pp. 17-31.
- Kuo, C. T., and Kuo, S. T. 1974. "Effect of Wave Breaking on Statistical Distribution of Wave Heights," *Proceedings of Civil Engineering in the Oceans, III*, American Society of Civil Engineers, pp. 1211-1231.
- Longuet-Higgins, M. S. 1952. "On the Statistical Distribution of the Heights of Sea Waves", *Journal of Marine Research*, Vol. 11, No. 3, pp. 245-266.
- Ochi, M. K., Malakar, S. B., and Wang, W. C. 1982. "Statistical Analysis of Coastal Waves Observed During the ARSLOE Project," UFL/COEL/TR-045, Coastal and Oceanographic Engineering Department, University of Florida, Gainesville, FL.
- Scheffner, N. W. 1986. "Biperiodic Waves in Shallow Water," *Proceedings of the 20th International Conference on Coastal Engineering*, American Society of Civil Engineers, pp. 724-736.
- Shore Protection Manual*. 1984. 4th ed., 2 Vols., US Army Engineer Waterways Experiment Station, Coastal Engineering Research Center, US Government Printing Office, Washington, DC.
- Thompson, E. F. 1974. "Results from the CERC Wave Measurement Program," *Proceedings of the International Symposium on Ocean Wave Measurement and Analysis*, American Society of Civil Engineers, pp. 836-855.
- Thompson, E. F., and Vincent, C. L. 1985. "Significant Wave Height for Shallow Water Design," *Journal of the Waterway, Port, Coastal, and Ocean Engineering Division*, American Society of Civil Engineers, Vol. 111, No. 5, pp. 828-842.

EXTREMAL SIGNIFICANT WAVE HEIGHT ANALYSIS

TABLE OF CONTENTS

Description	1-3-1
General Assumptions and Limitations	1-3-1
Data for Extremal Analysis	1-3-1
Extremal Distributions	1-3-2
Probability Distribution Functions	1-3-2
Return Period	1-3-3
Confidence Intervals	1-3-4
Probability of Wave Occurrence	1-3-6
Selection of a Distribution Function	1-3-6
References and Bibliography	1-3-6

EXTREMAL SIGNIFICANT WAVE HEIGHT ANALYSIS

DESCRIPTION

This application provides significant wave height estimates for various return periods. Confidence intervals are also provided. The approach developed by Goda (1988) is used to fit five candidate probability distributions to an input array of extreme significant wave heights. Candidate distribution functions are Fisher-Tippett Type I and Weibull with exponents ranging from 0.75 to 2.0. Goodness-of-fit information is provided for identifying the distributions which best match the input data.

GENERAL ASSUMPTIONS AND LIMITATIONS

General assumptions used in this approach are:

- All extreme wave heights come from a single statistical population of storm events. For example, the heights might represent only extratropical storms in the Northern Hemisphere at a site.
- Wave height properties for an event are reasonably represented by the significant height.
- Extreme wave heights are not limited by any physical factors such as shallow-water depth.

DATA FOR EXTREMAL ANALYSIS

The input array of significant wave heights for extremal analysis is extracted from a long-term data source of measurements, hindcasts, or observations. The reliability of predicted extremes is directly related to the accuracy of available data and the number of years of record. Therefore, the longest high-quality data source available should be used. As a general rule-of-thumb, heights can be extrapolated to return periods up to 3 times the length of record, K . Thus, 20 years of data can be used to estimate significant heights up to a 60-year return period. If return periods longer than $3K$ are requested, a warning message is generated.

Each significant height typically represents the maximum from a storm event. The array of significant heights is referred to as a partial duration series. Often only the more severe storms, with significant height above some minimum value, are considered. The total number, N_T , of events from the population during the length of record must be estimated. The parameter N_T can only be approximated, but results are fairly insensitive to the precise value. It is advisable to consider an average of at least one event per year in the partial duration series. If the average number of events per year, N_T/K , is less than one, a warning message is generated.

Another approach is to use only the highest significant height from each year to form an annual maximum series. The partial duration series is usually preferable for waves. Most sources cover relatively short time periods. The additional information available from a partial duration series can be helpful in increasing confidence in the extremal estimates and extrapolating to rare events.

EXTREMAL DISTRIBUTIONS

Probability Distribution Functions

There is no strong physical, theoretical, or empirical evidence for selecting a particular *pdf* for extreme wave heights. The approach commonly used is to try several candidate distributions with each data set and select the one that fits best. The candidate distributions suggested by Goda (1988) and used in this application are as follows:

- Fisher-Tippett Type I (FT-I) Distribution:

$$F(H_s \leq \hat{H}_s) = e^{-e^{\left(\frac{\hat{H}_s - B}{A}\right)}} \quad (1)$$

- Weibull Distribution:

$$F(H_s \leq \hat{H}_s) = 1 - e^{-\left(\frac{\hat{H}_s - B}{A}\right)^k} \quad (2)$$

where:

$F(H_s \leq \hat{H}_s)$ = probability of \hat{H}_s not being exceeded

H_s = significant wave height

\hat{H}_s = particular value of significant wave height

B = location parameter

A = scale parameter

k = shape parameter

The input data are ranked in descending order of significant height. A probability, or *plotting position*, is assigned to each height as follows (Goda 1988 based on previous work by Gringorten, 1963; Muir and El-Shaarawi, 1986; and Petruskas and Aagaard, 1970):

$$\begin{aligned}
 F(H_s \leq H_{sm}) &= 1 - \frac{m - 0.44}{N_T + 0.12} ; \quad FT-I \\
 F(H_s \leq H_{sm}) &= 1 - \frac{m - 0.20 - \frac{0.27}{\sqrt{k}}}{N_T + 0.20 + \frac{0.23}{\sqrt{k}}} ; \quad Weibull
 \end{aligned}
 \tag{3}$$

where:

$F(H_s \leq H_{sm})$ = probability of the m^{th} significant height not being exceeded

H_{sm} = m^{th} value in the ranked significant heights

m = rank of a significant height value
 $= 1, 2, \dots, N$

N_T = total number of events during the length of record
 (which may exceed the number of input significant heights)

The parameters A and B in Equations 1 and 2 are estimated by computing a least squares fit of the five candidate distribution functions to the data. Computations are based on linear regression analysis of the relationship

$$H_{sm} = \hat{A} y_m + \hat{B} \quad , \quad m = 1, 2, \dots, N \tag{4}$$

where:

$$\begin{aligned}
 y_m &= -\ln[-\ln F(H_s \leq H_{sm})] \quad , \quad FT-I \\
 y_m &= \{-\ln[1 - F(H_s \leq H_{sm})]\}^{\frac{1}{k}} \quad , \quad Weibull
 \end{aligned}
 \tag{5}$$

\hat{A} and \hat{B} = estimates of the scale and location parameters from linear regression analysis

Return Period

Return period is defined as the average time interval between successive events of an extreme significant wave height being equalled or exceeded. For example, the 25-year significant height can be expected to be equalled or exceeded an average of once every 25 years. Significant heights for various return periods are calculated from the probability distribution functions by the following equations:

$$H_{sr} = \hat{A} y_r + \hat{B} \tag{6}$$

where:

H_{sr} = significant wave height with return period T_r

$$y_r = -\ln \left[-\ln \left(1 - \frac{1}{\lambda T_r} \right) \right] , \quad FT-I \quad (7)$$

$$y_r = [\ln(\lambda T_r)]^{\frac{1}{k}} , \quad Weibull$$

λ = average number of events per year

$$= \frac{N_T}{K}$$

T_r = return period (years)

K = length of record (years)

Confidence Intervals

Estimation of confidence intervals is an essential part of extremal wave analysis. Typically the period of record is short, and the level of uncertainty in extremal estimates with long return periods is high. Confidence intervals give a quantitative indicator of the level of uncertainty in estimated extremal wave heights. The approach of Gumbel (1958) and Goda (1988) for estimating standard deviation of return value when the true distribution is known is used. The normalized standard deviation is calculated by

$$\sigma_{nr} = \frac{1}{\sqrt{N}} \left[1.0 + \alpha (y_r - c + \epsilon \ln v)^2 \right]^{\frac{1}{2}} \quad (8)$$

where:

σ_{nr} = normalized standard deviation of significant wave height with return period r

N = number of input significant heights

$$\alpha = \alpha_1 e^{\alpha_2 N^{-1.3} + \kappa \sqrt{-\ln v}} \quad (9)$$

$\alpha_1, \alpha_2, c, \epsilon, \kappa$ = empirical coefficients (Table 1-3-1)

v = censoring parameter

$$= \frac{N}{N_T}$$

Table 1-3-1
Coefficients of Empirical Standard Deviation Formula for Extreme
Significant Height (Goda, 1988)

Distribution	α_1	α_2	κ	c	ϵ
FT-I	0.64	9.0	0.93	0.0	1.33
Weibull (k=0.75)	1.65	11.4	-0.63	0.0	1.15
Weibull (k=1.0)	1.92	11.4	0.00	0.3	0.90
Weibull (k=1.4)	2.05	11.4	0.69	0.4	0.72
Weibull (k=2.0)	2.24	11.4	1.34	0.5	0.54

The absolute magnitude of the standard deviation of significant wave height is calculated by

$$\sigma_r = \sigma_{nr} \sigma_{H_s} \quad (10)$$

where:

σ_r = standard error of significant wave height with return period r

σ_{H_s} = standard deviation of input significant heights

Confidence intervals are calculated by assuming that significant height estimates at any particular return period are normally distributed about the assumed distribution function. Factors by which to multiply the standard error (Equation 10) to get bounds with various levels of confidence are given in Table 1-3-2. It is important to note that the width of confidence intervals depends on the distribution function, N , and v ; but it is not related to how well the data fit the distribution function.

Table 1-3-2
Confidence Interval Bounds For Extreme Significant Height

Confidence Level (%)	Confidence Interval Bounds Around H_{sr}	Probability of Exceeding Upper Bound (%)
80	$\pm 1.28\sigma_r$	10.0
85	$\pm 1.44\sigma_r$	7.5
90	$\pm 1.65\sigma_r$	5.0
95	$\pm 1.96\sigma_r$	2.5
99	$\pm 2.58\sigma_r$	0.5

PROBABILITY OF WAVE OCCURRENCE

The probability of wave occurrence is defined as the probability that a height with given return period will be equaled or exceeded during some time period. An example is the probability that the 25-year wave height will occur during a 10-year period. The probability of wave occurrence, expressed as a percent chance of occurrence, is calculated as (Headquarters, Department of the Army, 1989)

$$P_e = 100 \left[1 - \left(1 - \frac{1}{T_r} \right)^L \right] \quad (11)$$

where:

P_e = percent chance of occurrence

L = time period of concern (years)

SELECTION OF A DISTRIBUTION FUNCTION

The five distribution functions considered in this analysis are sufficiently different that only one or two can be expected to provide a good fit to any particular data set. Two statistics are provided to assist in selecting the best fit distribution function. The correlation between variables in the linear Equation 4 is the primary selection criterion. The distribution function that gives the highest correlation should be selected. The sum of the squares of residuals,

$$\sum_{m=1}^N [H_{sm} - (\hat{A}y_m + \hat{B})]^2 \quad (12)$$

is also provided. The sum is usually smallest for the distribution function with the highest correlation. Plots are also available to help judge the fit between data and distribution functions and the width of confidence intervals. If a second distribution function fits nearly as well as the best fit (i.e., the correlation is nearly as high and the sum of the squares of residuals is comparable), then it would be appropriate to consider extremal heights from both distributions. Extreme heights from the two distribution functions could be averaged together. Alternatively, the higher of the two could be used if a conservative estimate is desired.

REFERENCES AND BIBLIOGRAPHY

- Goda, Y. 1988. "On the Methodology of Selecting Design Wave Height," *Proceedings, Twenty-first Coastal Engineering Conference*, American Society of Civil Engineers, Costa del Sol-Malaga, Spain, pp. 899-913.
- Gringorten, I. I. 1963. "A Plotting Rule for Extreme Probability Paper," *Journal of Geophysical Research*, Vol. 68, No. 3, pp. 813-814.
- Gumbel, E. J. 1958. *Statistics of Extremes*, Columbia University Press, New York.

- Muir, L. R., and El-Shaarawi, A. H. 1986. "On the Calculation of Extreme Wave Heights: A Review," *Ocean Engineering*, Vol. 13, No. 1, pp. 93-118.
- Petrauskas, C., and Aagaard, P. M. 1970. "Extrapolation of Historical Storm Data for Estimating Design Wave Heights," *Proceedings, 2nd Offshore Technology Conference*, OTC1190.
- Headquarters, Department of the Army. 1989. "Water Levels and Wave Heights for Coastal Engineering Design," Engineer Manual 1110-2-1414, Washington, DC, Chapter 5, pp. 72-80.

CONSTITUENT TIDE RECORD GENERATION

TABLE OF CONTENTS

Description	1-4-1
Introduction	1-4-1
General Assumptions and Limitations	1-4-1
The Tide Prediction Equation	1-4-2
References and Bibliography	1-4-3

CONSTITUENT TIDE RECORD GENERATION

DESCRIPTION

This ACES application predicts a tide elevation record at a specific time and locale using known amplitudes and epochs for individual harmonic constituents.

INTRODUCTION

Tides are periodic in nature and are caused by the gravitational attraction of the sun and moon acting upon the rotating earth. The irregular distribution of land and water upon the planet, as well as the effects of friction, inertia, and the interactions of superimposed standing waves and progressive waves tend to complicate actual tidal motions induced by the gravitational forces. Around the year 1867, Lord Kelvin devised the method of reducing tides into constituents using harmonic analysis (Schureman, 1971). Harmonic analysis (as applied to tides) is the process by which observed tidal data at a location are reduced into a number of harmonic constituents. The quantities produced by such an analysis are known as harmonic constants and consist of amplitudes and phase relationships for each constituent. Harmonic prediction (the subject of this application) is accomplished by re-assembling the individual constituents in accordance with the appropriate astronomical relationships during the prediction period.

Harmonic tide prediction is a convenient tool for scheduling construction or maintenance work that may be affected by spring or neap tide conditions. It is also a useful tool in the application and verification of certain types of physical and hydrodynamic models where tide elevations are required either as boundary conditions or as stations for calibrating model parameters and verifying model performance.

GENERAL ASSUMPTIONS AND LIMITATIONS

The method is based upon the assumption that the tide elevation at a location can be expressed as a series of harmonic terms which are in turn dependent upon the gage location as well as the astronomical conditions during the prediction period. An individual harmonic term is represented as a simple cosine function consisting of an amplitude and phase relationship:

$$h_n = A_n \cos(\alpha_n t + \alpha_n) \quad (1)$$

Equation 1 expresses the contribution of an individual constituent (n) to the complete tide elevation. The expression contains an amplitude (A_n) and a phase relationship (the argument of the cosine function). The phase relationship is a function of the speed of the constituent (α_n), the time (t) measured from some initial epoch, and (α_n) which represents the initial phase of the constituent at the initial epoch ($t = 0$).

An important assumption in applying this methodology is that the observed record (from which the harmonic constants were derived) was of sufficient length, resolution, and quality to resolve the harmonic data adequately. Data from site-specific studies are usually short term in duration. Permanent recording stations provide longer and often more reliable records. Typical records chosen for analysis consist of hourly data analyzed in series lengths of 29 and 369 days. The latter series length is considered highly desirable for resolving most of the short period constituents and eliminating seasonal effects. Harmonic constants are often available from site-specific studies and from the National Ocean Survey.

The accuracy of the tide prediction is dependent upon the number of constituents included in the equation. In the United States, a maximum of 37 constituents (listed in Table A-5, Appendix A) are typically considered. However, in some areas, more constituents are included because of regional complexities. In many cases, a small number of constituents will represent the significant portion of the tide. For example, tides along the eastern coast of the United States are dominated by the M_2 constituent. Care should be taken to examine the amplitudes of the individual constituents in order to select those having the most significant influence on the amplitude and phase of the tide.

THE TIDE PREDICTION EQUATION

The general equation for the height of the tide at any time t can be determined from the formula:

$$h = H_0 + \sum_{n=1}^N f_n H_n \cos[\alpha_n t + (V_0 + u)_n - \kappa_n] \quad (2)$$

where

h = height of tide at time t

H_0 = mean height of water level above datum used for prediction

N = number of constituents to be considered

f_n = node factor of constituent n

H_n = amplitude of constituent n

α_n = speed of constituent n

t = time reckoned from some initial epoch

$(V_0 + u)_n$ = value of local equilibrium argument of constituent n at the initial epoch ($t = 0$)

κ_n = value of local phase lag or epoch of constituent n

In Equation 2, all quantities except h and t may be considered constant for a particular time period and location. Values of H_n and κ_n are the harmonic constants derived from analysis of past records. They must be specified (as input) for each of the constituents to be considered in the summation. The methodology implemented in ACES has algorithms for determining f_n , and $(V_0 + u)_n$ for each constituent as functions of the date and time of the initial epoch ($t = 0$), the total record length, and the longitude of the gage record. Essentially, they are determined by various combinations of astronomical functions (which are functions of time). Additionally, the equilibrium terms are also a function of longitude. In this application, their values are determined at Greenwich and translated to the gage longitude specified. The details of the computations are well described in Schureman (1971).

It should be noted that the results of some harmonic analysis are reported yielding a value of (κ'_n) which is a modified epoch (relative to Greenwich). In these cases the value of longitude at Greenwich ($= 0$) should be specified when using (κ'_n) .

REFERENCES AND BIBLIOGRAPHY

- Harris, D. L. 1981. "Tides and Tidal Datums in the United States," Special Report SR-7, US Army Engineer Waterways Experiment Station, Vicksburg, MS.
- Headquarters, Department of the Army. 1989. "Water Levels and Wave Heights for Coastal Engineering Design," Engineer Manual 1110-2-1414, Washington, DC, Chapter 2, pp. 5-10.
- Schureman, P. 1971 (reprinted). "Manual of Harmonic Analysis and Prediction of Tides," Coast and Geodetic Survey Special Publication No. 98, Revised (1940) Edition, US Government Printing Office, Washington, DC.

LINEAR WAVE THEORY

TABLE OF CONTENTS

Description	2-1-1
Introduction	2-1-1
General Assumptions and Limitations	2-1-1
Governing Equation	2-1-2
Boundary Conditions	2-1-3
Additional Simplifying Assumptions	2-1-3
Solution of the Governing Equation	2-1-4
Common Variables of Interest	2-1-5
References and Bibliography	2-1-6

LINEAR WAVE THEORY

DESCRIPTION

This application yields first-order approximations for various parameters of wave motion as predicted by the wave theory bearing the same name (also known as small amplitude, sinusoidal, or Airy theory). It provides estimates for engineering quantities such as water surface elevation, general wave properties, particle kinematics, and pressure as functions of wave height and period, water depth, and position in the wave form.

INTRODUCTION

The effects of water waves are of major importance in the field of coastal engineering. Waves are a major factor in determining geometry and composition of beaches and significantly influence planning and design of harbors, waterways, shore protection measures, coastal structures, and other coastal works.

In general, actual water-wave phenomena are complex and difficult to describe mathematically because of nonlinearities, three-dimensional characteristics, and apparent random behavior. The most elementary wave theory, referred to as small-amplitude or linear wave theory, was developed by Airy (1845). This nomenclature derives from the simplifying assumptions of its derivation. Additionally, it represents a first approximation resulting from a formal perturbation procedure for waves of finite amplitude.

GENERAL ASSUMPTIONS AND LIMITATIONS

A typical representation of a wave is depicted in Figure 2-1-1.

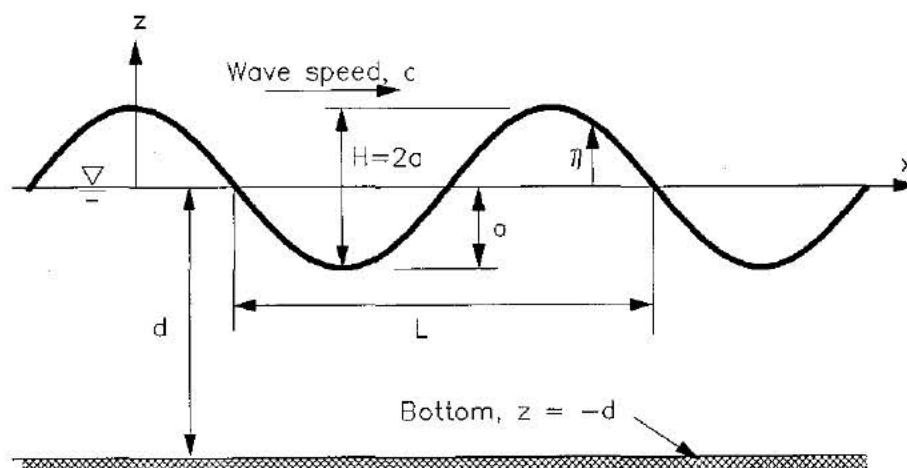


Figure 2-1-1. Progressive Wave

Common terminology for wave discussions includes:

d = still-water depth

η = free surface elevation relative to still water ($z = 0$)

α = wave amplitude

H = wave height = 2α for small-amplitude waves

L = wavelength

T = wave period

c = velocity of wave propagation (celerity) = L/T

k = wave number = $2\pi/L$

ω = wave angular frequency = $2\pi/T$

u, w = horizontal and vertical components of velocity vector \vec{u}

ϕ = velocity potential $\vec{u} = \nabla\phi$

g = acceleration of gravity

ρ = density of water

General assumptions and limitations used to derive wave theories are:

- Waves are two-dimensional (2-D) in the x-z plane.
- Waves propagate in a permanent form over a smooth horizontal bed of constant depth in the positive x-direction.
- There is no underlying current.
- Fluid is inviscid and incompressible, having no surface tension.
- Flow is irrotational.
- Coriolis effect is neglected.

GOVERNING EQUATION

The assumption of irrotational flow leads to the existence of a velocity potential. An ideal fluid must satisfy the mass continuity equation and can be expressed in primitive variables as:

$$\frac{\partial u}{\partial x} + \frac{\partial w}{\partial z} = 0 \quad (1)$$

or, in terms of the velocity potential:

$$\nabla^2 \phi = \frac{\partial^2 \phi}{\partial x^2} + \frac{\partial^2 \phi}{\partial z^2} = 0 \quad (2)$$

Equation 2 is the 2-D Laplace equation.

BOUNDARY CONDITIONS

The governing equation describes a boundary value problem. The various boundary conditions of the problem domain affect the form and complexity of the solution of the Laplace equation. The boundary conditions can be summarized as:

Bottom Boundary Condition (BBC). Fluid must not pass through the seafloor. Therefore at the sea bottom, the vertical component of the water particle velocity must vanish.

$$\frac{\partial \phi}{\partial z} = 0 \quad \text{at } z = -d \quad (3)$$

Kinematic Free Surface Boundary Condition (KFSBC). The fluid particle velocity normal to the free surface is equal to the velocity of the free surface itself. This condition implies that a water particle on the free surface remains there.

$$\frac{\partial \eta}{\partial t} + \frac{\partial \phi}{\partial x} \frac{\partial \eta}{\partial x} - \frac{\partial \phi}{\partial z} = 0 \quad \text{at } z = \eta \quad (4)$$

Dynamic Free Surface Boundary Condition (DFSBC). Expressed as the Bernoulli equation, the pressure at the free surface is constant. This requirement follows from an assumption that atmospheric pressure above the fluid is itself constant and no surface tension is present at the air-water interface.

$$\frac{\partial \phi}{\partial t} + \frac{1}{2} \left[\left(\frac{\partial \phi}{\partial x} \right)^2 + \left(\frac{\partial \phi}{\partial z} \right)^2 \right] + g\eta = f(t) \quad \text{at } z = \eta \quad (5)$$

Periodicity. The wave is periodic in time and space.

$$\begin{aligned} \phi(x, t) &= \phi(x + L, t) \\ \phi(x, t) &= \phi(x, t + T) \end{aligned} \quad (6)$$

ADDITIONAL SIMPLIFYING ASSUMPTIONS

The partial differential equations are difficult to solve because of problems associated with the free surface boundary conditions. They are nonlinear and occur at location $z = \eta$, which is initially unknown. Linear wave theory derives from applying simplifying assumptions to the free surface boundary conditions. The still-water wave height H is assumed to be very small relative to both the wavelength L and the still-water depth d :

$$H \ll L \quad \text{and} \quad H \ll d$$

The result of these assumptions is that the nonlinear terms which contain products of terms of order of H are then negligible in comparison with remaining linear terms of order H . Also, the free surface boundary conditions may now be applied at the still-water level $z = 0$. The simplified or linearized free surface boundary conditions then reduce to:

Kinematic Free Surface Boundary Condition (KFSBC).

$$\frac{\partial \phi}{\partial z} - \frac{\partial \eta}{\partial t} = 0 \quad \text{at } z = 0 \quad (7)$$

Dynamic Free Surface Boundary Condition (DFSBC).

$$\frac{\partial \phi}{\partial t} + g\eta = 0 \quad \text{at } z = 0 \quad (8)$$

SOLUTION OF THE GOVERNING EQUATION

The solution for the velocity potential is obtained by applying the method of separation of variables and the given boundary conditions. The resulting solution is stated below as well as the linear dispersion relation:

$$\phi = \frac{\pi H \cosh(ks)}{kT \sinh(kd)} \sin \theta \quad \text{or} \quad \phi = \frac{g H \cosh(ks)}{2\omega \cosh(kd)} \sin \theta \quad (9)$$

$$\omega^2 = gk \tanh(kd) \quad \text{or} \quad c^2 = \frac{g}{k} \tanh(kd) \quad (10)$$

where

$\Theta = k(x - ct) = kx - \omega t = \text{wave phase angle}$

$s = z + d$ measured upwards from the seabed

The dispersion relation describes the manner in which a field of propagating waves consisting of many frequencies would separate or "disperse" due to the different celerities of the various frequency components (Dean and Dalrymple, 1984). The linear dispersion relation is a transcendental function but may be readily evaluated using a Pade approximation (Hunt, 1979):

$$c^2 = gd \left[y + \left(1 + \sum_{n=1}^9 d_n y^n \right)^{-1} \right]^{-1} \quad (11)$$

where

$$y = \frac{\omega^2 d}{g}$$

$d_n = \text{constants}$

$d_1 = 0.66667$	$d_4 = 0.06320$	$d_7 = 0.00171$
$d_2 = 0.35550$	$d_5 = 0.02174$	$d_8 = 0.00039$
$d_3 = 0.16084$	$d_6 = 0.00654$	$d_9 = 0.00011$

This approximation has an accuracy better than 0.01 percent over the range $0 \leq y \leq \infty$.

COMMON VARIABLES OF INTEREST

The solution for ϕ and the linear dispersion relation provide a foundation for deriving expressions for other common variables of interest. These equations are listed below and can be found in many texts including Sarpkaya and Isaacson (1981) and the SPM (1984).

$$\text{Wavelength: } L = cT \quad (12)$$

$$\text{Group velocity: } C_g = \frac{1}{2} \left[1 + \frac{2kd}{\sinh(2kd)} \right] c \quad (13)$$

$$\text{Water surface elevation: } \eta = \frac{H}{2} \cos \theta \quad (14)$$

$$\text{Average energy density: } E = \frac{1}{8} \rho g H^2 \quad (15)$$

$$\text{Energy flux: } P = E C_g \quad (16)$$

$$\text{Pressure: } p = -\rho g z + \frac{1}{2} \rho g H \frac{\cosh(ks)}{\cosh(kd)} \cos \theta \quad (17)$$

$$\text{Horizontal particle displacement: } \xi = -\frac{H \cosh(ks)}{2 \sinh(kd)} \sin \theta \quad (18)$$

$$\text{Vertical particle displacement: } \zeta = \frac{H \sinh(ks)}{2 \sinh(kd)} \cos \theta \quad (19)$$

$$\text{Horizontal particle velocity: } u = \frac{\pi H \cosh(ks)}{T \sinh(kd)} \cos \theta \quad (20)$$

$$\text{Vertical particle velocity: } w = \frac{\pi H \sinh(ks)}{T \sinh(kd)} \sin \theta \quad (21)$$

$$\text{Horizontal particle acceleration: } \frac{\partial u}{\partial t} = \frac{2\pi^2 H \cosh(ks)}{T^2 \sinh(kd)} \sin \theta \quad (22)$$

$$\text{Vertical particle acceleration: } \frac{\partial w}{\partial t} = -\frac{2\pi^2 H \sinh(ks)}{T^2 \sinh(kd)} \cos \theta \quad (23)$$

A common parameter for the applicability of various wave theories is the Stokes (1847) or Ursell (1953) parameter, which is defined as:

$$U_r = \frac{H L^2}{d^3} \quad (24)$$

This parameter is reported for convenience.

REFERENCES AND BIBLIOGRAPHY

- Airy, G. B. 1845. "Tides and Waves," *Encyclopaedia Metropolitana*, Vol. 192, pp. 241-396.
- Dean, R. G., and Dalrymple, R. A. 1984. *Water Wave Mechanics for Engineers and Scientists*, Prentice-Hall, Englewood Cliffs, NJ, pp. 41-86.
- Hunt, J. N. 1979. "Direct Solution of Wave Dispersion Equation," *Journal of Waterway, Port, Coastal and Ocean Division*, American Society of Civil Engineers, Vol. 105, No. WW4, pp. 457-459.
- Sarpkaya, T., and Isaacson, M. 1981. *Mechanics of Wave Forces on Offshore Structures*, Van Nostrand Reinhold, New York, pp. 150-168.
- Shore Protection Manual*. 1984. 4th ed., 2 Vols., US Army Engineer Waterways Experiment Station, Coastal Engineering Research Center, US Government Printing Office, Washington, DC, Chapter 2, pp. 6-33.
- Stokes, G. G. 1847. "On the Theory of Oscillatory Waves," *Transactions of the Cambridge Philosophical Society*, Vol. 8, pp. 441-455.
- Ursell, F. 1953. "The Long-Wave Paradox in the Theory of Gravity Waves," *Proceedings of the Cambridge Philosophical Society*, Vol. 49, pp. 685-694.

CNOIDAL WAVE THEORY

TABLE OF CONTENTS

Description	2-2-1
Introduction	2-2-1
General Assumptions and Limitations	2-2-1
Governing Equation	2-2-2
Boundary Conditions	2-2-3
Cnoidal Wave Theory Considerations	2-2-3
Solution of the Governing Equations	2-2-5
Results from the Theory	2-2-7
First-Order Solutions	2-2-7
Second-Order Approximations	2-2-9
References and Bibliography	2-2-12

CNOIDAL WAVE THEORY

DESCRIPTION

This application yields various parameters of wave motion as predicted by first-order (Isobe, 1985) and second-order (Hardy and Kraus, 1987) approximations for cnoidal wave theory. It provides estimates for common items of interest such as water surface elevation, general wave properties, kinematics, and pressure as functions of wave height and period, water depth, and position in the wave form.

INTRODUCTION

The accurate description of waves in the nearshore region is an important element in the design and analysis process. The complexity of nonlinear wave theories has apparently discouraged their common application, especially for reconnaissance level investigations; yet they often provide significant improvements over linear wave theory descriptions. Today's common desktop microcomputers offer adequate computational power to implement many nonlinear wave theories.

Solutions for wave attributes described by this theory are expressed in terms of the Jacobian elliptic function cn , thus providing an explanation for the theory's name. The original source for the theory was a paper by the Dutch mathematicians Korteweg and de Vries (1895). More recent derivations for cnoidal wave theory include those of Keulegan and Patterson (1940), Keller (1948), Laitone (1960), Chappellear (1962), Fenton (1979), and Isobe and Kraus (1983) among others. Differences between the derivations consist primarily of choices in perturbation parameter, definition of celerity, and order of the solution. The following discussion is taken principally from Hardy and Kraus (1987), and Isobe and Kraus (1983).

GENERAL ASSUMPTIONS AND LIMITATIONS

A representative cnoidal wave profile is illustrated in Figure 2-2-1.

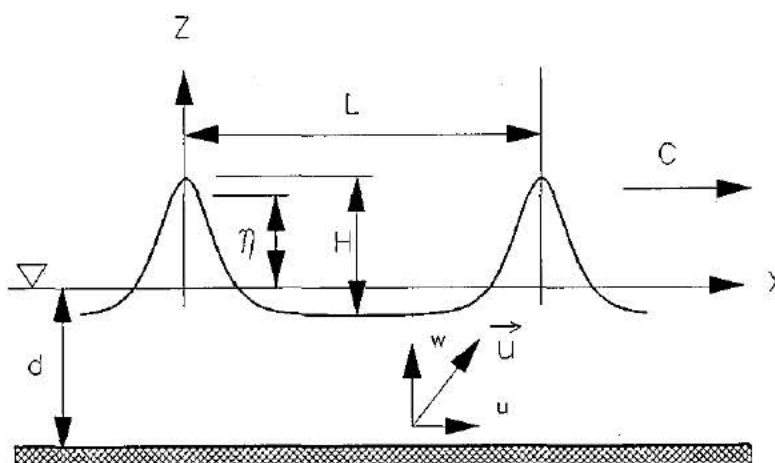


Figure 2-2-1. Cnoidal Wave Profile

The assumptions and terminology for general wave theories will be reviewed first, followed by specific assumptions and treatments associated with cnoidal wave theory. Terms common to wave discussions include:

d = still-water depth

η = free surface elevation relative to still water ($z = 0$)

α = wave amplitude

H = wave height = 2α for small-amplitude waves

L = wavelength

T = wave period

c = velocity of wave propagation (celerity) = L/T

\vec{u} = water particle velocity vector

u, w = horizontal and vertical components of velocity vector \vec{u}

ϕ = velocity potential $\vec{u} = \nabla \phi$

ψ = stream function

g = acceleration of gravity

ρ = density of water

p_B = Bernoulli constant

General assumptions and limitations used to derive wave theories include:

- Waves are two-dimensional in the x-z plane.
- Waves propagate in a permanent form over a smooth horizontal bed of constant depth in the positive x-direction.
- There is no underlying current.
- Fluid is inviscid and incompressible, having no surface tension.
- Flow is irrotational.

GOVERNING EQUATION

The assumption of irrotational flow leads to the existence of a velocity potential. An ideal fluid must satisfy the mass continuity equation and can be expressed in terms of the velocity potential as:

$$\nabla^2 \phi = 0 \quad (1)$$

This is the 2-D Laplace equation.

BOUNDARY CONDITIONS

The governing equation describes a boundary value problem. The various boundary conditions of the problem domain affect the form and complexity of the solution of the Laplace equation. The boundary conditions can be summarized as:

Bottom Boundary Condition (BBC). Fluid must not pass through the seafloor. Therefore, at the sea bottom, the vertical component of the water particle velocity must vanish.

$$\phi_z = 0 \quad \text{at } z = -d \quad (2)$$

Kinematic Free Surface Boundary Condition (KFSBC). The fluid particle velocity normal to the free surface is equal to the velocity of the free surface itself. This condition implies that a water particle on the free surface remains there. It also implies that the wave does not break.

$$\eta_t + \phi_x \eta_x - \phi_z = 0 \quad \text{at } z = \eta \quad (3)$$

Dynamic Free Surface Boundary Condition (DFSBC). Expressed as the Bernoulli equation, the pressure at the free surface is constant. This requirement follows from an assumption that atmospheric pressure above the fluid is itself constant and no surface tension is present at the air-water interface.

$$-\phi_t + \frac{1}{2}(\phi_x^2 + \phi_z^2) + gz = \frac{P_b}{\rho} \quad \text{at } z = \eta \quad (4)$$

Periodicity. The wave is periodic in time and space.

$$\phi(x, t) = \phi(x + L, t) \quad \phi(x, t) = \phi(x, t + T) \quad (5)$$

CNOIDAL WAVE THEORY CONSIDERATIONS

Cnoidal wave theory is valid in relatively shallow water. For deriving waves of finite amplitude, the simplifying assumptions which characterize small-amplitude (linear) wave theory ($H \ll L$) and ($H \ll d$) are not appropriate. For shallow water, the second assumption ($H \ll d$) is invalid. Consequently, the nonlinear terms of the free surface boundary conditions are retained in the solution of the boundary value problem.

The free surface boundary conditions can be simplified by adopting a moving coordinate system having the same velocity as the wave celerity. The unsteady terms (time derivatives) are then eliminated. However, this procedure requires an additional assumption for an initial definition of celerity. The two most common assumptions were originally proposed by Stokes (1847) and are stated below:

Stokes Definition 1
(avg horizontal velocity = 0)

$$\frac{1}{L} \int_0^L u \, dx = 0$$

Stokes Definition 2
(avg mass flux = 0)

$$\frac{1}{L} \int_0^L \int_{-d}^{\eta} u \, dz \, dx = 0 \quad (6)$$

The second definition of wave celerity was selected for this derivation. The tabulated approximations resulting from the derivation will be expressed relative to a fixed coordinate system.

Wave theories are often derived in any of three sets of variables: primitive variables (u, w), velocity potential ϕ , or stream function ψ . The assumption of 2-D, irrotational flow of an incompressible fluid leads to the following relationships between the three variables:

$$\psi_z = \phi_x = u \qquad -\psi_x = \phi_z = w \qquad (7)$$

Use of the stream function automatically satisfies the KFSBC (Equation 3) and consequently simplifies its form. The governing equation and boundary equations can then be restated in terms of stream function as:

$$\text{Laplace Equation:} \qquad \nabla^2 \psi = 0 \qquad (8)$$

$$\text{BBC:} \qquad \psi = 0 \qquad \text{at } z = -d \qquad (9)$$

$$\text{KFSBC:} \qquad \psi = q \qquad \text{at } z = \eta \qquad (10)$$

$$\text{DFSBC:} \qquad \frac{1}{2}(\psi_x^2 + \psi_z^2) + g\eta = \frac{P_b}{\rho} \qquad \text{at } z = \eta \qquad (11)$$

$$\text{Other Conditions:} \qquad \bar{\eta} = 0 \qquad (12)$$

$$\eta(0) - \eta\left(\frac{L}{2}\right) = H \qquad (13)$$

$$\text{Celerity Definition:} \qquad c = -\frac{q}{d} \qquad (14)$$

The variable q in the above expressions represents the unit flow rate. Expressions for the periodic nature of the wave have been recast into alternate forms. Equation 12 requires the average value of η taken over a wavelength to be zero, while Equation 13 defines the wave height.

In shallow water, the vertical and horizontal length scales are of different orders of magnitude. For convenience, the variables are nondimensionalized using the horizontal length scale (L), vertical length scale (H), and velocity scale \sqrt{gd} :

$$\begin{aligned} X &= \frac{x}{L} & Z &= \frac{z}{d} & N &= \frac{\eta}{d} & \Psi &= \frac{\psi}{d\sqrt{gd}} \\ Q &= \frac{q}{d\sqrt{gd}} & P &= \frac{P}{\rho g d} & P_B &= \frac{P_B}{\rho g d} \end{aligned} \qquad (15)$$

The complete boundary value problem restated in terms of these nondimensional variables is:

$$\text{Governing Equation:} \quad \Psi_{zz} + \left(\frac{d}{L}\right)^2 \Psi_{xx} = 0 \quad (16)$$

$$\text{BBC:} \quad \Psi = 0 \quad \text{at } z = -1 \quad (17)$$

$$\text{KFSBC:} \quad \Psi = q \quad \text{at } z = N \quad (18)$$

$$\text{DFSBC:} \quad \frac{1}{2} \left[\Psi_z^2 + \left(\frac{d}{L}\right)^2 \Psi_x^2 \right] + N = P_B \quad \text{at } z = N \quad (19)$$

$$\text{Other Conditions:} \quad \bar{N} = 0 \quad (20)$$

$$N(0) - N\left(\frac{1}{2}\right) = \frac{H}{d} \quad (21)$$

SOLUTION OF THE GOVERNING EQUATIONS

The boundary value problem consists of a set of nonlinear partial differential equations. The principal approach used to solve finite-amplitude wave behavior is the perturbation method. Dependent variables in the problem are assumed to be functions of an auxiliary parameter, δ , and are expanded in a power series of a small perturbation parameter, ϵ .

Waves of permanent form can be described by three independent variables, H , L , and d , from which two independent nondimensional quantities can be formed: (H/L) and (H/d) . One of these ratios is often selected as the perturbation parameter in finite-amplitude wave theories. In this derivation of cnoidal wave theory, the second quantity is selected as the perturbation parameter:

$$\epsilon = \frac{H}{d} \quad (22)$$

The modulus of the elliptic integral, κ , is selected as the auxiliary parameter.

The nondimensional variables of the boundary value problem are expanded as power series about ϵ :

$$\Psi(X, Z, \kappa, \epsilon) = \sum_{n=0}^{\infty} \Psi_n(X, Z, \kappa) \epsilon^n = \Psi_0 + \epsilon \Psi_1 + \epsilon^2 \Psi_2 + \epsilon^3 \Psi_3 + \dots \quad (23)$$

$$N(X, \kappa, \epsilon) = \sum_{n=1}^{\infty} N_n(X, \kappa) \epsilon^n = \epsilon N_1 + \epsilon^2 N_2 + \epsilon^3 N_3 + \dots \quad (24)$$

$$Q(\kappa, \epsilon) = \sum_{n=0}^{\infty} Q_n(\kappa) \epsilon^n = Q_0 + \epsilon Q_1 + \epsilon^2 Q_2 + \epsilon^3 Q_3 + \dots \quad (25)$$

$$P_B(\kappa, \epsilon) = \sum_{n=0}^{\infty} P_n(\kappa) \epsilon^n = P_0 + \epsilon P_1 + \epsilon^2 P_2 + \epsilon^3 P_3 + \dots \quad (26)$$

$$\left(\frac{d}{L}\right)^2 (\kappa, \epsilon) = \sum_{n=1}^{\infty} \delta_n(\kappa) \epsilon^n = \epsilon \delta_1 + \epsilon^2 \delta_2 + \epsilon^3 \delta_3 + \dots \quad (27)$$

The series expansions for N and $(d/L)^2$ (Equations 24 and 27) do not have *zero* terms because they are always smaller than ϵ .

The expanded forms for variables (Equations 23-27) are inserted into the Equations 16-21. For example, substituting the expanded form for Ψ in the governing Equation 16 yields:

$$\begin{aligned} & (\Psi_{0ZZ} + \epsilon \Psi_{1ZZ} + \epsilon^2 \Psi_{2ZZ} + \epsilon^3 \Psi_{3ZZ} + \dots) \\ & + (\epsilon \delta_1 + \epsilon^2 \delta_2 + \epsilon^3 \delta_3 + \dots) \times (\Psi_{0XX} + \epsilon \Psi_{1XX} + \epsilon^2 \Psi_{2XX} + \epsilon^3 \Psi_{3XX} + \dots) = 0 \end{aligned} \quad (28)$$

and at the bottom boundary (Equation 17):

$$\Psi_0 + \epsilon \Psi_1 + \epsilon^2 \Psi_2 + \epsilon^3 \Psi_3 + \dots = 0 \quad (29)$$

Equation 28 also provides some useful initial information. With the wave height equal to zero ($\epsilon = 0$), uniform flow conditions exist as a result of the moving coordinate system. Further, it can be seen that:

$$\Psi_0 = b_{00} Z \quad \Rightarrow \quad \Psi_{0XX} = \Psi_{0ZZ} = 0 \quad (30)$$

The term b_{00} is a constant to be determined later.

The free surface boundary conditions require special treatment because they occur at a location which is initially unknown. Instead of expansion with a power series, variables requiring evaluation at the free surface are expanded using a Taylor series about the known still-water level ($Z = 0$). For example, the Taylor series expansion for Ψ at the free surface is:

$$\Psi(X, N) = \Psi(X, 0) + N \Psi_z(X, 0) + \frac{N^2}{2} \Psi_{zz}(X, 0) + \dots \quad (31)$$

Continuing with the perturbation technique, for a given equation, terms are grouped by equal powers of ϵ , and terms of an individual order on the left side must equal terms of like order on the right side. For example, again consider the governing Equation 28:

$$\epsilon \text{ terms:} \quad \Psi_{1ZZ} = 0 \quad (32)$$

$$\epsilon^2 \text{ terms:} \quad \Psi_{2ZZ} + \delta_1 \Psi_{1XX} = 0 \quad (33)$$

$$\epsilon^3 \text{ terms:} \quad \Psi_{3ZZ} + \delta_1 \Psi_{2XX} + \delta_2 \Psi_{1XX} = 0 \quad (34)$$

This procedure is also applied to the remaining five boundary condition equations (17-21). The result is a set of equations for each order of ϵ . For example, the set of equations of second-order (ϵ^2) terms is:

$$\left[\begin{array}{l} \Psi_{2ZZ} + \delta_1 \Psi_{1XX} = 0 \\ \Psi_2 = 0 \quad \text{at } Z = -1 \\ \Psi_2 + b_{00} N_2 + N_1 \Psi_{1Z} = Q_2 \quad \text{at } Z = N \\ N_2 + b_{00} (\Psi_{2Z} + N_1 \Psi_{1ZZ}) + \frac{1}{2} (\Psi_{1Z})^2 = P_2 \quad \text{at } Z = N \\ \bar{N}_2 = 0 \\ N_2(0) - N_2\left(\frac{1}{2}\right) = 0 \end{array} \right] \quad (35)$$

The solution of n^{th} order equations requires information from the equations of $(n+1)^{\text{th}}$ order. In total, the algebraic manipulations are quite lengthy and are beyond the intent of this report. A short summary of the procedure follows. The equations of 0th order determine P_0 and Q_0 once b_{00} is determined. The equations of 1st order determine b_{00} such that a nontrivial solution of N_1 and Ψ_1 exists. In similar fashion, the 2nd order equations determine N_1 and Ψ_1 if a nontrivial solution of N_2 and Ψ_2 exists. The process continues upward to the desired order of solution. This particular ACES application will provide results for 1st and 2nd order solutions.

The solution for the cnoidal theory contains elliptic integrals and Jacobian elliptic functions which arise from the choice of κ as the auxiliary parameter and from the solution of certain nonlinear differential equations. Standard numerical methods described in Abramowitz and Stegun (1972) are employed for approximating these quantities.

RESULTS FROM THE THEORY

The resulting approximations for the critical elements of the wave description are summarized below. Integral properties, water particle kinematics, and other traditional quantities of interest are included in the tabulations. All quantities are relative to a fixed frame of reference.

First-Order Solutions

$$\text{Dispersion relation:} \quad \frac{16\kappa^2 K^2}{3} = \frac{gHT^2}{d^2} \quad (36)$$

$$\text{Celerity: } c = \sqrt{gd}(C_0 + \epsilon C_1) \quad (37)$$

$$C_0 = 1 \quad (37.1)$$

$$C_1 = \frac{1 + 2\lambda - 3\mu}{2} \quad (37.2)$$

$$\text{Wavelength: } L = cT \quad (38)$$

$$\text{Water surface elevation: } \eta = d(A_0 + A_1 \text{cn}^2\theta) \quad (39)$$

$$A_0 = \epsilon(\lambda - \mu) \quad (39.1)$$

$$A_1 = \epsilon \quad (39.2)$$

$$\text{Average energy density: } E = \rho g H^2 E_0 \quad (40)$$

$$E_0 = \frac{-\lambda + 2\mu + 4\lambda\mu - \lambda^2 - 3\mu^2}{3} \quad (40.1)$$

$$\text{Energy flux: } F = \rho g H^2 \sqrt{gd} F_0 \quad (41)$$

$$F_0 = E_0 \quad (41.1)$$

$$\text{Pressure: } p = p_b - \frac{\rho}{2}[(u - c)^2 + w^2] - g\rho(z + d) \quad (42)$$

$$p_b = \rho g d(P_0 + \epsilon P_1) \quad (42.1)$$

$$P_0 = \frac{3}{2} \quad (42.2)$$

$$P_1 = \frac{1 + 2\lambda - 3\mu}{2} \quad (42.3)$$

$$\text{Horizontal velocity: } u = \sqrt{gd}(B_{00} + B_{10} \text{cn}^2\theta) \quad (43)$$

$$B_{00} = \epsilon(\lambda - \mu) \quad (43.1)$$

$$B_{10} = \epsilon \quad (43.2)$$

$$\text{Vertical velocity: } w = \sqrt{gd} \frac{4Kd \operatorname{csd} \left(\frac{z+d}{d} \right)}{L} B_{10} \quad (44)$$

$$\text{Horizontal acceleration: } \frac{\partial u}{\partial t} = \sqrt{gd} B_{10} \frac{4K}{T} \operatorname{csd} \quad (45)$$

$$\text{Vertical acceleration: } \frac{\partial w}{\partial t} = \sqrt{gd} \frac{4Kd}{L} \left(\frac{z+d}{d} \right) B_{10} \frac{2K}{T} (\operatorname{sn} \theta \operatorname{dn} \theta - \operatorname{cn} \theta \operatorname{dn} \theta + \kappa^2 \operatorname{sn} \theta \operatorname{cn} \theta) \quad (46)$$

The following general symbols also require definition:

$$\kappa' = \sqrt{1 - \kappa^2} \quad (47)$$

$$\lambda = \frac{\kappa'^2}{\kappa^2} \quad (48)$$

$$\mu = \frac{E}{\kappa^2 K} \quad (49)$$

$$\theta = 2K \left[\left(\frac{x}{L} \right) - \left(\frac{t}{T} \right) \right] \quad (50)$$

K and E are the complete elliptic integrals of the first and second kind, respectively; $\operatorname{sn} \theta$, $\operatorname{cn} \theta$, $\operatorname{dn} \theta$ are the Jacobian elliptic functions, and

$$\operatorname{csd} = \operatorname{cn} \theta \operatorname{sn} \theta \operatorname{dn} \theta \quad (51)$$

Second-Order Approximations

$$\text{Dispersion relation: } \frac{16\kappa^2 K^2}{3} = \frac{gHT^2}{d^2} \left[1 - \epsilon \left(\frac{1+2\lambda}{4} \right) \right] \quad (52)$$

$$\text{Celerity: } c = \sqrt{gd} (C_0 + \epsilon C_1 + \epsilon^2 C_2) \quad (53)$$

$$C_0 = 1 \quad (53.1)$$

$$C_1 = \frac{1+2\lambda-3\mu}{2} \quad (53.2)$$

$$C_2 = \frac{-6 - 16\lambda + 5\mu - 16\lambda^2 + 10\lambda\mu + 15\mu^2}{40} \quad (53.3)$$

$$\text{Water surface elevation: } \eta = d(A_0 + A_1 \text{cn}^2\theta + A_2 \text{cn}^4\theta) \quad (54)$$

$$A_0 = \epsilon(\lambda - \mu) + \epsilon^2 \left(\frac{-2\lambda + \mu - 2\lambda^2 + 2\lambda\mu}{4} \right) \quad (54.1)$$

$$A_1 = \epsilon - \frac{3}{4}\epsilon^2 \quad (54.2)$$

$$A_2 = \frac{3}{4}\epsilon^2 \quad (54.3)$$

$$\text{Average energy density: } E = \rho g H^2 (E_0 + \epsilon E_1) \quad (55)$$

$$E_0 = \frac{-\lambda + 2\mu + 4\lambda\mu - \lambda^2 - 3\mu^2}{3} \quad (55.1)$$

$$E_1 = \frac{1}{30}(\lambda - 2\mu - 17\lambda\mu + 3\lambda^2 - 17\lambda^2\mu + 2\lambda^3 + 15\mu^3) \quad (55.2)$$

$$\text{Energy flux: } F = \rho g H^2 \sqrt{gd} (F_0 + \epsilon F_1) \quad (56)$$

$$F_0 = E_0 \quad (56.1)$$

$$F_1 = \frac{1}{30}(-4\lambda + 8\mu + 53\lambda\mu - 12\lambda^2 - 60\mu^2 + 53\lambda^2\mu - 120\lambda\mu^2 - 8\lambda^3 + 75\mu^3) \quad (56.2)$$

$$\text{Pressure: } p = p_b - \frac{\rho}{2}[(u - c)^2 + w^2] - g\rho(z + d) \quad (57)$$

$$p_b = \rho g d (P_0 + \epsilon P_1 + \epsilon^2 P_2) \quad (57.1)$$

$$P_0 = \frac{3}{2} \quad (57.2)$$

$$P_1 = \frac{1 + 2\lambda - 3\mu}{2} \quad (57.3)$$

$$P_2 = \frac{-1 - 16\lambda + 15\mu - 16\lambda^2 + 30\lambda\mu}{40} \quad (57.4)$$

Horizontal velocity: $u = \sqrt{gd}[(B_{00} + B_{10} \operatorname{cn}^2 \theta + B_{20} \operatorname{cn}^4 \theta) - \frac{1}{2} \left(\frac{z+d}{d} \right)^2 (B_{01} + B_{11} \operatorname{cn}^2 \theta + B_{21} \operatorname{cn}^4 \theta)]$ (58)

$$B_{00} = \epsilon(\lambda - \mu) + \epsilon^2 \left(\frac{\lambda - \mu - 2\lambda^2 + 2\mu^2}{4} \right) \quad (58.1)$$

$$B_{10} = \epsilon + \epsilon^2 \left(\frac{1 - 6\lambda + 2\mu}{4} \right) \quad (58.2)$$

$$B_{20} = -\epsilon^2 \quad (58.3)$$

$$B_{01} = \frac{3\lambda}{2} \epsilon^2 \quad (58.4)$$

$$B_{11} = 3\epsilon^2(1 - \lambda) \quad (58.5)$$

$$B_{21} = -\frac{9}{2} \epsilon^2 \quad (58.6)$$

Vertical velocity: $w = \sqrt{gd} \frac{4Kd \operatorname{csd}}{L} \times \left[\left(\frac{z+d}{d} \right) (B_{10} + 2B_{20} \operatorname{cn}^2 \theta) - \frac{1}{6} \left(\frac{z+d}{d} \right)^3 (B_{11} + 2B_{21} \operatorname{cn}^2 \theta) \right]$ (59)

Horizontal acceleration: $\frac{\partial u}{\partial t} = \sqrt{gd} \left\{ \left[B_{10} - \frac{1}{2} \left(\frac{z+d}{d} \right)^2 B_{11} \right] \frac{4K}{T} \operatorname{csd} + \left[B_{20} - \frac{1}{2} \left(\frac{z+d}{d} \right)^2 B_{21} \right] \frac{8K}{T} \operatorname{cn}^2 \theta \operatorname{csd} \right\}$ (60)

Vertical acceleration: $\frac{\partial w}{\partial t} = \sqrt{gd} \frac{4Kd}{L} \left\{ \frac{8K}{T} \operatorname{csd}^2 \left[\left(\frac{z+d}{d} \right) B_{20} - \frac{1}{6} \left(\frac{z+d}{d} \right)^3 B_{21} \right] + \left[\left(\frac{z+d}{d} \right) (B_{10} + 2B_{20} \operatorname{cn}^2 \theta) - \frac{1}{6} \left(\frac{z+d}{d} \right)^3 (B_{11} + 2B_{21} \operatorname{cn}^2 \theta) \right] \times [\operatorname{sn} \theta \operatorname{dn} \theta - \operatorname{cn} \theta \operatorname{dn} \theta + \kappa^2 \operatorname{sn} \theta \operatorname{cn} \theta] \right\}$ (61)

REFERENCES AND BIBLIOGRAPHY

- Abramowitz, M., and Stegun, I. A. 1972. *Handbook of Mathematical Functions*, Dover Publications, New York, 1046 pp.
- Chappelear, J. E. 1962. "Shallow Water Waves," *Journal of Geophysical Research*, Vol. 67, No. 12, pp. 4693-4704.
- Davis, H. T. 1962. *Introduction to Nonlinear Differential and Integral Equations*, Dover Publications, New York, 596 pp.
- Fenton, J. D. 1979. "A High Order Cnoidal Wave Theory," *Journal of Fluid Mechanics*, Vol. 94, pp. 129-161.
- Hardy, T. A., and Kraus, N. C. 1987. "A Numerical Model for Shoaling and Refraction of Second-Order Cnoidal Waves over an Irregular Bottom," Miscellaneous Paper CERC-87-9, US Army Engineer Waterways Experiment Station, Vicksburg, MS.
- Isobe, M. 1985. "Calculation and Application of First-Order Cnoidal Wave Theory," *Coastal Engineering*, Vol. 9, pp. 309-325.
- Isobe, M., and Kraus, N. C. 1983. "Derivation of a Second-Order Cnoidal Wave Theory," Hydraulics Laboratory Report No. YNU-HY-83-2, Department of Civil Engineering, Yokohama National University, 43 pp.
- Keller, J. B. 1948. "The Solitary Wave and Periodic Waves in Shallow Water," *Communication of Pure and Applied Mathematics*, Vol. 1, pp. 323-339.
- Keulegan, G. H., and Patterson, G. W. 1940. "Mathematical Theory of Irrotational Translation Waves," *Journal of Research of the National Bureau of Standards*, Vol. 24, pp. 47-101.
- Korteweg, D. J., and de Vries, G. 1895. "On the Change of Form of Long Waves Advancing in a Rectangular Canal, and on a New Type of Long Stationary Waves," *Philosophy Magazine*, Series 5, Vol. 39, pp. 422-443.
- Laitone, E. V. 1960. "The Second Approximation to Cnoidal and Solitary Waves," *Journal of Fluid Mechanics*, Vol. 9, pp. 430-444.
- Shore Protection Manual*. 1984. 4th ed., 2 Vols., US Army Engineer Waterways Experiment Station, Coastal Engineering Research Center, US Government Printing Office, Washington, DC, Chapter 2, pp. 44-55.
- Stokes, G. G. 1847. "On the Theory of Oscillatory Waves," *Transactions of the Cambridge Philosophical Society*, Vol. 8, pp. 441-455.

FOURIER SERIES WAVE THEORY

TABLE OF CONTENTS

Description	2-3-1
Introduction	2-3-1
General Assumptions and Terminology	2-3-2
Governing Equation and Boundary Conditions	2-3-3
Additional Considerations Relative to the Dispersion Relation	2-3-4
Solution and Method	2-3-5
Solution Aids and Insights	2-3-9
Maximum Wave Checks	2-3-9
Derived Results	2-3-10
Kinematics and Other Derived Variables	2-3-10
Integral Properties	2-3-11
References and Bibliography	2-3-12

FOURIER SERIES WAVE THEORY

DESCRIPTION

This application yields various parameters for progressive waves of permanent form, as predicted by Fourier series approximation. It provides estimates for common engineering parameters such as water surface elevation, integral wave properties, and kinematics as functions of wave height, period, water depth, and position in the wave form which is assumed to exist on a uniform co-flowing current. Stokes first and second approximations for celerity (i.e., values of the mean Eulerian current or mean mass transport rate) may be specified. Fourier series of up to 25 terms may be selected to approximate the wave. In addition to providing kinematics at a given point in the wave, this application provides graphical presentations of kinematics over two wavelengths (at a given z coordinate), and the vertical profile of selected kinematics under the wave crest. The methodology is based upon a series of papers by J. D. Fenton (Reinecker and Fenton, 1981; Fenton, 1988a; Fenton, 1988b; Fenton, 1990) and R. J. Sobey (Sobey, Goodwin, Thieke, and Westberg, 1987). LINPACK routines (Dongarra et al., 1979) are used to solve the set of up to 60 simultaneous equations to determine the Fourier coefficients for the series.

INTRODUCTION

The accurate description of the steady wave is an important element in the design and analysis process. While linear wave theory has traditionally (and often correctly) been used for a large group of wave applications, nonlinear wave theories often provide significant improvements over linear wave theory descriptions, particularly where wavelengths are long or short relative to water depth. Recent developments and technology enable engineers to easily employ higher order wave theories to increase the accuracy of their estimates of wave properties. Today's common desktop microcomputers offer adequate computational power to implement many nonlinear wave theories.

Common practice includes the use of Stokes' theory in deep water, cnoidal theory in shallow water, and Fourier series wave theory in deep, transitional, and shallow water. Contemporary versions of Stokes' and cnoidal theory are readily accessible at fifth order, and Fourier series theory at any order, though 15th to 20th order appears adequate to resolve even highly nonlinear waves. All are capable of incorporating a uniform underlying current. Stokes and cnoidal theory have limited regions of physical validity, and at higher orders, can be quite accurate. The domain of applicability for Fourier approximation wave theory includes that of both Stokes and cnoidal theory. It is based upon a numerical approach, and substitutes computational effort for the limited domain of the above perturbation methods. It is easily tractable at any desired order (subject to machine precision), and has become a well-established, robust, and accurate engineering tool for the steady wave problem.

Several variations of Fourier series wave theory have been presented in recent years: (Chappelear, 1961; Dean, 1965, and 1974; Schwartz, 1974; Dalrymple, 1974; Cokelet, 1977; Chaplin, 1980; Reinecker and Fenton, 1981; Le Mehaute, et al., 1984; Fenton, 1988a, and 1988b). Differences between the various approaches are well summarized by Sobey (Sobey, et al., 1987), and can be generally categorized by choice of field variable (stream function versus velocity potential), form of the terms in the cosine series and behavior in deep water, inclusion of a current (none, uniform, or shear), and formulation, extensibility, treatment, and efficiency of numerical approaches for the problem. The methodology of Fenton (1988a and 1988b) is utilized here to formulate the problem and determine the Fourier series coefficients, while revised derivations for wave properties have been taken from Sobey (1988) and Klopman (1990).

GENERAL ASSUMPTIONS AND TERMINOLOGY

A representative wave profile is illustrated in Figure 2-3-1.

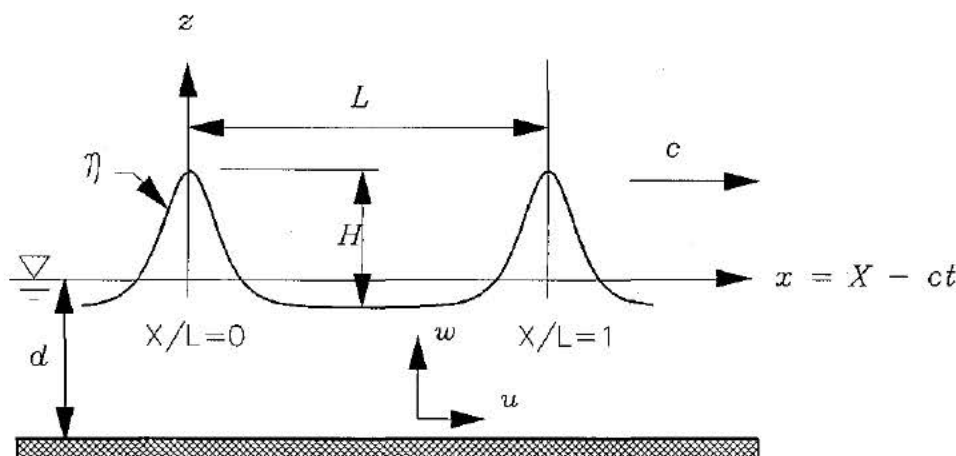


Figure 2-3-1. Wave in Steady Reference Frame (which Moves at Wave Speed c)

Assumptions applicable to the above progressive wave include:

- The wave is two-dimensional in the x - z plane.
- It propagates in a permanent form over a smooth horizontal bed of constant depth in the positive x -direction.
- There is a uniform underlying current.
- The fluid is inviscid and incompressible, having no surface tension.
- The flow is irrotational.

Terminology relevant to the following discussion includes:

(X, Z) = coordinates in Fixed (non-translating) Reference Frame

$(x, z) = (X - ct, Z)$ = coordinates in Steady Reference Frame (which moves at wave speed c)

d = still-water depth ($z = 0$)

$\eta(x)$ = water surface elevation

H = wave height

L = wavelength

T = wave period

$$k = \frac{2\pi}{\lambda} = \text{wave number}$$

$$c = \text{wave speed}$$

$$\bar{u} = \text{mean value of horizontal fluid velocity for a constant value of } z, \text{ over one wavelength}$$

$$\overline{u_1} = \text{time-mean Eulerian current (corresponding to Stokes First approximation for } c)$$

$$\overline{u_2} = \text{depth-averaged mass transport velocity (corresponding to Stokes Second approximation for } c)$$

$$\psi(x, z) = \text{stream function}$$

$$Q = \text{constant volume flow rate per unit width under the steady wave}$$

$$q = \bar{u}d - Q = \text{constant volume flow rate per unit width due to wave}$$

$$R = \text{Bernoulli constant}$$

$$r = R - gd = \text{Bernoulli constant (separated for convenience in treatment of deep water)}$$

$$(U, W) = \text{velocity components in Fixed Reference Frame}$$

$$(u, w) = (U - c, W) = \text{velocity components in Steady Reference Frame}$$

$$g = \text{acceleration of gravity}$$

$$\rho = \text{density of water}$$

GOVERNING EQUATION AND BOUNDARY CONDITIONS

The steady wave problem is a boundary value problem consisting of the two-dimensional Laplace equation as the governing field equation, boundary conditions at the free surface and bottom, and the assertion that the wave is periodic in space and time.

The wave problem has traditionally been formulated in three sets of variables: primitive variables (u, w) , velocity potential ϕ , or stream function ψ . The assumption of two-dimensional, irrotational flow of an incompressible fluid leads to the following relationships between the three variables:

$$\psi_z = \phi_x = u \qquad -\psi_x = \phi_z = w \qquad (1)$$

The formulation in stream function, and the adoption of a steady (i.e., moving at wave speed c) coordinate system (as depicted in Figure 2-3-1) simplifies the form of some of the boundary conditions for the problem. The governing equation and boundary conditions formulated in stream function for the selected coordinate system can be summarized as follows:

Governing (Laplace) Equation. The governing field equation is the two-dimensional Laplace equation. It represents the conservation of mass and momentum within the fluid field.

$$\frac{\partial^2 \psi(x, z)}{\partial x^2} + \frac{\partial^2 \psi(x, z)}{\partial z^2} = 0 \quad (2)$$

Bottom Boundary Condition (BBC). The seabed is considered impermeable. Therefore, at the sea bottom, the flow rate through the bottom boundary must be 0.

$$\psi(x, -d) = 0 \quad \text{at } z = -d \quad (3)$$

Kinematic Free Surface Boundary Condition (KFSBC). The fluid particle velocity normal to the free surface is equal to the velocity of the free surface itself. This condition implies that all water particles on the free surface remain there. Therefore, at the free surface, the flow rate through the boundary must also be 0. It also implies that the wave does not break.

$$\psi(x, \eta) = -Q \quad \text{at } z = \eta \quad (4)$$

Dynamic Free Surface Boundary Condition (DFSBC). Expressed as the Bernoulli equation, this boundary condition asserts that the pressure at the free surface is constant (equal to atmospheric pressure). This requirement follows from the preliminary assumptions that atmospheric pressure above the free surface is itself constant and that surface tension may be neglected at the air-sea interface.

$$\frac{1}{2} \left\{ \left(\frac{\partial \psi(x, \eta)}{\partial x} \right)^2 + \left(\frac{\partial \psi(x, \eta)}{\partial z} \right)^2 \right\} + g\eta(x) = R \quad \text{at } z = \eta \quad (5)$$

Periodicity. The wave is periodic in time and space.

$$\psi(x, t) = \psi(x + L, t) \quad \psi(x, t) = \psi(x, t + T) \quad (6)$$

ADDITIONAL CONSIDERATIONS RELATIVE TO THE DISPERSION RELATION

The adoption of a moving coordinate system (having the same velocity as the wave phase speed) simplifies the form of the KFSBC by eliminating a time derivative. However, this simplification yields some additional complexities which have been emphasized by Fenton (1988a, 1988b, 1990) and Sobey et al. (1987). The exact wave speed is correctly predicted by the wave theory only for the singular case of zero underlying current. It is more rational to assert that the wave theory predicts the wave phase speed relative to the underlying current, which is seldom zero in a realistic environment. A principal consequence of an underlying current is a Doppler shift of the apparent wave period (relative to a stationary observer or gage). Hence, the underlying current velocity must also be known in order to resolve the wave problem.

Some confusion results from consideration of the above concerns relative to the traditional definitions of Stokes (1847) for wave speed. Concerning the first definition, consider a given time-mean Eulerian current (\bar{u}_1) which is a time-mean horizontal fluid velocity at any point (X, Z) wholly in the fluid (within the fixed, non-moving frame of reference). This corresponds to the current recorded by a stationary meter. By considering $-\bar{u}$ to be the mean fluid velocity (i.e., at

a fixed z coordinate, but averaged over one wavelength) in the steady (moving) frame of reference, the relationship between the wave speed and the time-mean Eulerian current applied to Stokes' first definition is:

$$c = \bar{u} + \bar{u}_1 \quad (7)$$

The special case of $\bar{u}_1 = 0$ corresponds exactly to Stokes first definition of wave speed where $c = \bar{u}$.

An alternate estimate of the wave phase speed is a function of the depth-averaged mass transport velocity (Stokes' drift velocity) (\bar{u}_2). By considering Q to be the volume flow rate (per unit width) under the wave in the steady (moving) frame of reference, the depth-averaged fluid velocity is then $-Q/d$. The relationship between wave speed and the mass transport velocity is suggested by Stokes' second definition as:

$$c = \frac{Q}{d} + \bar{u}_2 \quad (8)$$

The special case of $\bar{u}_2 = 0$ corresponds to Stokes' second definition of wave speed where $c = Q/d$. It is a condition that is commonly imposed in wave flumes or any situation where mass transport is actually or assumed to be restricted. It is not, however, generally true in open water sea states.

The above two equations include the principle of an underlying current in the dispersion relation and can represent the shift in wave period due to the current. A final consideration in formulating the dispersion relationship involves the boundary condition requiring the wave to be periodic in space and time. This condition implicitly requires the wave speed to satisfy the familiar relation $c = L/T$. The dispersion relation is declared in the wave problem by selecting the definition of wave speed, and providing the appropriate value for either the mean Eulerian velocity, or the Stokes drift velocity:

Stokes' *First* Approximation
of Wave Speed

$$c = \frac{L}{T} = \frac{2\pi}{kT} = \bar{u} + \bar{u}_1$$

(specify mean Eulerian velocity \bar{u}_1)

Stokes' *Second* Approximation
of Wave Speed

$$c = \frac{L}{T} = \frac{2\pi}{kT} = \frac{Q}{d} + \bar{u}_2 \quad (9)$$

(specify Stokes' drift velocity \bar{u}_2)

SOLUTION AND METHOD

Fourier series wave theory derives its name from an approximate (but potentially very accurate) solution to the governing wave equation using a Fourier cosine series in kx , as follows:

$$\psi(x, z) = -\bar{u}(d+z) + \left(\frac{g}{k^3}\right)^{\frac{1}{2}} \sum_{j=1}^N B_j \frac{\sinh jk(d+z)}{\cosh jkd} \cos jkx \quad (10)$$

where

B_j = dimensionless Fourier coefficients

The solution is obtained by numerically computing the N Fourier coefficients to satisfy a system of simultaneous equations that consist of the two free-surface boundary conditions (evaluated at $N+1$ evenly spaced points on the free surface between a crest and following trough) as well as the dispersion relation when given the wave height, wave period, water depth, and either the mean Eulerian velocity, or the Stokes drift velocity. The set of dimensionless variables and equations as described by Fenton (1988a and 1988b) are listed in Tables 2-3-1 through 2-3-3.

Table 2-3-1 Vector of Dimensionless Problem Variables (Fenton, 1988)			
Variable	Dimensionless Form	Variable	Dimensionless Form
depth	$z_1 = kd$	free surface elevation at crest ($x = 0$)	$z_{10} = k\eta_0$
wave height	$z_2 = kH$	free surface elevation at ($x = \frac{L}{2N}$)	$z_{11} = k\eta_1$
wave period	$z_3 = T(gk)^{1/2}$	free surface elevation at ($x = \frac{L}{N}$)	$z_{12} = k\eta_2$
wave speed	$z_4 = c(k/g)^{1/2}$
mean Eulerian velocity	$z_5 = \overline{u_1}(k/g)^{1/2}$	free surface elevation at trough ($x = \frac{L}{2}$)	$z_{N+10} = k\eta_N$
Stokes' drift velocity	$z_6 = \overline{u_2}(k/g)^{1/2}$	Fourier series coefficient	$z_{N+11} = \beta_1$
mean fluid velocity	$z_7 = \overline{u}(k/g)^{1/2}$...	$z_{N+12} = \beta_2$
volume flow rate per unit width	$z_8 = q(k^3/g)^{1/2}$
Bernoulli constant	$z_9 = r(k/g)$...	$z_{2N+10} = \beta_N$

Table 2-3-1 lists the name and order of dimensionless variables for use in the system of equations. Table 2-3-2 lists the relationships being formalized and their order as a system of equations to be solved simultaneously. Table 2-3-3 identifies some special forms of the equations used for numerical stability or speed in deepwater environments. Deepwater simplifications are automatically employed when $(d/L > 3/2)$ with L initially estimated by a linear wave theory approximation.

Table 2-3-2
System of Equations

(Fenton, 1988)

Relation	Equation
H to d	$f_1(z_{1,2}) = kH - (H/d)kd = 0$
H to T	$f_2(z_{2,3}) = kH - \left(\frac{H}{gT^2}\right)(T(gk)^{1/2})^2 = 0$
$c = \frac{L}{T} = \frac{2\pi}{kT}$	$f_3(z_{3,4}) = c(k/g)^{1/2}T(gk)^{1/2} - 2\pi = 0$
$c = \bar{u} + \bar{u}_1$	$f_4(z_{4,5,7}) = \bar{u}_1(k/g)^{1/2} + \bar{u}(k/g)^{1/2} - c(k/g)^{1/2} = 0$
$c = \frac{g}{d} + \bar{u}_2$	$f_5(z_{1,4,6,7,8}) = \bar{u}_2(k/g)^{1/2} + \bar{u}(k/g)^{1/2} - c(k/g)^{1/2} - \frac{g(k^3/g)^{1/2}}{kd} = 0$
apply selected approx for c $u_c = \bar{u}_1$ or \bar{u}_2	$f_6(z_{2,5,6}) = u_c(k/g)^{1/2} - \frac{u_c}{(gH)^{1/2}}(gH)^{1/2} = 0$
$\bar{\eta}(x) = 0$	$f_7(z_{10,N+10,m+10}) = k\eta_0 + k\eta_N + 2 \sum_{m=1}^{N-1} k\eta_m = 0$
$H = \eta_0 - \eta_N$	$f_8(z_{2,10,N+10}) = k\eta_0 - k\eta_N - kH = 0$
KFSBC: solved at $m = 0 \dots N$ points on free surface	$f_{m+9}(z_{1,7,8,m+10,N+j+10}) = -q\left(\frac{k^3}{g}\right)^{1/2} - k\eta_m \bar{u}\left(\frac{k}{g}\right)^{1/2} + \sum_{j=1}^N B_j \left[\frac{\sinh j(kd + k\eta_m)}{\cosh jkd} \right] \cos \frac{j m \pi}{N} = 0$
DFSBC: solved at $m = 0 \dots N$ points on free surface	$f_{N+10+m}(z_{1,7,9,10,m+10,N+j+10}) = k\eta_m - \frac{rk}{g} + \frac{1}{2} \left(-\bar{u}\left(\frac{k}{g}\right)^{1/2} + \sum_{j=1}^N jB_j \left[\frac{\cosh j(kd + k\eta_m)}{\cosh jkd} \right] \cos \frac{j m \pi}{N} \right)^2 + \frac{1}{2} \left(\sum_{j=1}^N jB_j \left[\frac{\sinh j(kd + k\eta_m)}{\cosh jkd} \right] \sin \frac{j m \pi}{N} \right)^2 = 0$

Table 2-3-3 System of Equations (Special Variations for Deep Water) (Fenton, 1988)	
Relation	Equation
proxy	$f_1(z_1) = kd + 1 = 0$
$c = \frac{q}{d} + \overline{u_2}$	$f_5(z_{4,6,7}) = \overline{u_2}(k/g)^{1/2} + \overline{u}(k/g)^{1/2} - c(k/g)^{1/2} = 0$
KFSBC: solved at $m = 0 \dots N$ points on free surface	$f_{m+9}(z_{7,8,m+10,N+1+10}) = -q\left(\frac{k^3}{g}\right)^{1/2} - k\eta_m \overline{u}\left(\frac{k}{g}\right)^{1/2}$ $+ \sum_{j=1}^N B_j e^{jk\eta_m} \cos \frac{j m \pi}{N} = 0$
DFSBC: solved at $m = 0 \dots N$ points on free surface	$f_{N+10+m}(z_{7,9,m+10,N+1+10}) = k\eta_m - \frac{rk}{g}$ $+ \frac{1}{2} \left(-\overline{u}\left(\frac{k}{g}\right)^{1/2} + \sum_{j=1}^N j B_j e^{jk\eta_m} \cos \frac{j m \pi}{N} \right)^2$ $+ \frac{1}{2} \left(\sum_{j=1}^N j B_j e^{jk\eta_m} \sin \frac{j m \pi}{N} \right)^2 = 0$

Tables 2-3-1 and 2-3-2 describe a system of $2N + 10$ equations:

$$\mathbf{f}(\mathbf{z}) = \{f_i(\mathbf{z}), i = 1 \dots 2N + 10\} = \mathbf{0} \quad (11)$$

The system of equations is solved iteratively using Newton's method:

$$\left[\frac{\partial f_i}{\partial z_j} \right]^{(n)} \cdot (\mathbf{z}^{(n+1)} - \mathbf{z}^{(n)}) = -\mathbf{f}(\mathbf{z}^{(n)}) \quad (12)$$

where

n = Iteration index

$\mathbf{z}^{(n)}$ = Values of $(z_i, i = 1 \dots 2N + 10)$ at iteration n

$\mathbf{z}^{(n+1)}$ = Values of $(z_i, i = 1 \dots 2N + 10)$ at iteration $n + 1$

$\mathbf{f}(\mathbf{z}^{(n)})$ = Values of $\{f_i(\mathbf{z}), i = 1 \dots 2N + 10\}$ evaluated at iteration n

$\left[\frac{\partial f_i}{\partial z_j} \right]^{(n)}$ = Jacobian matrix evaluated at iteration n as:

$$\frac{\partial f_i}{\partial z_j} \approx \frac{f_i(z_1, \dots, z_j + \Delta_j, \dots, z_{2N+10}) - f_i(z_1, \dots, z_j, \dots, z_{2N+10})}{\Delta_j} \quad (13)$$

Note: The Jacobian matrix may be evaluated analytically or numerically. As indicated by Equation (13), in this implementation the Jacobian matrix is evaluated numerically. Each of $2N+10$ equations were evaluated a total of $2N+10$ times with the value of Δ_j as below:

$$\Delta_j = z_j / 100 \text{ for } z_j > 10^{-4}$$

$$\Delta_j = 10^{-5} \text{ for } z_j \leq 10^{-4}$$

Iterations continue until the solution converges to the following criteria:

$$\sum_{j=1}^{2N+10} |z_j^{(n+1)} - z_j^{(n)}| < 10^{-6} \quad (14)$$

within ($n_{\max} \leq 9$) iterations. Double precision LINPACK (Dongarra et al; 1979) routines are employed to solve the matrix Equation (12) at each iteration. As currently implemented in ACES, the square matrix is dimensioned to a maximum rank of 60, and the solved matrix rank is $2N+10$, which allows a maximum of ($N_{\max} = 25$) terms in the Fourier series approximation.

Solution Aids and Insights

Several researchers (Dalrymple and Solana, 1986), (Fenton, 1988) and (Sobey, 1988) have noted that Fourier theory formulations can potentially admit the odd harmonics ($L, L/3, L/5, \dots, L/N$) singularly, or in combinations, particularly in shallow water. Sobey (1988) notes that two features of the formulation (symmetry about crest, and periodicity at lateral boundary conditions) permit the manifestation of these apparent multicrested solutions. Several strategies for achieving the fundamental solution (rather than higher odd harmonics) have been discussed in the cited literature, and the method employed by Fenton (1988) is implemented in this version. A "ramping" mechanism is provided to solve the problem by initially (internally) solving for a lower wave height, and approaching the specified wave height in a specified (as input) number of evenly spaced steps. The approach eliminates the problem at the expense of additional iterations to achieve the final fundamental solution for the specified wave height.

Maximum Wave Checks

Most wave theories (both analytic and numerically based) are capable of yielding valid mathematical solutions to physically implausible data; particularly with regards to wave steepness and depth-related breaking. In part, this is a consequence of some of the assumptions imposed upon the boundary problem formulation. As an aid in restricting solutions to an observed physically valid domain, empirical data and formulations are often employed to estimate the validity of the given wave. The following expression (Fenton, 1990) is used for estimating the greatest wave as a function of both wavelength and depth:

$$H_{\max} = d \left\{ \frac{.141063 \frac{L}{d} + .0095721 \left(\frac{L}{d} \right)^2 + .0077829 \left(\frac{L}{d} \right)^3}{1 + .078834 \frac{L}{d} + .0317567 \left(\frac{L}{d} \right)^2 + .0093407 \left(\frac{L}{d} \right)^3} \right\} \quad (15)$$

In the limits, the leading term in the numerator of the above expression provides the familiar steepness limit for short waves ($H_{\max}/L \rightarrow .141063$), and as ($\lim L/d \rightarrow \infty$) the ratio of coefficients of the cubic terms provides the familiar ratio ($.0077829(L/d)^2/.0093407(L/d)^3 \rightarrow .83322$). This simple empirical test is applied using the given water depth, and solved wavelength as a rough filter for implausible wave specifications.

DERIVED RESULTS

Traditional engineering quantities of interest about the wave are derived from the solution of the governing equation. Since the solution is expressed as a Fourier series, many of the derived quantities will also be functions of the series. Formulas for kinematics, integral properties, and other relevant items are included in the following tabulations. All quantities are relative to the stationary (non-moving) frame of reference.

Kinematics and Other Derived Variables

Velocities:

$$\text{Horizontal: } u(x, z) = \frac{\partial \psi}{\partial z} = -\bar{u} + \left(\frac{g}{k}\right)^{\frac{1}{2}} \sum_{j=1}^N j B_j \frac{\cosh jk(d+z)}{\cosh jkd} \cos jkx \quad (16)$$

$$\text{Vertical: } w(x, z) = -\frac{\partial \psi}{\partial x} = \left(\frac{g}{k}\right)^{\frac{1}{2}} \sum_{j=1}^N j B_j \frac{\sinh jk(d+z)}{\cosh jkd} \sin jkx \quad (17)$$

Accelerations:

$$\text{Horizontal: } a_x(x, y) = \frac{du}{dt} = u \frac{\partial u}{\partial x} + w \frac{\partial u}{\partial z} \quad (18)$$

$$\text{Vertical: } a_z(x, y) = \frac{dw}{dt} = u \frac{\partial w}{\partial x} + w \frac{\partial w}{\partial z} = u \frac{\partial u}{\partial z} - w \frac{\partial u}{\partial x} \quad (19)$$

where

$$\frac{\partial u}{\partial x} = -(gk)^{\frac{1}{2}} \sum_{j=1}^N j^2 B_j \frac{\cosh jk(d+z)}{\cosh jkd} \sin jkx$$

$$\frac{\partial u}{\partial z} = (gk)^{\frac{1}{2}} \sum_{j=1}^N j^2 B_j \frac{\sinh jk(d+z)}{\cosh jkd} \cos jkx$$

$$\text{Pressure: } p(x, y) = \rho r - \rho g z - \frac{1}{2} \rho (u^2 + w^2) \quad (20)$$

$$\text{Water Surface: } \eta(x) = \sum_{j=1}^{N-1} f_j \cos jkx + \frac{1}{2} f_N \cos Nkx \quad (21)$$

where

$$f_j = \frac{2}{N} \left\{ \frac{1}{2} \eta_0 + \sum_{m=1}^{N-1} \eta_m \cos \frac{j m \pi}{N} + \frac{1}{2} \eta_N \cos j\pi \right\}$$

Notes:

$$\begin{aligned} X &= x + ct, \quad Z = z \\ U(X, Z, t) &= u(x, z) + c \\ W(X, Z, t) &= w(x, z) \\ P(X, Z, t) &= p(x, z) \end{aligned}$$

$$r = R - gd$$

Integral Properties

Potential Energy:
(per unit horizontal area)

$$E_p = \overline{\int_0^\eta (\rho g Z) dZ} \quad (22)$$

$$E_p = \frac{1}{2} \rho g \overline{\eta^2}$$

Momentum:
(per unit horizontal area)
(Impulse)

$$I = \overline{\int_{-d}^\eta (\rho U) dZ} \quad (23)$$

$$I = \rho (cd - Q)$$

Kinetic Energy:
(per unit horizontal area)

$$E_k = \overline{\int_{-d}^\eta \left(\frac{1}{2} \rho (U^2 + W^2) \right) dZ} \quad (24)$$

$$E_k = \frac{1}{2} (cI - \rho \overline{u_1 Q})$$

Mean Square of Bed Velocity:

$$\overline{U_b^2} = \frac{1}{L} \int_0^L U^2(X, -d, t) dX \quad (25)$$

$$\overline{U_b^2} = 2(R - gd) - c^2 + 2\overline{u_1 c}$$

Energy Flux:
(per unit length of crest)
(Wave Power)

$$F = \overline{\int_{-d}^\eta \left(P + \frac{1}{2} \rho (U^2 + W^2) + \rho g Z \right) U dZ} \quad (26)$$

$$F = (3E_k - 2E_p - 2\overline{u_1 I})c + \frac{1}{2} \overline{U_b^2} (I + \rho cd)$$

Radiation Stress:

$$S_{xx} = \overline{\int_{-d}^\eta (P + \rho U^2) dZ} - \frac{1}{2} \rho g d^2 \quad (27)$$

$$S_{xx} = 4E_k - 3E_p + \rho d \overline{U_b^2} - 2\overline{u_1 I}$$

Notes:

$$\begin{aligned} X &= x + ct, \quad Z = z \\ U(X, Z, t) &= u(x, z) + c \\ W(X, Z, t) &= w(x, z) \end{aligned}$$

$$\begin{aligned} P(X, Z, t) &= p(x, z) \\ \int () &\Rightarrow \text{averaged over one wavelength} \end{aligned}$$

REFERENCES AND BIBLIOGRAPHY

- Chaplin, J. R., 1980. "Developments of Stream-Function Wave Theory," *Coastal Engineering*, Vol. 3, pp. 179-205.
- Chappelear, J. E., 1961. "Direct Numerical Calculation of Wave Properties," *Journal of Geophysical Research*, Vol. 66, No. 2, pp. 501-508.
- Cokelet, E. D., 1977. "Steep Gravity Waves in Water of Arbitrary Uniform Depth," *Proceedings of the Royal Society of London, Series A*, Vol. 286, pp. 183-230.
- Dalrymple, R. A., 1974. "A Finite Amplitude Wave on a Linear Shear Current," *Journal of Geophysical Research*, Vol. 79, No. 30, pp. 4498-4504.
- Dalrymple, R. A., and Solana, P., 1986. "Nonuniqueness in Stream Function Wave Theory," *Journal of Waterway, Port, Coastal and Ocean Division*, American Society of Civil Engineers, Vol. 112, No. 2, pp. 333-337.
- Dean, R. G., 1965. "Stream Function Representation of Nonlinear Ocean Waves," *Journal of Geophysical Research*, Vol. 70, No. 18, pp. 4561-4572.
- Dean, R. G., 1974. "Evaluation and Development of Water Wave Theories for Engineering Application," Special Report No. 1, Coastal Engineering Research Center, 2 Vols.
- Dongarra, J. J., Moler, C. B., Bunch, J. R., and Stewart, G. W., 1979. LINPACK User's Guide, S. I. A. M., Philadelphia.
- Fenton, J. D., 1988a. "The Numerical Solution of Steady Water Wave Problems," *Computers and Geoscience*, Vol. 14, No. 3, pp. 357-368.
- Fenton, J. D., 1988b. Discussion of "Nonuniqueness in Stream Function Wave Theory," by R. A. Dalrymple and P. Solana, *Journal of Waterway, Port, Coastal and Ocean Division*, American Society of Civil Engineers, Vol. 114, No. 1, pp. 110-112.
- Fenton, J. D., 1990. "Nonlinear Wave Theories," Ocean Engineering Science, The Sea, Vol. 9, Part A, Edited by Le Mehaute, B., and Hanes, D., John Wiley and Sons, New York, pp. 3-25.
- Klopman, G., 1990. "A Note on Integral Properties of Periodic Gravity Waves in the Case of a Non-zero Mean Eulerian Velocity," *Journal of Fluid Mechanics*, Vol. 211, pp. 609-615.
- Le Mehaute, B., Lu, C. C., and Ulmer, E. W., 1984. "Parametized Solution to Nonlinear Wave Problem," *Journal of Waterway, Port, Coastal and Ocean Division*, American Society of Civil Engineers, Vol. 110, No. 3, pp. 309-320.
- Reinecker, M. M., and Fenton, J. D., 1981. "A Fourier Approximation Method for Steady Water Waves," *Journal of Fluid Mechanics*, Vol. 104, pp. 119-137.
- Schwartz, L. W., 1974. "Computer Extension and Analytical Continuation of Stokes' Expansion for Gravity Waves," *Journal of Fluid Mechanics*, Vol. 62, Part 3, pp. 553-578.
- Sobey, R. J., 1988. Discussion of "Nonuniqueness in Stream Function Wave Theory," by R. A. Dalrymple and P. Solana, *Journal of Waterway, Port, Coastal and Ocean Division*, American Society of Civil Engineers, Vol. 114, No. 1, pp. 112-114.
- Sobey, R. J., Goodwin, P., Thieke, R. J., Westberg, R. J. Jr., 1987. "Application of Stokes, Cnoidal, and Fourier Wave Theories," *Journal of Waterway, Port, Coastal and Ocean Division*, American Society of Civil Engineers, Vol. 113, No. 6, pp. 565-587.
- Stokes, G. G., 1847. "On the Theory of Oscillatory Waves," *Transactions of the Cambridge Philosophical Society*, Vol. 8, pp. 441-455.

LINEAR THEORY WITH SNELL'S LAW

TABLE OF CONTENTS

Description	3-1-1
Introduction	3-1-1
General Assumptions and Limitations	3-1-1
Shoaling and Refraction Coefficients	3-1-2
References and Bibliography	3-1-3

LINEAR WAVE THEORY WITH SNELL'S LAW

DESCRIPTION

This application provides a simple estimate for the transformation of monochromatic waves. It considers two common processes of wave transformation: refraction (using Snell's law) and shoaling using wave properties predicted by linear wave theory (Airy, 1845). Given wave properties and a crest angle at a known depth, this application predicts the values in deep water and at a subject location specified by a new water depth. An important assumption is that all depth contours are assumed to be straight and parallel. In addition to the wave transformation results, this application reports common bulk wave properties from linear wave theory. More detailed discussion of these methods can be found in the SPM (1984), Dean and Dalrymple (1984), Sarpkaya and Isaacson (1981), as well the section of this reference manual entitled **Linear Wave Theory**.

INTRODUCTION

In deep water, waves often referred to as ocean swell have a profile that is very nearly sinusoidal, with long, low crests. As the waves propagate into shallow water, they undergo a transformation, starting where the waves are affected by the seabed at a depth approximately one-half of the deepwater wavelength. The wave velocity, height, and length alter. This process is called wave shoaling.

When waves travel at an angle to underwater contours, the portion of the wave in deeper water is moving faster than the part in shallower water. This variation causes the wave crest to bend toward alignment with the contours. This process is called wave refraction.

GENERAL ASSUMPTIONS AND LIMITATIONS

Important assumptions and limitations made in this shoaling and refraction discussion are:

- Wave energy between wave orthogonals remains constant. A wave orthogonal is a locus of points that define the minimum time of travel for wave propagation between two points (Le Mehaute, 1976). The wave orthogonals (Figure 3-1-1) are drawn perpendicular to the wave crest.
- Direction of wave advance is perpendicular to the wave crest.
- Speed of a wave of a given period at a particular location depends only on the depth at that location.
- Changes in bottom topography are gradual.
- Waves are based on small-amplitude wave theory.
- Effects of current, winds, and reflections from beaches and underwater topographic variations are ignored.
- Offshore contours are straight and parallel to the shoreline.

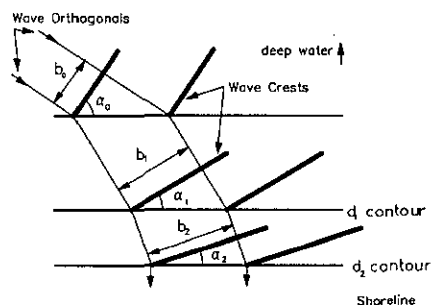


Figure 3-1-1. Snell's Law and Wave Refraction

SHOALING AND REFRACTION COEFFICIENTS

It has been observed that the decrease in wave celerity with decreasing water depth is analogous to the decrease in the speed of light with an increase in the refractive index of the transmitting medium. Using this analogy, O'Brien (1942) suggested the use of Snell's law of geometrical optics for addressing the problem of water-wave refraction by changes in depth.

Using deep water as a reference, the general form of Snell's law is:

$$\frac{c}{c_0} = \frac{\sin \alpha}{\sin \alpha_0} \quad (1)$$

where

c, c_0 = wave velocity at the depth contour

α, α_0 = angle between a wave crest and the depth contour

As stated earlier, the rate of energy transfer between wave orthogonals is assumed to remain constant and is given by average energy flux:

$$\bar{P}_0 = \bar{P} \quad (2)$$

where

Deep Water	Shallow Water	Item
$\bar{P}_0 = \bar{E}_0 C_{g0}$	$\bar{P} = \bar{E} C_g$	Energy flux
b_0	b	Distance between orthogonals
$\bar{E}_0 = \frac{\rho g H_0^2}{8}$	$\bar{E} = \frac{\rho g H^2}{8}$	Average energy density
C_{g0}	C_g	Group velocity

Rearranging terms and solving for H/H_o yields:

$$\frac{H}{H_o} = \sqrt{\frac{C_{g0}}{C_g}} \sqrt{\left(\frac{b_o}{b}\right)} \quad (3)$$

The term $\sqrt{C_{g0}/C_g}$ is known as the *shoaling coefficient* K_s , and the term $\sqrt{b_o/b}$ is known as the *refraction coefficient* K_R .

The assumption of straight and parallel depth contours leads to a simple geometrical relationship between b and α and a resulting expression for K_R :

$$K_R = \sqrt{\frac{b_o}{b}} = \sqrt{\frac{\cos \alpha_o}{\cos \alpha}} \quad (4)$$

A final expression for this simplified wave transformation approach is then:

$$\frac{H}{H_o} = K_R K_s \quad (5)$$

REFERENCES AND BIBLIOGRAPHY

- Airy, G. B. 1845. "Tides and Waves," *Encyclopaedia Metropolitana*, Vol. 192, pp. 241-396.
- Dean, R. G., and Dalrymple, R. A. 1984. *Water Wave Mechanics for Engineers and Scientists*, Prentice-Hall, Englewood Cliffs, NJ, pp. 41-86, 104-105.
- Hunt, J. N. 1979. "Direct Solution of Dispersion Equation," *Journal of Waterway, Port, Coastal and Ocean Division*, American Society of Civil Engineers, Vol. 107, No. WW4, pp. 457-459.
- Le Mehaute, B. 1976. *An Introduction to Hydrodynamics and Water Waves*, Springer-Verlag, New York, pp. 228-232.
- O'Brien, M. P. 1942. "A Summary of the Theory of Oscillatory Waves," Technical Report No. 2, US Army Corps of Engineers, Beach Erosion Board, Washington, DC.
- Sarpkaya, T., and Isaacson, M. 1981. *Mechanics of Wave Forces on Offshore Structures*, Van Nostrand Reinhold, New York, pp. 150-168, 237-242.
- Shore Protection Manual*. 1984. 4th ed., 2 Vols., US Army Engineer Waterways Experiment Station, Coastal Engineering Research Center, US Government Printing Office, Washington, DC, Chapter 2, pp. 6-33, 60-66.
- Singamsetti, S. R., and Wind, H. G. 1980. "Characteristics of Shoaling and Breaking Periodic Waves Normally Incident to Plane Beaches of Constant Slope," *Breaking Waves Publication No. M1371*, Waterstaat, The Netherlands, pp. 23-27.
- Weggel, J. R. 1972. "Maximum Breaker Height," *Journal of Waterways, Harbors and Coastal Engineering Division*, American Society of Civil Engineers, Vol. 98, No. WW4, pp. 529-548.

IRREGULAR WAVE TRANSFORMATION (GODA'S METHOD)

TABLE OF CONTENTS

Description	3-2-1
General Assumptions and Limitations	3-2-1
Theory	3-2-2
References and Bibliography	3-2-6

IRREGULAR WAVE TRANSFORMATION (GODA'S METHOD)

DESCRIPTION

This application yields cumulative probability distributions of wave heights as a field of irregular waves propagate from deep water through the surf zone. The application is based on two random-wave theories by Yoshimi Goda (1975 and 1984). The 1975 paper concerns transformation of random waves shoaling over a plane bottom with straight parallel contours. This analysis treated breaking and broken waves and resulted in cumulative probability distributions for wave heights given a water depth. It did not include refraction, however. The 1984 article details a refraction procedure for random waves propagating over a plane bottom with straight parallel contours assuming a particular incident spectrum. This ACES application combines the two approaches by treating directional random waves propagating over a plane bottom with straight parallel contours. This application also uses the theory of Shuto (1974) for the shoaling calculation. The theories assume a Rayleigh distribution of wave heights in the nearshore zone and a Bretschneider-Mitsuyasu incident directional spectrum. The processes modeled include:

- ° Wave refraction
- ° Wave shoaling
- ° Wave breaking
- ° Wave setup
- ° Surf beat

GENERAL ASSUMPTIONS AND LIMITATIONS

General assumptions and limitations in this irregular wave transformation discussion are:

- ° The incident wave spectrum is of the Bretschneider-Mitsuyasu type.
- ° The incident wave height distribution is of the Rayleigh type.
- ° Waves propagate over a smooth, absorbent beach (no reflection) with straight, parallel contours.
- ° Irregular wave shoaling may be approximated by shoaling of monochromatic waves.
- ° The probability distribution of broken wave heights is proportional to that of unbroken wave heights.
- ° An empirical relation determines the surf beat level.

These assumptions dictate the following theoretical limitations:

- ° The Bretschneider-Mitsuyasu wave spectrum is a narrow-banded spectrum. Thus, this application should not be used where broad-banded spectra or multiple-peaked spectra are present.

- ° This application should not be used in areas with complex bathymetry; contours should be roughly parallel to shore.

In addition, the following limitations were implemented:

- ° Peak period must not exceed 16 sec.
- ° The smallest depth of interest that can be represented is 10 ft or 3.04 m.
- ° Principal direction of incidence must not exceed 75 deg from shore normal.

THEORY

The development of the theory begins by considering the incident Bretschneider-Mitsuyasu spectrum:

$$S(f) = 0.257 (H_{1/3})^2 T_{1/3} (T_{1/3} f)^{-5} e^{[-1.03(T_{1/3} f)^{-4}]} \quad (1)$$

where

$S(f)$ = spectral density ($m^2 \text{ sec}$)

$H_{1/3}$ = significant wave height (m)

$T_{1/3}$ = significant wave period (sec)

f = wave frequency (rad/sec)

This incident wave spectrum is assumed to propagate over straight parallel bathymetric contours at a principal direction to shore normal. The spectrum is also assumed to have a directional spread of 135 deg, 67.5 deg to either side of the principal direction. The spreading function $G(f, \theta)$ used in this application is that of Mitsuyasu (1975):

$$G(f, \theta) = G_0 \cos^{2s} \left(\frac{\theta}{2} \right) \quad (2)$$

where

θ = angular deviation from principal direction

$$G_0 = \frac{2^{2s-1}}{\pi} \frac{\Gamma^2(s+1)}{\Gamma(2s+1)} \quad (3)$$

s = parameter representing directional energy concentration around a peak

s_{\max} = peak value of s

= 10 for wind waves

= 25 for steep swell

= 75 for flat swell

Γ = Gamma function

The effective refraction coefficient for the spectrum is defined as the *average* refraction coefficient for the entire spectrum. The *directional* Bretschneider-Mitsuyasu spectrum is defined as (Goda, 1984):

$$S(f, \theta) = S(f) G(f, \theta) \quad (4)$$

From this an expression for the effective refraction coefficient $(K_r)_{eff}$ is given as:

$$(K_r)_{eff} = \left[\frac{1}{m} \int_0^\infty \int_{\theta_{min}}^{\theta_{max}} S(f, \theta) K_s^2(f) K_r^2(f, \theta) d\theta df \right]^{1/2} \quad (5)$$

where

$$m = \int_0^\infty \int_{\theta_{min}}^{\theta_{max}} S(f, \theta) K_s^2(f) d\theta df \quad (6)$$

$K_s(f)$ = individual shoaling coefficient

$K_r(f, \theta)$ = individual refraction coefficient

As the incident wave spectrum propagates into shallow water, individual waves within the spectrum refract, shoal, and break at rates dependent upon their individual heights, periods, and directions. Since these processes would occur at different rates (due to the irregularity of the wave field), any wave height prediction model would also have to be irregular. One way to describe the wave field during transformation and still retain irregularity is by using a probability distribution of wave heights. In this application, Goda's irregular wave height distribution model (1975) is used.

In the absence of wave breaking and assuming a Rayleigh distribution of wave heights, a probability density function of wave height normalized by H_o is given by:

$$P_o(x) = 2a^2 x e^{-\left(\frac{a^2}{x^2}\right)} \quad (7)$$

where

$P_o(x)$ = probability density function

$x = \frac{H}{H_o}$ = normalized wave height

$$\alpha = \frac{1.416}{K_s}$$

K_s = shoaling coefficient

The Rayleigh distribution does not have an upper limit on the normalized wave height; it approaches zero asymptotically. However, normalized wave height in nature is limited by wave breaking. This is the primary difference between Goda's model and the ideal Rayleigh model.

If wave breaking is assumed to occur between x_2 and x_1 , the unbroken wave heights are restricted in Equation 7 by the following equations:

$$P_r(x) = \begin{cases} P_0(x) & x \leq x_2 \\ P_0(x) - \left(\frac{x - x_2}{x_1 - x_2} \right) P_0(x_1) & x_2 < x \leq x_1 \\ 0 & x_1 \leq x \end{cases} \quad (8)$$

It is assumed that broken waves carry a small amount of energy. This assumption is accounted for by redistributing the energy along the top of the distribution. This redistribution leads to Goda's form of the probability density function for irregular waves:

$$P(x) = \alpha P_r(x) \quad (9)$$

where

$$\frac{1}{\alpha} = \int_0^{x_1} P_r(x) dx = 1 - [1 + \alpha^2 x_1 (x_1 - x_2)] e^{-\alpha^2 x_1^2} \quad (10)$$

NOTE: $P_r(x)$ is restricted by Equation 8 and α is defined in Equation 7.

At this point, essentially two different theories are represented in the method: Goda's refraction algorithm (Equations 1-6) and Goda's irregular wave height distribution model (Equations 7-10). The wave parameter in common with the two theories is the wave height, more specifically, the breaking wave height. Goda (1975) gave the following expression for normalized breaking wave height based on wave shoaling only:

$$X_b = \frac{H_b}{H_0} = 0.17 \frac{L_0}{H_0'} \left\{ 1 - e^{\left[\frac{-1.5\pi h}{H_0'} \frac{H_0'}{L_0} \left(1 + 1.5 \tan^{\frac{4}{3}} \theta \right) \right]} \right\} \quad (11)$$

where

H_b = breaking wave height

H'_0 = equivalent deepwater significant wave height

L_0 = deepwater wavelength

h = water depth of interest

n = bottom slope

By multiplying Equation 11 by $(K_r)_{eff}$, Goda's irregular wave distribution model is extended to include refraction effects. Shoaling, surf beat, and wave setup are also included in the application and are used to determine water depth and wave height for input into Equation 11. The equations for surf beat, wave setup, and wave shoaling follow:

Surf beat

$$\xi_{rms} = \frac{0.01 H'_0}{\sqrt{\frac{H'_0}{L_0} \left(1 + \frac{h}{H'_0} \right)}} \quad (12)$$

Wave setup

$$\frac{d\bar{\eta}}{dx} = \frac{-1}{(\bar{\eta} + h)} \frac{d}{dx} \left[\frac{1}{8} H_{rms}^2 \left(\frac{1}{2} + \frac{2kh}{\sinh 2kh} \right) \right] \quad (13)$$

where

$\frac{d\bar{\eta}}{dx}$ = set-up gradient

x = offshore-onshore coordinate

$\bar{\eta}$ = wave setup

k = wave number

Wave shoaling (Shuto, 1974)

$$\begin{aligned}
 0 < \frac{gH(T_{1/3})^2}{h^2} &\leq 30 : \text{use linear wave theory} \\
 30 < \frac{gH(T_{1/3})^2}{h^2} &\leq 50 : Hh^{\frac{2}{3}} = \text{constant} \\
 50 < \frac{gH(T_{1/3})^2}{h^2} < \infty : Hh^{\frac{5}{2}} \left(\sqrt{\frac{gH(T_{1/3})^2}{h^2}} - 2\sqrt{3} \right) &= \text{constant}
 \end{aligned} \tag{14}$$

where

g = gravitational acceleration

REFERENCES AND BIBLIOGRAPHY

- Goda, Y. 1975. "Irregular Wave Deformation in the Surf Zone," *Coastal Engineering in Japan*, Vol. 18, pp. 13-26.
- Goda, Y. 1984. *Random Seas and Design of Maritime Structures*, University of Tokyo Press, Tokyo, Japan, pp. 41-46.
- Mitsuyasu, H. 1975. "Observation of the Directional Spectrum of Ocean Waves Using a Cloverleaf Buoy," *Journal of Physical Oceanography*, Vol. 5, No. 4, pp. 750-760.
- Shuto, N. 1974. "Nonlinear Long Waves in a Channel of Variable Section," *Coastal Engineering in Japan*, Vol. 17, pp. 1-12.

COMBINED DIFFRACTION AND REFLECTION BY A VERTICAL WEDGE

TABLE OF CONTENTS

Description	3-3-1
Introduction	3-3-1
General Assumptions and Limitations	3-3-1
Theoretical Background	3-3-2
References	3-3-5

COMBINED DIFFRACTION AND REFLECTION BY A VERTICAL WEDGE

DESCRIPTION

This application estimates wave height modification due to combined diffraction and reflection near jettied harbor entrances, quay walls, and other such structures. Jetties and breakwaters are approximated as a single straight, semi-infinite breakwater by setting the wedge angle to zero. Corners of docks and quay walls may be represented by setting the wedge angle equal to 90 deg. Additionally, such natural diffracting and reflecting obstacles as rocky headlands can be approximated by setting a particular value for the wedge angle.

INTRODUCTION

In coastal and ocean engineering practice, it is often important to be able to determine wave height near such coastal structures as jetties, breakwaters, platforms, and docks. Such information aids engineers in evaluating coastal structure designs, especially in the areas of energy transmission, sediment transport, and structural strength. Wave heights in the vicinity of a structure have traditionally been presented in the form of dimensionless wave diffraction and reflection coefficients defined as the ratio of diffracted/reflected wave height to incident wave height. Early studies presented a dimensionless graphical solution based on theory by Penny and Price (1952) for diffraction by a semi-infinite breakwater (Wiegel, 1962). Subsequently these diagrams have been incorporated into every edition of the SPM (1984). They remain useful tools for preliminary engineering design.

Limitations of the traditional diagrams include monochromatic and unidirectional wave assumption, constant water depth assumption, no reflection, and simple structure shape with vertical walls. Recently Chen (1987) presented an analytical solution for wave height modification in the vicinity of a structure. The solution is more general than the traditional approach in that it includes reflection as well as diffraction and it allows a wedge-shaped structure with vertical walls. Other limitations of the traditional approach still apply. Chen's (1987) solution was implemented in a computer code, PCDFRAC, by Kaihatu and Chen (1988). Output consists of a wave height modification coefficient (ratio of combined diffracted and reflected height to incident height) and a wave phase for any selected point in the vicinity of the structure. The code PCDFRAC has been modified to reside in ACES.

GENERAL ASSUMPTIONS AND LIMITATIONS

Assumptions inherent in the approach include linear, monochromatic, unidirectional waves, and constant water depth. The structure is assumed to be straight and semi-infinite in length with vertical walls. The walls are treated as fully reflecting.

Modified wave heights in areas strongly affected by reflection, such as the area immediately in front of the wedge, are variable in space because of interference between the incident and reflected waves. Such variability would not be expected in natural wave conditions.

Solutions are not available beyond about 10 wavelengths from the wedge tip. The approach is based on an analytical solution which includes summation of an infinite number of terms. The summation is computed with as many terms as needed to satisfy a convergence criterion. There is a limit on the maximum number of terms allowed. More terms are required for convergence as distance from the wedge tip increases. The limit is usually reached at distances of 10 to 15 wavelengths.

THEORETICAL BACKGROUND

The general boundary value problem of linear wave reflection and diffraction by a vertical wedge of arbitrary angle has been well formulated and presented by Stoker (1957) among many other investigators. The technique to obtain an analytical solution for the problem is also given by Stoker (1957). However, analytical solutions were available only for the special case of wave diffraction by a thin semi-infinite breakwater, that is, a wedge with angle equal to zero. The more general solution by Chen (1987) is the basis for the model PCDFRAC.

A cylindrical coordinate system (r, θ, z) is adopted, where $z = 0$ represents the undisturbed free surface and the positive z -axis is positioned vertically upward. The tip of the wedge is chosen to be the origin of the coordinate system, and the two rigid walls of the wedge are at $\theta = 0$ and $\theta = \theta_0$, respectively (Figure 3-3-1). Cartesian coordinates (x, y, z) , also shown in Figure 3-3-1, are used for specifying input to the routine. The wedge angle is defined as $2\pi - \theta_0$, while the water domain is defined as $0 \leq \theta \leq \theta_0$ and $0 \geq z \geq -h$.

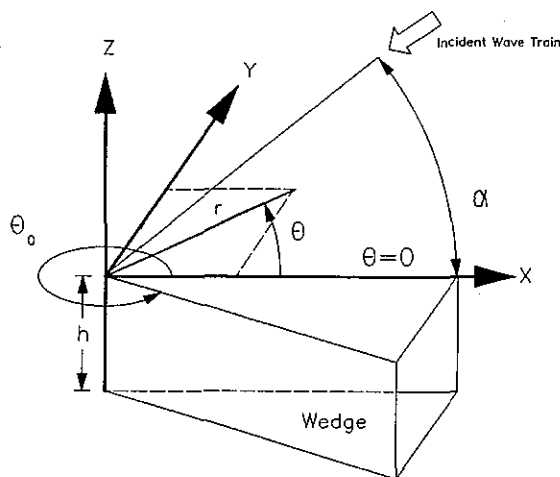


Figure 3-3-1. A Vertical Wedge of Arbitrary Angle

For the problem at hand, the velocity field for wave motion in an ideal fluid may be represented by the velocity potential $\Phi(r, \theta, z, t)$. This may be expressed as follows:

$$\Phi(r, \theta, z, t) = A_0 \frac{\cosh k(z+h)}{\cosh(kh)} \phi(r, \theta) e^{i\omega t} \quad (1)$$

where:

$\phi(r, \theta)$ = velocity potential function in the horizontal plane

t = time variable

$$A_0 = \frac{-iga_0}{\omega}$$

$$i = \sqrt{-1}$$

g = gravitational acceleration

a_0 = incident wave amplitude

ω = radian frequency

k = wave number

The wave number k must be real and satisfy the following linear dispersion equation:

$$\omega^2 = gk \tanh(kh) \quad (2)$$

Several properties of wave mechanics are dependent on the velocity potential component $\phi(r, \theta)$. For example, the free surface elevation η may be expressed in terms of $\phi(r, \theta)$ as follows:

$$\eta = a_0 \phi(r, \theta) e^{i\omega t} \quad (3)$$

The flow velocity u may be expressed in polar coordinates as follows:

$$u_r = \frac{\partial \phi}{\partial r} = A_0 \frac{\cosh k(z+h)}{\cosh(kh)} \frac{\partial \phi}{\partial r} e^{i\omega t} \quad (4)$$

$$u_\theta = \frac{1}{r} \frac{\partial \phi}{\partial \theta} = A_0 \frac{\cosh k(z+h)}{\cosh(kh)} \frac{1}{r} \frac{\partial \phi}{\partial \theta} e^{i\omega t} \quad (5)$$

where the subscripts, r and θ , refer to the r - and θ - directions. The absolute values of u_r and u_θ are the maximum flow velocities for each component direction, while the phases of u_r and u_θ contain the wave phase information. It is clear the solution to Equation 1 and Equations 3-5 lies in finding $\phi(r, \theta)$.

For an incident plane wave train coming from the α direction (Figure 3-3-1), the free surface elevation of the incident wave may be described by:

$$\eta_i = a_0 e^{ikr_i \cos(\alpha + \omega t)} \quad (6)$$

where r_i defines a point on the incident wave.

The analytical solution for a wave field by a vertical wedge of arbitrary wedge angle, based on the linearized wave theory, may be written as follows (Chen, 1987):

$$\phi(r, \theta) = \frac{2}{v} \left[J_0(kr) + 2 \sum_{n=1}^{\infty} e^{\frac{in\pi}{2v}} J_{\frac{n}{v}}(kr) \cos \frac{n\alpha}{v} \cos \frac{n\theta}{v} \right] \quad (7)$$

where:

$$v = \frac{\theta_0}{\pi} \quad (8)$$

J_0 = zero order Bessel function of the first kind

$J_{n/v}$ = n/v order Bessel function of the first kind

The semi-infinite breakwater is a special case of the diffraction/reflection problem, where the wedge angle is equal to zero ($\theta_0 = 2\pi$) and $v = 2$. The solution of Equation 1 for this case is:

$$\phi(r, \theta) = J_0(kr) + 2 \sum_{n=1}^{\infty} e^{\frac{in\pi}{4}} J_{\frac{n}{2}}(kr) \cos \frac{n\alpha}{2} \cos \frac{n\theta}{2} \quad (9)$$

NOTE: Equations 7 and 9 show a summation of an infinite number of terms. This has been accommodated in the program by carrying the summation out to a term followed by eight successive terms in which the absolute value of the Bessel function is 10^{-8} or less. If the value of the solution is of the order one, this corresponds to a truncation error of 10^{-8} or less.

The velocity potential function $\phi(r, \theta)$ in Equations 7 and 9 is a complex function and may be expressed as:

$$\phi = |\phi| e^{i\beta} \quad (10)$$

where:

$$|\phi|^2 = [Im(\phi)]^2 + [Re(\phi)]^2 \quad (\text{amplitude of } \phi) \quad (11)$$

$Im \phi$ = imaginary part of $\phi(r, \theta)$

$Re \phi$ = real part of $\phi(r, \theta)$

$$\beta = \tan^{-1} \left[\frac{Im(\phi)}{Re(\phi)} \right] \quad (\text{phase of } \phi) \quad (12)$$

Substituting Equation 10 into Equation 3, the following is obtained:

$$\eta = \alpha_0 |\phi| e^{i(\beta + \omega t)} \quad (13)$$

This expression represents the actual water surface elevation at a point in the water domain bounded by a vertical wedge of arbitrary wedge angle. Since the incident wave train is expressed in Equation 6, the normalized water surface elevation in the near field may be expressed as:

$$\frac{\eta}{\eta_i} = |\phi| e^{i(\beta - kr_i \cos \alpha)} \quad (14)$$

where:

η_i = incident free surface elevation

It is clear that the term $|\phi| e^{i(\beta - kr_i \cos \alpha)}$ is a factor that modifies the incident wave elevation to account for reflection and diffraction effects. The amplitude of the normalized surface elevations, which is comparable to diffraction and reflection coefficients defined in the SPM (1984), may be expressed as the following wave diffraction/reflection coefficient:

$$\left| \frac{\eta}{\eta_i} \right| = |\phi| \quad (15)$$

The phase of Equation 14 is the phase difference between incident and modified waves.

$$\text{Phase difference} \quad \frac{\eta}{\eta_i} = \beta - kr_i \cos \alpha \quad (16)$$

Output of PCDFRAC is composed of $|\phi|$ and β . The diffraction/reflection coefficient $|\phi|$ (modification factor) is then multiplied by the incident wave height to obtain the modified wave height. The phase difference β related to the modified wave is a quantity not usually required in engineering practice; however, it may be useful on some occasions.

REFERENCES

- Chen, H. S. 1987. "Combined Reflection and Diffraction by a Vertical Wedge," Technical Report CERC-87-16, US Army Engineer Waterways Experiment Station, Vicksburg, MS.
- Chen, H. S., and Thompson, E. F. 1985. "Iterative and Pade Solutions for the Water - Wave Dispersion Relation," Miscellaneous Paper CERC-85-4, US Army Engineer Waterways Experiment Station, Vicksburg, MS.
- Kaihatu, J. A., and Chen, H. S. 1988. "Combined Diffraction and Reflection by a Vertical Wedge: PCDFRAC User's Manual," Technical Report CERC-88-9, US Army Engineer Waterways Experiment Station, Vicksburg, MS.
- Morris, A. H., Jr. 1984. "NSWC Library of Mathematics Subroutines," NSWC TR 84 -143, Strategic Systems Department, Naval Surface Weapons Center, Dahlgren, Va.

BREAKWATER DESIGN USING HUDSON AND RELATED EQUATIONS

DESCRIPTION

A rubble structure is often composed of several layers of random-shaped or random-placed stones, protected with a cover layer of selected armor units of either quarystone or specially shaped concrete units. This ACES application provides estimates for the armor weight, minimum crest width, armor thickness, and the number of armor units per unit area of a breakwater using Hudson's and related equations. The material presented herein can be found in Chapter 7 of the SPM (1984).

INTRODUCTION

Until about 1930, design of rubble structures was based only on experience and general knowledge of site conditions. Empirical methods have been developed that, if used with care, will give satisfactory determination of the stability characteristics of these structures when under attack by storm waves.

GENERAL ASSUMPTIONS AND LIMITATIONS

Empirical formulas that were developed for the design of rubble-mound structures are generally expressed in terms of the stone weight required to withstand design wave conditions. These formulas have been largely derived from physical model studies. They are guides and must be used with experience and engineering judgment. Physical modeling is often a cost-effective measure to determine the final cross-section design for most rubble-mound structures.

STABILITY OF RUBBLE STRUCTURES

A proposed breakwater may necessarily be designed for either nonbreaking or breaking waves depending upon positioning of the breakwater and severity of anticipated wave action during its economic life. Some local wave conditions may be of such severity that the protective cover layer must consist of specially shaped concrete armor units in order to provide economic construction of a stable breakwater. The following four sections describe empirical formulas used in the ACES package for design of rubble structures.

Weight of Primary Armor Unit

Comprehensive investigations were made by Hudson (1953, 1959, 1961a, 1961b) to develop a formula to determine the stability of armor units on rubble structures. The stability formula, based on the results of extensive small-scale model testing and some preliminary verification by large-scale model test, is

$$W = \frac{w_r H_t^3}{K_D (S_r - 1)^3 \cot \theta} \quad (1)$$

where

W = weight of individual armor unit in the primary cover layer

w_r = unit weight of armor unit material

H_i = design wave height

K_D = armor unit stability coefficient (see Table A-1 of Appendix A)

$S_r = w_r/w_w$ = specific gravity of armor material

w_w = unit weight of water

Θ = angle between seaward structure slope and horizontal

The dimensionless stability coefficient, K_D , accounts for factors other than structure slope, wave height, and the specific gravity of water at the site. The most important of these variables include

- Shape of armor units.
- Number of units comprising the thickness of the armor layer.
- Manner of placing armor units.
- Surface roughness and sharpness of edges of the armor units (degree of interlocking of the armor units).
- Type of wave attacking structure (breaking or nonbreaking).
- Part of the structure being attacked (trunk or head).
- Angle of incident wave attack.

These stability coefficients (Table A-1 of Appendix A) were derived from large- and small-scale tests that used many various shapes and sizes of both natural and artificial armor units. Values are reasonably definitive and are recommended for use in the design of rubble-mound structures, supplemented by physical model test results when economically warranted.

Crest Width

The width of the crest depends greatly on the degree of allowable overtopping; where there will be no overtopping, crest width is not critical. Little study has been made of crest width of a rubble structure subject to overtopping. As a general guide for overtopping conditions, the minimum crest width should equal the combined widths of three armor units ($n = 3$). The crest should be wide enough to accommodate any construction and maintenance equipment that may be operated from the structure. Crest width is obtained from the following equation:

$$B = nk_{\Delta} \left(\frac{W}{w_r} \right)^{1/3} \quad (2)$$

where

B = crest width

n = number of armor units (ACES application sets $n = 3$)

k_{Δ} = layer coefficient (see Table A-2 of Appendix A)

W = weight of individual armor unit in the primary cover layer

w_r = unit weight of armor unit material

Thickness of the Armor Layer

The thickness of the cover layer is determined from the following formula:

$$r = nk_{\Delta} \left(\frac{W}{w_r} \right)^{1/3} \quad (3)$$

where

r = average layer thickness

n = number of layers of armor units

Armor Unit Placement Density

The placing density is given by the following formula:

$$N_r = Ank_{\Delta} \left(1 - \frac{p}{100} \right) \left(\frac{w_r}{W} \right)^{2/3} \quad (4)$$

where

N_r = number of armor units for a given surface area

A = surface area (assumed as 1000)

p = average porosity of cover layer (see Table A-2 of Appendix A)

REFERENCES AND BIBLIOGRAPHY

- Headquarters, Department of the Army. 1986. "Design of Breakwaters and Jetties," Engineer Manual 1110-2-2904, Washington, DC, p. 4-10.
- Hudson, R. Y. 1953. "Wave Forces on Breakwaters," *Transactions of the American Society of Civil Engineers*, American Society of Civil Engineers, Vol. 118, p. 653.
- Hudson, R. Y. 1959. "Laboratory Investigations of Rubble-Mound Breakwaters," *Proceedings of the American Society of Civil Engineers*, American Society of Civil Engineers, Waterways and Harbors Division, Vol. 85, NO. WW3, Paper No. 2171.
- Hudson, R. Y. 1961a. "Laboratory Investigation of Rubble-Mound Breakwaters," *Transactions of the American Society of Civil Engineers*, American Society of Civil Engineers, Vol. 126, Pt IV.

- Hudson, R. Y. 1961b. "Wave Forces on Rubble-Mound Breakwaters and Jetties," Miscellaneous Paper 2-453, US Army Engineer Waterways Experiment Station, Vicksburg, MS.
- Markel, D. G., and Davidson, D. D. 1979. "Placed-Stone Stability Tests, Tillamook, Oregon; Hydraulic Model Investigation," Technical Report HL-79-16, US Army Engineer Waterways Experiment Station, Vicksburg, MS.
- Shore Protection Manual*. 1984. 4th ed., 2 Vols., US Army Engineer Waterways Experiment Station, Coastal Engineering Research Center, US Government Printing Office, Washington, DC, Chapter 7, pp. 202-242.
- Smith, O. P. 1986. "Cost-Effective Optimization of Rubble-Mound Breakwater Cross Sections," Technical Report CERC-86-2, US Army Engineer Waterways Experiment Station, Vicksburg, MS, p. 48.
- Zwamborn, J. A., and Van Niekerk, M. 1982. *Additional Model Tests--Dolos Packing Density and Effect of Relative Block Density*, CSIR Research Report 554, Council for Scientific and Industrial Research, National Research Institute for Oceanology, Coastal Engineering and Hydraulics Division, Stellenbosch, South Africa.

TOE PROTECTION DESIGN

TABLE OF CONTENTS

Description	4-2-1
Introduction	4-2-1
General Assumptions and Limitations	4-2-1
Width of Toe Apron	4-2-2
Toe Stone Weight	4-2-4
Stability Number	4-2-4
References and Bibliography	4-2-5

TOE PROTECTION DESIGN

DESCRIPTION

Toe protection consists of armor for the beach or bottom material fronting a structure to prevent wave scour. This application determines armor stone size and width of a toe protection apron for *vertical* faced structures such as seawalls, bulkheads, quay walls, breakwaters, and groins. Apron width is determined by the geotechnical and hydraulic guidelines specified in Engineer Manual 1110-2-1614 (Headquarters, Department of the Army, 1985). Stone size is determined by a method (Tanimoto, Yagyu, and Goda, 1982) whereby a stability equation is applied to a single rubble unit placed at a position equal to the width of the toe apron and subjected to standing waves.

INTRODUCTION

Coastal structures rely upon the foundation material for vertical support. Some types of retaining walls also rely upon the bottom material for lateral support. Wave action resulting in loss of bottom material can cause damage and ultimate collapse of a protective structure. While a variety of methods for wave scour protection are employed in practice, this application addresses a simple toe protection design using an apron of armor stones fronting a structure with a vertical seaward face. Unbroken waves are assumed to be normally incident to the structure and are assumed to produce standing waves above the toe protection apron. Stone size is determined by consideration of the stability of a single stone subjected to the standing waves and situated at the seaward edge of the apron.

GENERAL ASSUMPTIONS AND LIMITATIONS

The methodology represented in this application is a composite of largely empirical guidance for the width of the toe apron, and a semi-empirical formulation for the toe stone weight. General assumptions include the following:

- ° Waves are normally incident to the structure.
- ° Standing waves form as a result of wave interaction with a vertical (seaward) face of the structure and remain unbroken in the water depth above the toe apron.
- ° Linear wave theory approximations are adequate to predict the standing wave properties.
- ° Rankine theory is adequate for evaluating the stability of the soil wedge beneath the toe apron.
- ° Rubble-mound material is used as the toe protection material.

In general, this application considers the stability of an armor stone at the seaward crest of the toe protection apron. It does not offer any guidance for preparation or detailed protection of foundation material at the dredge line.

The method for stone weight (Tanimoto, Yagyu, and Goda, 1982) is based upon irregular waves (characterized by significant wave height, H_s) acting on composite breakwaters. To be formally consistent with Tanimoto's approach, the normally incident wave train should use H_s values and structure configurations limited to those tested in the original research. Sheet-pile designs were not considered in the development of the method. In general, Tanimoto's method has not been verified by model tests within the Corps of Engineers. The empirical guidance used for estimating the toe protection width (Engineer Manual 1110-2-1614) has no physical coupling with Tanimoto's method for determining the toe stone weight, yet has significant impact on the formulas for stone weight.

In using Rankine theory as part of the guidance for determining toe protection width for pile structures, a common practice is to use the effective penetration depth of the pile which is less than the full driven depth. The actual computations will apply the user-specified value, and engineering judgment should be applied to adjust d_e as an input parameter.

Official guidance regarding toe protection is being revised to a less conservative design, and this interim methodology will be revised at a later date.

WIDTH OF TOE APRON

The width of the toe apron is estimated using hydraulic and geotechnical factors. Sketches depicting geotechnical and hydraulic factors considered in the estimation of the apron width for a typical sheet-pile wall and a gravity type breakwater are shown in Figures 4-2-1 and 4-2-2 respectively.

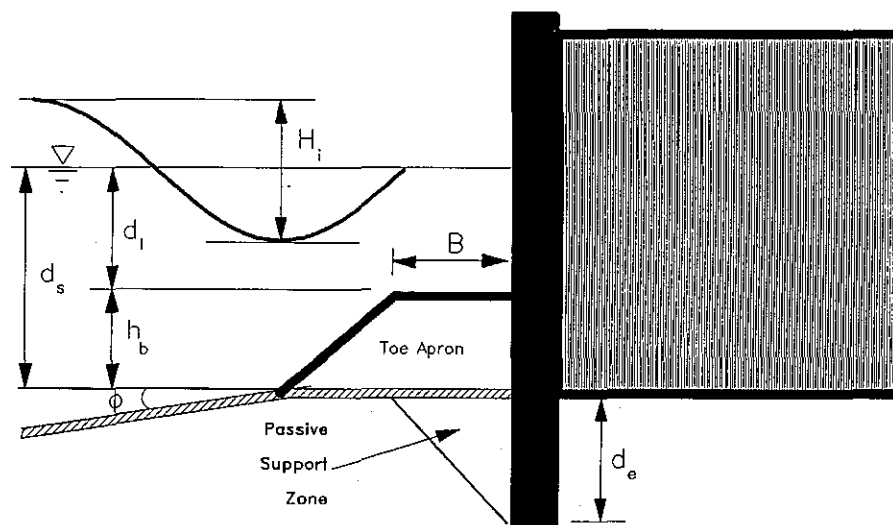


Figure 4-2-1. Typical Toe Apron for Sheet-Pile Walls

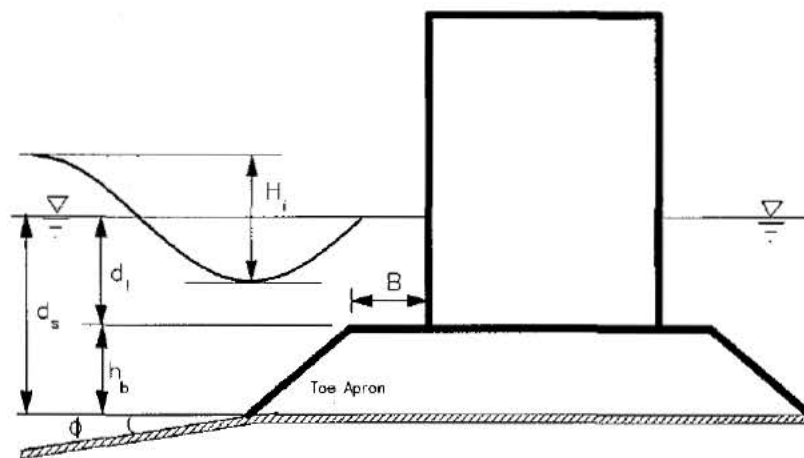


Figure 4-2-2. Typical Toe Apron for Breakwaters

The minimum width of the toe apron, B , from a geotechnical perspective is associated with structure-soil equilibrium considerations and is estimated using Rankine theory (Eckert, 1983 and Eckert and Callendar, 1987):

$$B_1 = K_p d_s \quad (1)$$

where

K_p = coefficient of passive earth pressure

d_s = sheet-pile penetration depth (0 if no pile)

The minimum width of the toe apron, B , from a hydraulics perspective is estimated from simple criteria stated as (EM 1110-2-1614):

$$B_2 = 2 H_i \quad (2)$$

or

$$B_3 = 0.4 d_s \quad (3)$$

where

H_i = incident wave height

d_s = water depth at structure (in absence of toe protection)

The design width for the apron is taken as the largest value predicted by the various criteria considered in Equations 1-3.

$$B = \max(B_1, B_2, B_3) \quad (4)$$

TOE STONE WEIGHT

The stability equation (SPM, 1984) used to determine the armor stone weight in the toe protection apron is cast in the form of the equation derived by Hudson (1959) for armor units for rubble-mound breakwaters.

$$W = \frac{w_r H_i^3}{N_s^3 (S_r - 1)^3} \quad (5)$$

where

W = weight of individual armor stone

w_r = unit weight of armor stone

N_s = stability number

$S_r = w_r / w_w$ = specific gravity of armor stone

w_w = unit weight of water

Stability Number

The stability number, N_s , is semi-empirically formulated on the basis of irregular wave tests conducted by Tanimoto, Yagyu, and Goda (1982). It is determined as:

$$N_s = \max \left\{ 1.3 \left(\frac{1-K}{K^{\frac{1}{3}}} \right) \left(\frac{d_t}{H_i} \right) + 1.8 e^{\left[-1.5 \frac{(1-K)^2 d_t}{K^{\frac{1}{3}} H_i} \right]} ; 1.8 \right\} \quad (6)$$

where

K = parameter associated with the maximum horizontal velocity at the edge of the apron determined from standing waves as described by linear wave theory

$$= \frac{\frac{4\pi d_t}{L}}{\sinh\left(\frac{4\pi d_t}{L}\right)} \left(\sin \frac{2\pi B}{L} \right)^2$$

d_t = water depth (at top of toe protection)

L = wavelength at depth d_t predicted by linear wave theory

REFERENCES AND BIBLIOGRAPHY

- Eckert, J. W. 1983. "Design of Toe Protection for Coastal Structures," *Proceedings of the Coastal Structures '83 Conference*, American Society of Civil Engineers, Arlington, VA, pp. 331-341.
- Eckert, J. W., and Callendar, G. 1987. "Geotechnical Engineering in the Coastal Zone," Instructional Report CERC-87-1, US Army Engineer Waterways Experiment Station, Vicksburg, MS, Chapter 8, pp. 36-38.
- Headquarters, Department of the Army. 1985. "Design of Coastal Revetments, Seawalls, and Bulkheads," Engineer Manual 1110-2-1614, Washington, DC, Chapter 2, pp. 15-19.
- Hudson, R. Y. 1959. "Laboratory Investigations of Rubble-Mound Breakwaters," *Proceedings of the American Society of Civil Engineers*, American Society of Civil Engineers, Waterways and Harbors Division, Vol. 85, NO. WW3, Paper No. 2171.
- Shore Protection Manual*. 1984. 4th ed., 2 Vols., US Army Engineer Waterways Experiment Station, Coastal Engineering Research Center, US Government Printing Office, Washington, DC, Chapter 7, pp. 242-249.
- Tanimoto, K., Yagyu, T., and Goda, Y. 1982. "Irregular Wave Tests for Composite Breakwater Foundations," *Proceedings of the 18th Coastal Engineering Conference*, American Society of Civil Engineers, Cape Town, Republic of South Africa, Vol. III, pp. 2144-2161.

NONBREAKING WAVE FORCES AT VERTICAL WALLS

TABLE OF CONTENTS

Description	4-3-1
Introduction	4-3-1
General Assumptions and Limitations	4-3-1
Sainflou Method	4-3-3
Free Surface Elevation	4-3-3
Sainflou Pressure	4-3-4
Miche-Rundgren Method	4-3-5
Free Surface Elevation	4-3-5
Miche-Rundgren Pressure	4-3-7
Implementation	4-3-8
Numerical Implementation	4-3-8
Implementation Notes	4-3-9
References and Bibliography	4-3-9

NONBREAKING WAVE FORCES AT VERTICAL WALLS

DESCRIPTION

This application provides the pressure distribution and resultant force and moment loading on a vertical wall caused by normally incident, *nonbreaking* regular waves. The results can be used to design vertical structures in protected or fetch-limited regions when the water depth at the structure is greater than about 1.5 times the maximum expected wave height. The application provides the same results as found using the design curves given in Chapter 7 of the SPM (1984).

INTRODUCTION

The pressure distribution on the seaward side of a vertical wall exposed to wave action is composed of two components, the hydrostatic pressure due to the depth of water at the wall and the wave-induced dynamic pressure caused by acceleration of the fluid particles. Estimates of wave-induced pressure are required to design vertical walls that will resist the applied loads without loss of functionality.

Design curves presented in the SPM (1984) provide a means of determining nonbreaking wave forces and moments as a function of water depth, water specific weight, incident wave height, and wave period. One set of curves applies to the case of complete reflection ($\chi = 1.0$) whereas the other set is for a slightly less ($\chi = 0.9$) reflective case.

The curves in the SPM represent a composite method using two solution methods for the wave-induced pressure distribution on a vertical wall. The Miche-Rundgren method provides better fit to laboratory data for steep, nonbreaking waves, but the theory begins to overpredict as the wavelength is increased. On the other hand, the Sainflou method provides better estimates for long, low-steepness waves, but it overpredicts as the waves become steeper. Therefore, the curves in the SPM use the Sainflou method for low-steepness waves and the Miche-Rundgren method for steeper waves. Transition from one method to the other is determined simply by whichever method provides the minimum force or moment for given values of wave steepness and wave height-to-depth ratio.

The major disadvantage of using the design curves in the SPM (other than inconvenience and potential for error) is determination of resultant forces and moments for values of wave height-to-depth ratio that fall between the curves. Additionally, the designer is restricted to using a reflection coefficient of either $\chi = 1.0$ or $\chi = 0.9$.

GENERAL ASSUMPTIONS AND LIMITATIONS

Hydrodynamic assumptions invoked in derivation of both the Sainflou and the Miche-Rundgren equations are typical for theoretical wave motion theories. These assumptions include:

- Nonviscous flow, i.e., ideal fluid in which there are no tangential stresses between adjacent water particles.

- ° Incompressible fluid of constant density.
- ° Irrotational flow in two dimensions.
- ° The absolute pressure at the surface is equal to atmospheric pressure everywhere (so surface pressure is defined as zero).

The above assumptions allow the wave motion problem at a reflecting vertical wall to be expressed in terms of potential flow theory.

Both methods are derived in the Lagrangian system, which follows individual water particles rather than remaining stationary. The primary advantage of Lagrangian coordinates is better representation of the hydrodynamic pressure above the still-water level when the crest of the standing wave is at the wall. Hydrodynamic pressure exerted on the vertical wall is hydrostatic pressure due to the depth of water, and wave pressure due to transformation of wave kinetic energy into pressure energy when wave motion acts on the wall. Most applications of the theories usually omit the hydrostatic pressure component of the total pressure, and this custom has been followed in this ACES application.

Both methods assume normally incident, monochromatic waves being reflected by a vertical wall. The waves are nonbreaking and of constant form, and it is assumed that no overtopping of the wall occurs. The bottom fronting the vertical wall is assumed horizontal. A definition sketch for a nonbreaking, normally incident, monochromatic wave being reflected from a vertical wall is shown on Figure 4-3-1.

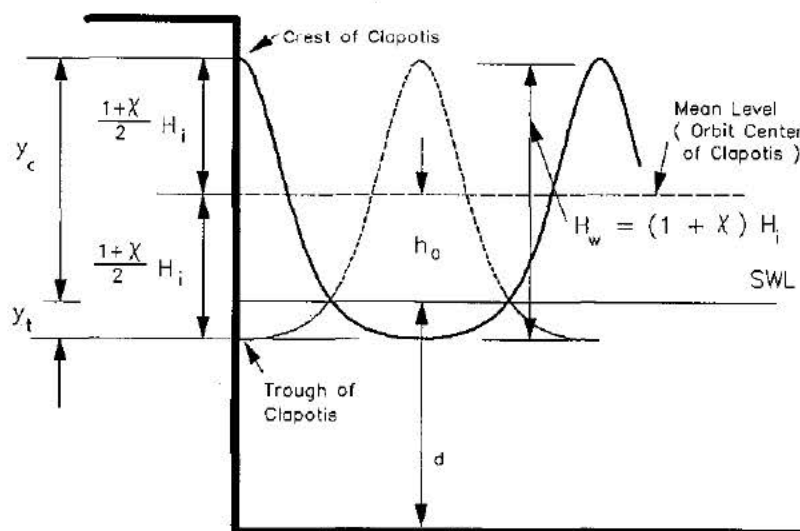


Figure 4-3-1. Definition Sketch

Primary drawbacks to using the Sainflou or Miche-Rundgren method of calculating wave-induced pressure distributions and resulting forces and moments are the facts that they are monochromatic theories and they do not give breaking wave forces. There may be waves in an

equivalent irregular wave train that produce greater force loading than predicted using monochromatic waves. Also waves breaking directly on the wall can produce significantly higher forces than nonbreaking waves.

The only limitation in applying the Miche-Rundgren method is the restriction that the reflection coefficient can vary only over the range $0.9 < \chi < 1.0$. This range is based on recommendations given in the SPM. The Sainflou method accommodates only a reflection coefficient equal to unity $\chi = 1.0$. Consequently, predictions from this method may sometimes be conservative.

SAINFLOU METHOD

Sainflou (1928) published a theoretical solution for the pressure distribution at a vertical wall for a perfectly reflected monochromatic wave of incident height, H_i . His derivation was based on the classical hydrodynamic equations of continuity and momentum. Sainflou developed his equations as a simplification of second-order wave theory in which he omitted some of the second-order terms in the expressions. Consequently, his solution is partly of second-order in the parameter H/L . He assumed that ambient atmospheric pressure is constant everywhere on the free surface, and his expression for pressure due to the wave motion does not include any atmospheric pressure contribution.

Free Surface Elevation

In the Lagrangian coordinate system, Sainflou derived the following expressions for the vertical elevations of water particles of a standing wave at a vertical wall under the crest and trough:

Crest

$$y_{cr} = y_0 + H_i \frac{\sinh\left[\frac{2\pi}{L}(d + y_0)\right]}{\sinh\left(\frac{2\pi d}{L}\right)} + \pi H_i \left(\frac{H_i}{L}\right) \frac{\sinh\left[\frac{2\pi}{L}(d + y_0)\right] \cosh\left[\frac{2\pi}{L}(d + y_0)\right]}{\sinh\left(\frac{2\pi d}{L}\right)} \quad (1)$$

Trough

$$y_{tr} = y_0 - H_i \frac{\sinh\left[\frac{2\pi}{L}(d + y_0)\right]}{\sinh\left(\frac{2\pi d}{L}\right)} + \pi H_i \left(\frac{H_i}{L}\right) \frac{\sinh\left[\frac{2\pi}{L}(d + y_0)\right] \cosh\left[\frac{2\pi}{L}(d + y_0)\right]}{\sinh\left(\frac{2\pi d}{L}\right)} \quad (2)$$

where

H_i = incident wave height

L = wavelength

d = water depth

y_0 = initial vertical elevation of a water particle at rest

The free surface at rest is given by $y_0 = 0$. Therefore, the elevation of the free surface relative to still-water level (SWL) when the crest or trough of the standing wave is at the wall is found by substituting $y_0 = 0$ into Equations 1 and 2, yielding:

where

$$\Theta_1 = 1 + \frac{3}{4 \sinh^2\left(\frac{2\pi d}{L}\right)} - \frac{1}{4 \cosh^2\left(\frac{2\pi d}{L}\right)} \quad (10)$$

$$\Theta_2 = \frac{3}{4 \sinh^2\left(\frac{2\pi d}{L}\right)} + \frac{1}{4 \cosh^2\left(\frac{2\pi d}{L}\right)} \quad (11)$$

The free surface elevation (relative to SWL) when the crest or trough is at the wall is found by substituting $y_0 = 0$ into Equations 8 and 9, resulting in the expressions:

Crest

$$\eta_{cr} = \frac{H_i}{2}(1 + \chi) + \frac{\pi H_i}{4} \left(\frac{H_i}{L} \right) \coth\left(\frac{2\pi d}{L}\right) [(1 + \chi)^2 \Theta_1 + (1 - \chi)^2 \Theta_2] \quad (12)$$

Trough

$$\eta_{tr} = -\frac{H_i}{2}(1 + \chi) + \frac{\pi H_i}{4} \left(\frac{H_i}{L} \right) \coth\left(\frac{2\pi d}{L}\right) [(1 + \chi)^2 \Theta_1 + (1 - \chi)^2 \Theta_2] \quad (13)$$

In the Miche-Rundgren formulation, the height of the orbit center above the SWL is represented by the second term in Equations 12 and 13, i.e.,

$$\frac{h_0}{H_i} = \frac{\pi}{4} \left(\frac{H_i}{L} \right) \coth\left(\frac{2\pi d}{L}\right) [(1 + \chi)^2 \Theta_1 + (1 - \chi)^2 \Theta_2] \quad (14)$$

The similarity between the Miche-Rundgren equations and the Sainflou equations is easily recognized. In the case of complete reflection when $\chi = 1.0$, the only difference between the corresponding equations is the Θ_1 -term present in the Miche-Rundgren equations.

Miche-Rundgren Pressure

The pressure at any vertical elevation under a standing wave when the crest or trough is at the vertical wall was given by Rundgren (1958) as:

Crest

$$\begin{aligned} \frac{p_{cr}}{\gamma} = & -y_0 - \frac{H_i}{2}(1+\chi) \frac{\sinh\left(\frac{2\pi y_0}{L}\right)}{\sinh\left(\frac{2\pi d}{L}\right)\cosh\left(\frac{2\pi d}{L}\right)} \\ & - \frac{\pi H_i}{4} \left(\frac{H_i}{L}\right) \frac{\sinh\left(\frac{2\pi y_0}{L}\right)}{\sinh^2\left(\frac{2\pi d}{L}\right)} [(1+\chi)^2 \Theta_3 + (1-\chi)^2 \Theta_4] \end{aligned} \quad (15)$$

Trough

$$\begin{aligned} \frac{p_{tr}}{\gamma} = & -y_0 + \frac{H_i}{2}(1+\chi) \frac{\sinh\left(\frac{2\pi y_0}{L}\right)}{\sinh\left(\frac{2\pi d}{L}\right)\cosh\left(\frac{2\pi d}{L}\right)} \\ & - \frac{\pi H_i}{4} \left(\frac{H_i}{L}\right) \frac{\sinh\left(\frac{2\pi y_0}{L}\right)}{\sinh^2\left(\frac{2\pi d}{L}\right)} [(1+\chi)^2 \Theta_3 + (1-\chi)^2 \Theta_4] \end{aligned} \quad (16)$$

where

$$\begin{aligned} \Theta_3 = & \left[1 - \frac{1}{4 \cosh^2\left(\frac{2\pi d}{L}\right)} \right] \cosh\left[\frac{2\pi}{L}(2d+y_0)\right] - 2 \tanh\left(\frac{2\pi d}{L}\right) \sinh\left[\frac{2\pi}{L}(2d+y_0)\right] \\ & + \frac{3}{4} \left[\frac{\cosh\left(\frac{2\pi y_0}{L}\right)}{\sinh^2\left(\frac{2\pi d}{L}\right)} - \frac{2 \cosh\left[\frac{2\pi}{L}(d+y_0)\right]}{\cosh\left(\frac{2\pi d}{L}\right)} \right] \end{aligned} \quad (17)$$

$$\begin{aligned} \Theta_4 = & \frac{\cosh\left[\frac{2\pi}{L}(2d+y_0)\right]}{4 \cosh^2\left(\frac{2\pi d}{L}\right)} - 2 \tanh\left(\frac{2\pi d}{L}\right) \sinh\left[\frac{2\pi}{L}(2d+y_0)\right] \\ & + \frac{3}{4} \left[\frac{\cosh\left(\frac{2\pi y_0}{L}\right)}{\sinh^2\left(\frac{2\pi d}{L}\right)} - \frac{2 \cosh\left[\frac{2\pi}{L}(d+y_0)\right]}{\cosh\left(\frac{2\pi d}{L}\right)} \right] \end{aligned} \quad (18)$$

IMPLEMENTATION

The determination of wave forces and moments acting on a vertical wall (when the crest or trough of a standing wave is at the wall) is accomplished in this ACES application by numerically integrating the equations given in the preceding sections.

Numerical Implementation

After performing initial bookkeeping chores, the numerical code first determines the sea surface elevation for when the crest and when the trough are at the wall (corresponds to $y_0 = 0$). This calculation is performed using Equations 12 and 13 from the Miche-Rundgren method. The resulting values for crest and trough elevation are taken as valid for both the Miche-Rundgren solution and for the Sainflou solution. The corresponding Sainflou equations (Equations 3 and 4) would give similar results, but the increased accuracy produced by the fully second-order Miche-Rundgren equations, and the fact that reduced reflection could be accommodated, led to the decision of using only the Miche-Rundgren result. The nomogram method in the SPM also follows this convention.

Next, the water depth is divided into 90 equal increments for calculation of wave pressure. Each incremental depth represents an at-rest value of y_0 for use in the Lagrangian equations for vertical elevation. During each program loop at an incremental depth, the following values are calculated and stored:

Sainflou Method

- Vertical elevation of particle when crest is at wall (Equation 1).
- Vertical elevation of particle when trough is at wall (Equation 2).
- Pressure when crest is at wall (Equation 6).
- Pressure when trough is at wall (Equation 7).
- Incremental component to overturning moment about the bottom of the wall, given as $p_{cr}(y_{cr} + d)$ and $p_{tr}(y_{tr} + d)$ for the crest and trough, respectively.

Miche-Rundgren Method

- Vertical elevation of particle when crest is at wall (Equation 8).
- Vertical elevation of particle when trough is at wall (Equation 9).
- Pressure when crest is at wall (Equation 15).
- Pressure when trough is at wall (Equation 16).
- Incremental component to overturning moment about the bottom of the wall, given as $p_{cr}(y_{cr} + d)$ and $p_{tr}(y_{tr} + d)$ for the crest and trough, respectively.

After all loops have been completed, the total force per unit horizontal width of the wall is found for both methods by integrating the pressure over the entire water column (summing the incremental pressure values calculated at each depth). Corresponding overturning moments are found by integrating the incremental moment components.

Implementation Notes

Forces and moments per unit length of wall calculated by this program are those caused by the wave action and hydrostatic water pressure. The designer must add any other external force loads due to soil pressure from backfill, etc.

As mentioned previously, the Miche-Rundgren method overpredicts when the waves are very long (low steepness), whereas the Sainflou method provides a more realistic answer for this condition. Conversely, the Miche-Rundgren method is better for steeper wave conditions. This application reports answers from both methods, with the recommendation of using the smaller values for force and moment.

The Sainflou method *does not* include provision for reflection coefficients less than one. Therefore, it gives conservative results if reflection is less than complete. The SPM (1984) gives the following guidance on choosing the reflection coefficient:

It should be assumed that smooth vertical walls completely reflect incident waves and $\chi = 1.0$. Where wales, tiebacks, or other structural elements increase the surface roughness of the wall by retarding vertical motion of the water, a lower value of χ may be used. A lower value of χ also may be assumed when the wall is built on a rubble base or when rubble has been placed seaward of the structure toe. Any value of χ less than 0.9 should not be used for design purposes.

This application should provide results that closely match the design curves given in the SPM. An exception may occur in determination of crest and trough elevation at very low values of H_i/gT^2 using SPM Figures 7-90 or 7-93. The SPM method first determines h_0 and then calculates η_{cr} and η_{tr} as a distance $H_i(1 + \chi)/2$ above or below h_0 . As H_i/gT^2 approaches zero, the curves for h_0 in the SPM were forced to a value of $h_0/H_i = 1.0$, representing the limit of a solitary wave. On the other hand, this ACES application calculates η_{cr} and η_{tr} directly, and the values of h_0 obtained from Equations 5 and 14 may be different from the SPM at very small values of wave steepness.

REFERENCES AND BIBLIOGRAPHY

- Miche, R. 1944. "Mouvements ondulatoires de la mer en profondeur constante ou décroissante," *Annales des Ponts et Chaussées*, Paris, Vol. 114.
- Rundgren, L. 1958. "Water Wave Forces," Bulletin No. 54, Royal Institute of Technology, Division of Hydraulics, Stockholm, Sweden.
- Sainflou, M. 1928. "Essay on Vertical Breakwaters," *Annals des Ponts et Chaussées*, Paris (Translated by Clarence R. Hatch, Western Reserve University, Cleveland, OH).
- Shore Protection Manual*. 1984. 4th ed., 2 Vols., US Army Engineer Waterways Experiment Station, Coastal Engineering Research Center, US Government Printing Office, Washington, DC, Chapter 7, pp. 161-173.

RUBBLE-MOUND REVETMENT DESIGN

TABLE OF CONTENTS

Description	4-4-1
Introduction	4-4-1
General Assumptions and Limitations	4-4-1
Riprap Armor Stability Formula	4-4-2
CERC Stability Number	4-4-2
Dutch Stability Number	4-4-3
Surf Similarity Parameter	4-4-5
Revetment Design	4-4-6
Weight of Armor Unit	4-4-6
Armor Layer Thickness	4-4-6
Filter Layer Thickness	4-4-6
Stone Sizes (Gradation)	4-4-7
Irregular Wave Runup on Riprap	4-4-8
References and Bibliography	4-4-9

RUBBLE-MOUND REVETMENT DESIGN

DESCRIPTION

Quarystone is the most commonly used material for protecting earth embankments from wave attack because high-quality stone, where available, provides a stable and unusually durable revetment armor material at relatively low cost. This ACES application provides estimates for revetment armor and bedding layer stone sizes, thicknesses, and gradation characteristics. Also calculated are two values of runup on the revetment, an expected extreme and a conservative runup value.

INTRODUCTION

Structures are often needed along either bluff or beach shorelines to provide protection from wave action or to retain in situ soil or fill. Vertical structures are classified as either seawalls or bulkheads, according to their function, and protective materials laid on slopes are called revetments.

Revetments are generally constructed of durable stone or other material that will provide sufficient armoring for protected slopes. They consist of an armor layer, filter layer, and toe protection. The filter layer assures drainage and retention of the underlaying soil. Toe protection is needed to provide stability against undermining at the bottom of the structure.

GENERAL ASSUMPTIONS AND LIMITATIONS

Empirical formulas that were developed for the design of rubble-mound structures are generally expressed in terms of the stone weight required to withstand design wave conditions. These formulas have been largely derived from physical model studies. They are guides and must be used with experience and engineering judgment. Physical modeling is often a cost-effective measure to determine the final cross-section design for most rubble-mound structures. A definition sketch for some of the terms used in this section is shown in Figure 4-4-1.

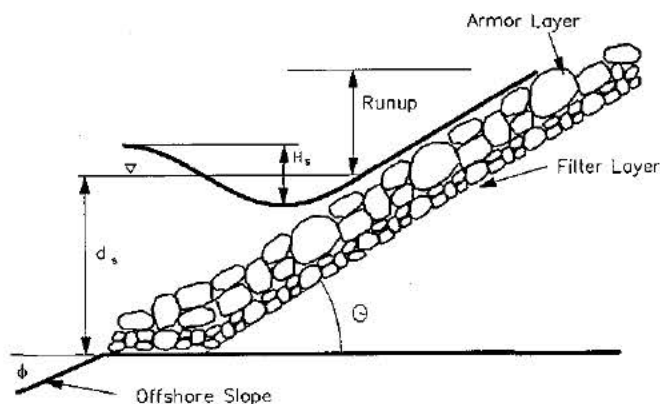


Figure 4-4-1. Definition Sketch for Riprap Revetments

RIPRAP ARMOR STABILITY FORMULA

For irregular wave conditions, a stability formula is defined that is similar to the one developed by Hudson (1958) for monochromatic waves:

$$W_{50} = w_r \left[\frac{H_s}{N_s \left(\frac{w_r}{w_w} - 1 \right)} \right]^3 \quad (1)$$

where

- W_{50} = median weight of the armor stone
- w_r = unit weight of the armor stone
- H_s = significant wave height
- N_s = stability number
- w_w = unit weight of water

The following sections present two stability numbers for use in Equation 1. These stability numbers are based on riprap stability studies conducted at CERC and by the Dutch. This ACES application uses the larger of the two in Equation 1 to compute the required stone weight for the revetment.

CERC Stability Number

Based on findings of Broderick (1983), the *zero-damage* riprap stability number given in Ahrens (1981) as:

$$N_{s-zero} = 1.45 (\cot \theta)^{\frac{1}{6}} \quad (2)$$

should be changed to:

$$N_{s-zero} = \frac{1.45}{1.27} (\cot \theta)^{\frac{1}{6}} \quad (3)$$

where

$\cot \theta$ = cotangent of structure slope

The factor, 1.27, is the ratio between the average of the highest 10 percent of the waves and the significant wave height in a Rayleigh distribution. By changing the coefficient in the stability number equation, the significant wave height can continue to be used in the stability formula, and at the same time the essential findings of Broderick can be addressed. Broderick found that a wave height greater than the significant gave better correlation to damage observed in laboratory tests of riprap stability. Broderick suggested that the average of the highest 10 percent of the waves was the appropriate wave height to use in a riprap stability formula.

Dutch Stability Number

Based on findings of Van der Meer and Pilarczyk (1987) and Van der Meer (1988a, 1988b) two formulas for riprap stability numbers were derived, one for plunging waves and one for surging (nonbreaking) waves. Basic assumptions for the formulas are:

- A rubble-mound structure with an armor layer consisting of rock.
- Little or no overtopping (less than 10 to 15 percent of the waves).
- The slope of the structure should be generally uniform.

The formulas are:

Plunging Waves

$$N_s = 6.2 P^{0.18} \left(\frac{S}{\sqrt{N}} \right)^{0.2} (\zeta_z)^{-0.5} \quad (4)$$

Surging (Nonbreaking) Waves

$$N_s = 1.0 P^{-0.13} \left(\frac{S}{\sqrt{N}} \right)^{0.2} \sqrt{\cot \theta} \zeta_z^P \quad (5)$$

where

P = permeability coefficient (Figure 4-4-2)

S = damage level (Table 4-4-1)

N = number of waves

NOTE: The equations are valid in the range $1,000 < N < 7,000$, so $N = 7,000$ represents a logical limiting value that is used in this ACES application and should be conservative.

ζ_z = surf similarity parameter (see Equation 6)

The permeability coefficient P was introduced to describe the influence of the permeability of the structure on its stability. Van der Meer investigated three structures. The lower boundary value of P is that given by an impermeable core (clay or sand) (see Figure 4-4-2(a)). The ratio of armor/filter stone diameter was 4.5. With this impermeable core, a value of $P = 0.1$ was assumed. The upper boundary value of P is that given by a homogeneous structure, consisting only of armor stones (see Figure 4-4-2(d)). For this structure, a value of $P = 0.6$ was assumed. The third structure consisted of a two-diameter-thick armor layer on a permeable core. The ratio of armor/core stone diameter was 3.2 (see Figure 4-4-2(c)). For this structure, a value of $P = 0.5$ was assumed. The value of P for other structures with, for example, more than one layer of stones (Figure 4-4-2(b) or a thicker armor layer must be estimated from the values established for the three specific structures. The design engineer's experience is obviously important when selecting a value of P .

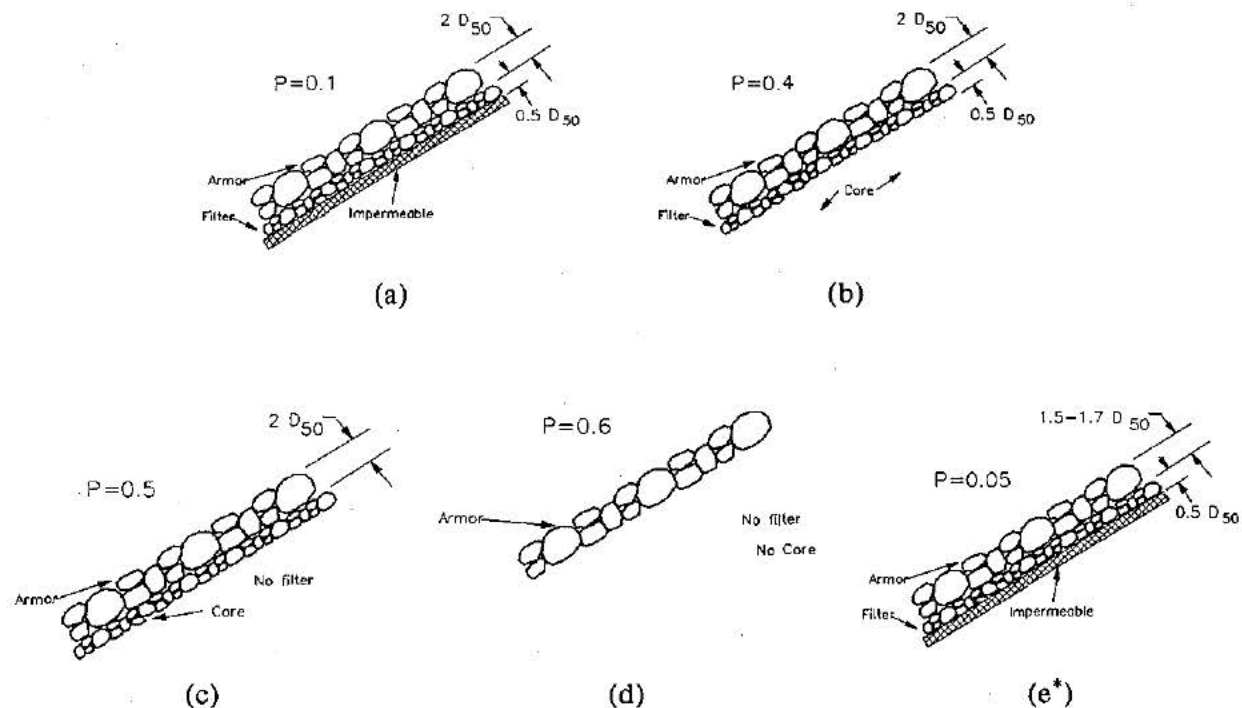


Figure 4-4-2. Permeability Coefficient (Van der Meer, 1988a; Bradbury, Allsop, and Latham, 1990*)

Table 4-4-1 Damage Levels for Two Diameter Thick Rock Slopes (Van der Meer, 1988a)		
cot θ	Damage Level S	
	Start of Damage	Failure (Filter Layer Visible)
2.0	2	8
3.0	2	12
4.0	3	17
6.0	3	17

Equations 4 and 5 were developed for deepwater wave conditions, and Van der Meer (1988a) recommends a correction for shallow-water conditions. This ACES application uses a factor of 1.2 for the correction.

The next section describes the surf similarity parameter and how it is used in this ACES application.

Surf Similarity Parameter

The surf similarity parameter has been found to be a very useful variable to characterize the breaker conditions on coastal structures or beaches. For irregular waves the surf similarity parameter can be defined as (Battjes, 1974):

$$\zeta_z = \frac{\tan \theta}{\left(\frac{2\pi H_s}{gT_z^2} \right)^{1/2}} \quad (6)$$

where

$$T_z = \text{average wave period} \\ = T_s \left(\frac{0.67}{0.80} \right)$$

NOTE: This ratio, (0.67/0.80), is based on laboratory data collected by Ahrens (1987).

The surf similarity parameter is used to determine which of the Van der Meer/Pilarczyk formulas for stability number (Equations 4 or 5) should be compared with the CERC stability number and finally used in the stability formula (Equation 1). Van der Meer (1988a) derives the following formula for the surf similarity parameter, ζ_{ztp} , at the transition point from plunging to surging waves:

$$\zeta_{ztp} = \left(-6.2 P^{0.31} \sqrt{\tan \theta} \right)^{\frac{1}{(P-0.5)}} \quad (7)$$

The following criteria are used to determine which of the Van der Meer/Pilarczyk stability numbers (Equations 4 or 5) is to be compared with the CERC stability number (Equation 3):

$$\zeta_z \leq \zeta_{ztp} \rightarrow \text{use Equation 4}$$

$$\zeta_z > \zeta_{ztp} \rightarrow \text{use Equation 5}$$

REVETMENT DESIGN

The following sections describe the formulas for median weight and other percentiles of stone, armor and filter layer thicknesses, and stone dimensions used in this ACES application for design of rubble-mound revetments.

Weight of Armor Unit

The median weight of the armor unit is computed using Equation 1.

$$W_{50} = w_r \left[\frac{H_s}{N_s \left(\frac{w_r}{w_w} - 1 \right)} \right]^3$$

The stability number, N_s , used in Equation 1 is the larger of the CERC stability number (Equation 3) or the Dutch stability number (Equation 4 or 5).

Armor Layer Thickness

The minimum armor layer thickness is given as:

$$r_{armor} = 2 \left(\frac{W_{50}}{w_r} \right)^{\frac{1}{3}} \quad (8)$$

Filter Layer Thickness

The filter layer thickness is given as the maximum of:

$$r_{filter} = \frac{r_{armor}}{4} \quad \text{or} \quad 1 \text{ foot} \quad (9)$$

The total horizontal thickness of the armor layer and first underlayer, l , must satisfy the following relation:

$$l \geq 2H_s \quad (10)$$

where

$$l = r_t \sqrt{1 + \cot^2 \theta} \quad (11)$$

$$r_t = r_{armor} + r_{filter} \quad (12)$$

The purpose of Equation 10 is to ensure there is sufficient stone between the violent wave attack on the surface of the riprap and the geotextile filter cloth to dissipate a considerable portion of the wave energy. A geotextile filter cloth is relatively permeable to ground-water seepage but not to the short duration loads and high velocity impacts of breaking waves.

Stone Sizes (Gradation)

Armor Layer

Gradation is based on guidance given in EM 1110-2-2300 (1971), which specifies that the maximum and minimum weight of the riprap stone is given by:

$$W_{\max} = 4W_{50} \quad (13)$$

$$W_{\min} = \frac{1}{8}W_{50} \quad (14)$$

where W_{\max} and W_{\min} are the weight of the largest and smallest stone respectively in the gradation.

In addition, laboratory tests (Ahrens, 1975) provide the following approximate relations:

$$W_{85} = 1.96W_{50} \quad (15)$$

$$W_{15} = 0.4W_{50} \quad (16)$$

where the subscript indicates the percentage of the total weight of gradation contributed by stones of lesser weight.

Stone dimensions, D , are computed by the following relationship:

$$D_x = \left(\frac{W_x}{w_r} \right)^{\frac{1}{3}} \quad (17)$$

where the subscript x indicates the percentage of the weight of the total gradation contributed by stones of lesser weight.

Filter Layer

The ratio of the filter layer stone size to armor stone size is given by Ahrens (1981) as:

$$\frac{D_{15(\text{armor})}}{D_{85(\text{filter})}} = 4.0 \quad (18)$$

Knowing $D_{85(filter)}$, the following relationship is used to calculate the median stone dimension, $D_{50(filter)}$, of the filter layer:

$$\frac{D_x}{D_{50}} = e^{(0.01157x - 0.5785)} \quad (19)$$

where

$$x = 85$$

Knowing $D_{50(filter)}$, Equation 19 is used to determine stone dimensions for the 0 (minimum), 15, and 100 (maximum) percentile size of the filter layer. Equation 17 is then used to determine corresponding stone weights for the filter layer.

IRREGULAR WAVE RUNUP ON RIPRAP

Recent research by Ahrens and Heimbaugh (1988) provides an improved method to estimate the maximum runup caused by irregular waves on riprap revetments. An unusual advantage of this method is that it works well for both shallow and deep water at the toe of the revetment. The approach is based on the surf parameter discussed earlier. In this instance the surf parameter is calculated using the energy-based variables H_{mo} and T_p . The energy-based surf parameter, ζ , is defined as:

$$\zeta = \frac{\tan \theta}{\left(\frac{2\pi H_{mo}}{gT_p^2} \right)^{1/2}} \quad (20)$$

where

T_p = period of peak energy density of the wave spectrum

$$= \frac{T_s}{0.80} \quad (21)$$

H_{mo} = energy-based zero-moment wave height

T_s = average period of the highest one-third of the waves

In this ACES application, the energy-based zero-moment wave height, H_{mo} , is computed by two methods, and the smaller value is then selected for use in the runup equation. The two methods for calculating H_{mo} are:

$$H_{mo} = 0.10 L_p \tanh\left(\frac{2\pi d_s}{L_p}\right) \quad (22)$$

or

$$H_{mo} = \frac{H_s}{\exp\left[C_o\left(\frac{d}{gT_p^2}\right)^{-C_1}\right]} \quad (23)$$

where

$$C_o = 0.00089$$

$$C_1 = 0.834$$

The expected maximum runup is calculated using the following equation:

$$R_{max} = H_{mo} \frac{\alpha \zeta}{1 + b \zeta} \quad (24)$$

where

α and b = dimensionless runup coefficients

In research for improved estimates of runup, Ahrens and Heimbaugh (1988) conducted investigations of the systematic error in predicting the maximum runup. They found approximately 25 percent of their tests had a percent error greater than ± 10 percent. Because of this, they suggest that it may be useful in some critical situations to use a conservative value of runup. Therefore, two sets of runup coefficients are provided in this ACES application, one for the maximum runup and the other for a conservative runup:

Expected Maximum Runup

$$a = 1.022 ; b = 0.247$$

Conservative Runup

$$a = 1.286 ; b = 0.247$$

REFERENCES AND BIBLIOGRAPHY

- Ahrens, J. P. 1975. "Large Wave Tank Tests of Riprap Stability," CERC Technical Memorandum 51, US Army Engineer Waterways Experiment Station, Vicksburg, MS.
- Ahrens, J. P. 1977. "Prediction of Irregular Wave Overtopping," CERC CETA 77-7, US Army Engineer Waterways Experiment Station, Vicksburg, MS.
- Ahrens, J. P. 1981. "Design of Riprap Revetments for Protection Against Wave Attack," CERC TP 81-5, US Army Engineer Waterways Experiment Station, Vicksburg, MS.
- Ahrens, J. P. 1987. "Characteristics of Reef Breakwaters," Technical Report CERC-87-17, US Army Engineer Waterways Experiment Station, Vicksburg, MS.

- Ahrens, J. P., and Heimbaugh, M. S. 1988. "Approximate Upperlimit of Irregular Wave Runup on Riprap," Technical Report CERC-88-5, US Army Engineer Waterways Experiment Station, Vicksburg, MS.
- Ahrens, J. P., and McCartney B. L. 1975. "Wave Period Effect on the Stability of Riprap," *Proceedings of Civil Engineering in the Oceans/III*, American Society of Civil Engineers, pp. 1019-1034.
- Battjes, J. A. 1974. "Surf Similarity," *Proceedings of the 14th Coastal Engineering Conference*, Copenhagen, Denmark.
- Bradbury, A. P., Ailsop, N. W. H., and Latham, L-P. 1990. "Rock Armor Stability Formulae-Influence of Stone Shape and Layer Thickness," *Proceedings of the 22nd International Conference on Coastal Engineering*, Delft, The Netherlands.
- Broderick, L. L. 1983. "Riprap Stability, A Progress Report," *Proceedings of the Coastal Structures '83 Conference*, American Society of Civil Engineers, Arlington, VA, pp. 320-330.
- Broderick, L. L., and Ahrens, J. P. 1982. "Riprap Stability Scale Effects," CERC TP 82-3, US Army Engineer Waterways Experiment Station, Vicksburg, MS.
- Headquarters, Department of the Army. 1971. "Earth and Rock-Fill Dams, General Design and Constructions Operations," Engineer Manual 1110-2-2300, Washington, DC.
- Hudson, R. Y. 1958. "Design of Quarry Stone Cover Layers for Rubble Mound Breakwaters," Research Report 2-2, US Army Engineer Waterways Experiment Station, Vicksburg, MS.
- Shore Protection Manual*. 1984. 4th ed., 2 Vols., US Army Engineer Waterways Experiment Station, Coastal Engineering Research Center, US Government Printing Office, Washington, DC, Chapter 7.
- Van der Meer, J. W., and Pilarczyk, K. W. 1987. "Stability of Breakwater Armor Layers Deterministic and Probabilistic Design," Delft Hydraulics Communication No. 378, Delft, The Netherlands.
- Van der Meer, J. W. 1988a. "Deterministic and Probabilistic Design of Breakwater Armor Layers," *Journal of Waterways, Port, Coastal, and Ocean Engineering*, American Society of Civil Engineers, Vol. 114, No. 1, pp. 66-80.
- Van der Meer, J. W. 1988b. "Rock Slopes and Gravel Beaches Under Wave Attack," Ph.d. Thesis, Department of Civil Engineering, Delft Technical University; also Delft Hydraulics Communication No. 396, Delft, The Netherlands.

IRREGULAR WAVE RUNUP ON BEACHES

TABLE OF CONTENTS

Description	5-1-1
General Assumptions and Limitations	5-1-1
Wave Runup Equation	5-1-2
References and Bibliography	5-1-2

IRREGULAR WAVE RUNUP ON BEACHES

DESCRIPTION

This application provides an approach to calculate runup statistical parameters for wave runup on smooth slope linear beaches. To account for permeable and rough slope natural beaches, the present approach needs to be modified by multiplying the results for the smooth slope linear beaches by a reduction factor. However, there is no guidance for such a reduction due to the sparsity of good field data on wave runup. The approach used in this ACES application is based on existing laboratory data on irregular wave runup (Mase and Iwagaki, 1984; Mase, 1989).

GENERAL ASSUMPTIONS AND LIMITATIONS

At present there are no theoretical approaches to calculate either monochromatic or irregular wave runup on beaches. The lack of a theoretical approach to solve the problem is due to the numerous difficulties inherent in the runup prediction problem such as:

- ° Nonlinear transformation of wave energy in the breaking wave zone.
- ° Wave reflection effects.
- ° Three-dimensional effects such as standing or progressive edge waves.
- ° Permeability.
- ° Porosity.
- ° Roughness.
- ° Ground-water table level.

Present approaches to calculating monochromatic wave runup on smooth steep slope coastal structures have been limited to empirical expressions of a Hunt (1959) equation form with limiting runup as determined via analytical breaking wave steepness limiting expressions (Walton and Ahrens, 1989; Walton, et al., 1989). Additionally, empirical nonlinear power law expressions exist for predicting irregular wave runup on smooth linear slopes (Mase, 1989) for the following runup statistics in a stationary wave train:

R_{\max} = maximum wave runup

R_2 = runup value exceeded by 2 percent of the runups

$R_{1/10}$ = average of the highest one-tenth of the wave runups

$R_{1/3}$ = significant or average of the highest third of the runups

\bar{R} = average wave runup

This ACES application calculates these runup statistics and quantiles based on the coefficients provided by Mase (1989).

WAVE RUNUP EQUATION

The methodology is based on a fitting of the relative wave runup, R , via an equation of the form:

$$R_p = H_{s0} \alpha_p I^{(b_p)} \quad (1)$$

where

$$-_p = \text{quantile or statistic value desired} \\ \left(\text{max, 2\%, } \frac{1}{3}, \frac{1}{10}, \text{average} \right)$$

α_p, b_p = constants based on the statistic or quantile value of desired runup

I = Iribarren number

$$I = \frac{\tan \theta}{\left(\frac{H_{s0}}{L_o} \right)^{\frac{1}{2}}} \quad (2)$$

$\tan \theta$ = tangent of the beach slope

H_{s0} = deepwater significant wave height

L_o = deepwater wavelength

Until further research is conducted, it is suggested that the beach foreshore slope be used as the required beach slope in Equation (1).

REFERENCES AND BIBLIOGRAPHY

- Hunt, I. A. 1959. "Design of Seawalls and Breakwaters," *Journal of the Waterway, Port, Coastal, and Ocean Engineering Division*, American Society Civil Engineers, Vol. 85, No. 3, pp. 123-152.
- Mase, H. 1989. "Random Wave Runup Height on Gentle Slopes," *Journal of the Waterway, Port, Coastal, and Ocean Engineering Division*, American Society Civil Engineers, Vol. 115, No. 5, pp. 649-661.
- Mase, H., and Iwagaki, Y. 1984. "Runup of Random Waves on Gentle Slopes," *Proceedings of the 19th International Conference on Coastal Engineering*, Houston, TX, American Society Civil Engineers, pp. 593-609.
- Walton, T. L., Jr., and Ahrens, J. P. 1989. "Maximum Periodic Wave Run-Up on Smooth Slopes," *Journal of the Waterway, Port, Coastal, and Ocean Engineering Division*, American Society Civil Engineers, Vol. 115, No. 5, pp. 703-708.
- Walton, T. L., Jr., Ahrens, J. P., Truitt, C. L., and Dean, R. G. 1989. "Criteria for Evaluating Coastal Flood-Protection Structures," Technical Report CERC-89-15, US Army Engineer Waterways Experiment Station, Vicksburg, MS.

WAVE RUNUP AND OVERTOPPING ON IMPERMEABLE STRUCTURES

TABLE OF CONTENTS

Description	5-2-1
Introduction	5-2-1
General Assumptions and Limitations	5-2-1
Wave Runup	5-2-2
Rough Slope Runup	5-2-2
Smooth Slope Runup	5-2-3
Overtopping Rate	5-2-4
Monochromatic Wave Overtopping	5-2-5
Wind Effects	5-2-5
Irregular Wave Overtopping	5-2-6
References and Bibliography	5-2-7

WAVE RUNUP AND OVERTOPPING ON IMPERMEABLE STRUCTURES

DESCRIPTION

This application provides estimates of wave runup and overtopping on rough and smooth slope structures that are assumed to be impermeable. Run-up heights and overtopping rates are estimated independently or jointly for monochromatic or irregular waves specified at the toe of the structure. The empirical equations suggested by Ahrens and McCartney (1975), Ahrens and Titus (1985), and Ahrens and Burke (unpublished report) are used to predict runup, and Weggel (1976) to predict overtopping. Irregular waves are represented by a significant wave height and are assumed to conform to a Rayleigh distribution (Ahrens, 1977). The overtopping rate is estimated by summing the overtopping contributions from individual runups in the distribution. Portions of the material presented herein can also be found in Chapter 7 of the SPM (1984).

INTRODUCTION

As waves encounter certain types of coastal structures, the water rushes up and sometimes over the structure. These closely related phenomena, wave runup and wave overtopping, often strongly influence the design and the cost of coastal projects. Wave runup is defined as the vertical height above still-water level to which a wave will rise on the structure (of assumed infinite height). Overtopping is the flow rate of water over the top of the finite height structure as a result of wave runup. Waves are assumed to be normally incident to the structure.

GENERAL ASSUMPTIONS AND LIMITATIONS

The various relationships for runup and overtopping employed in this application are empirically derived from physical model studies originally conducted for specific structures and wave climates. General assumptions applicable to the various expressions can be summarized as:

- Waves are normally incident to the structure and are unbroken in the vicinity of the structure toe.
- Waves are considered to be monochromatic. Irregular wave conditions are characterized by significant wave height H_s .
- Waves are specified at the structure location. Linear wave theory is applied to determine unrefracted deepwater wave height where necessary.
- The crest of the structure must be above still-water level.
- For run-up estimates, structures are considered to be impermeable and to have infinite height and simple plane slopes.
- For overtopping estimates, the actual finite structure height is employed. Results for additional structure configurations (such as curved and recurved walls) can be obtained if runup is known.

As reported in the references, the expressions for runup were primarily determined by empirical curve fitting procedures and consequently do not formally represent "best fit" curves derived by statistical procedures. The exception is the expression for smooth slope runup for nonbreaking wave conditions that was developed using regression analysis.

Similarly, the expression for overtopping rate was originally derived by a graphical curve fitting procedure (Weggel, 1976). In practice, the empirical coefficients required for the overtopping rate equation are often difficult to obtain. While a representative value of α is easy to estimate as a function of the structure slope, no satisfactory functional approximations for Q_o^* are available. An estimate is usually made by interpolation or extrapolation of the values presented in the SPM (1984), which are tabulations derived from the original data set and curve fitting procedure.

While expressions empirically derived from model data represent a useful and valid technology, engineering judgment should always be applied to the results, particularly when applying the formulas in situations much different from the bounds and character of the original data from which they were derived.

WAVE RUNUP

Numerous laboratory tests have been conducted over the years resulting in data for wave runup. Figure 5-2-1 shows parameters involved in discussing wave runup, and the next two sections present equations used in ACES for rough and smooth slopes.

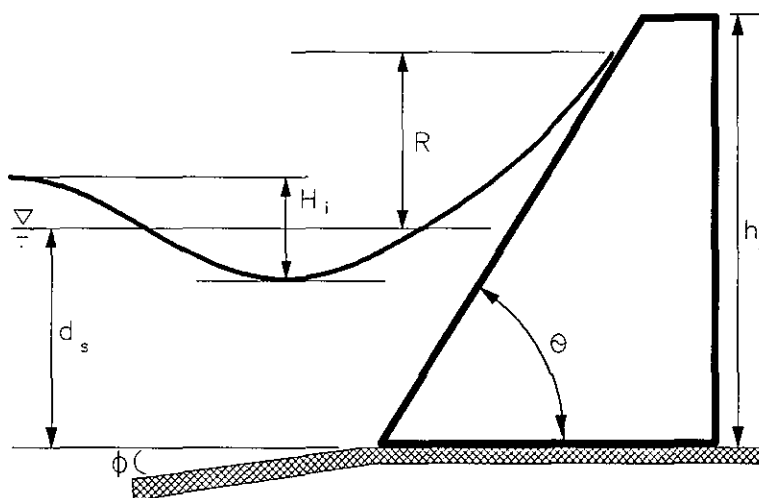


Figure 5-2-1. Wave Runup and Overtopping

Rough Slope Runup

Ahrens and McCartney (1975) present an empirical method for estimating the runup on structures protected by various types of primary armor faces. In their method, the runup is predicted as a nonlinear function of the surf parameter, ξ .

$$R = H_i \frac{\alpha \xi}{1 + b \xi} \quad (1)$$

where

R = runup

H_i = incident wave height

a, b = empirical coefficients associated with corresponding types of armor unit (see Table A-3 of Appendix A)

$$\xi = \frac{\tan \theta}{\sqrt{\frac{H_i}{L_o}}} \quad (2)$$

θ = angle between structure seaward face and horizontal (a measure of structure slope)

L_o = deepwater wavelength

Smooth Slope Runup

Ahrens and Titus (1985) recommend the following general equation for runup on smooth slopes:

$$R = CH_i \quad (3)$$

The coefficient C is characterized by the surf parameter ξ according to the following three wave-structure regimes:

- ° ($\xi \leq 2$) waves plunging directly on the run-up slope.
- ° ($\xi \geq 3.5$) wave conditions that are nonbreaking and are regarded as standing or surging waves.
- ° ($2 < \xi < 3.5$) transition conditions where breaking characteristics are difficult to define.

Recommended expressions for coefficient C corresponding to these regimes are then:

- ° *Plunging wave conditions* ($\xi \leq 2$)

$$C_p = 1.002\xi \quad (4)$$

- *Nonbreaking wave conditions* ($\xi \geq 3.5$)

$$C_{nb} = 1.181 \left(\frac{\pi}{2\theta} \right)^{0.375} \exp \left[3.187 \left(\frac{\eta_c}{H_i} - 0.5 \right)^2 \right] \quad (5)$$

where

η_c = crest height of the wave above the still-water level
calculated using the Stream Function Wave Theory
(Dean, 1974)

- *Transitional wave conditions* ($2 < \xi < 3.5$)

$$C_t = \left(\frac{3.5 - \xi}{1.5} \right) C_p + \left(\frac{\xi - 2}{1.5} \right) C_{nb} \quad (6)$$

This ACES application uses a more convenient but less accurate expression for the coefficient under nonbreaking conditions derived by Ahrens and Burke (unpublished report):

$$C_{nb} = 1.087 \sqrt{\frac{\pi}{2\theta}} + 0.775 \Pi \quad (7)$$

where

Π = Goda's (1983) nonlinearity parameter

$$= \frac{\frac{H_i}{L}}{\tanh^3 \left(\frac{2\pi d_s}{L} \right)} \quad (8)$$

L = incident wavelength

OVERTOPPING RATE

Several consequences of overtopping are important to engineers designing coastal structures. For structures along the shoreline (seawalls, bulkheads, or revetments), the volume of water that flows over the structure significantly impacts backside flooding. For breakwaters, wave transmission to the leeward side is an important criterion in harbor design. Also for breakwaters, the stability of armor material on the backslope of the structure is an important consideration. This ACES methodology estimates the overtopping flow rate for simple structures.

Monochromatic Wave Overtopping

The method implemented within this ACES application was developed by Weggel (1976) using data reported by Saville (1955) and by Saville and Caldwell (1953). It consists of an empirical expression for the monochromatic-wave overtopping rate:

$$Q = C_w \sqrt{g Q_0^* H_0^3} \left(\frac{R+F}{R-F} \right)^{\frac{-0.1085}{\alpha}} \quad (9)$$

where

Q = overtopping rate/unit length of structure

C_w = wind correction factor

g = gravitational acceleration

Q_0^*, α = empirical coefficients (see SPM (1984) figures)

Note: An average value for $\bar{\alpha}$ as a function of structure slope may be approximated by:

$$\bar{\alpha} = 0.06 - 0.0143 \ln(\sin \theta)$$

This option is available in the application.

H_0 = unrefracted deepwater wave height

R = runup

$F = h_s - d_s$ = freeboard

h_s = height of structure

d_s = water depth at structure

Wind Effects

Onshore winds can increase the overtopping rate at a barrier. The effect is dependent upon wind velocity, direction with respect to the axis of the structure, and structure characteristics. This increased overtopping rate is approximated by adjusting the above value for Q with a wind correction factor C_w (SPM, 1984):

$$C_w = 1 + W_f \left(\frac{F}{R} + 0.1 \right) \sin \theta \quad (10)$$

where

$$W_f = \frac{U^2}{1800} \quad (11)$$

U = onshore wind speed (mph)

Irregular Wave Overtopping

Douglass (1986) presents a summary of methods available for estimating overtopping rates from irregular waves. The method summarized below is that of Ahrens (1977) and embodies the following assumptions:

- Run-up values caused by an irregular sea will follow a Rayleigh distribution.
- Significant deepwater wave, $H_{1/3}$, causes the significant runup, $R_{1/3}$.
- α , Q_o^* , and H_o in Weggel's overtopping equation remain constant for all members of the distribution.

Ahrens estimates the overtopping rate by summing the overtopping contributions from the individual members of the run-up distribution:

$$Q = \frac{1}{199} \sum_{i=1}^{199} Q_i \quad (12)$$

where

Q = volume rate of overtopping caused by irregular waves

Q_i = volume rate of overtopping caused by one runup on the run-up distribution

$$= C_w \sqrt{g Q_o^* (H_{so})^3} \left(\frac{R_i + F}{R_i - F} \right)^{\frac{-0.1085}{\alpha}} \quad (13)$$

H_{so} = deepwater significant wave height

R_i = run-up value having exceedance probability p

$$= \sqrt{\frac{\ln \frac{1}{p}}{2}} R_s \quad (14)$$

$$p = 0.005 * i, i = 1, 2, 3, \dots, 199$$

R_s = runup with a given deepwater significant wave height and period

These equations *modify* Weggel's monochromatic expressions to account for the effect of irregular waves when the freeboard, F , is less than the runup of the significant wave, R_s . When the freeboard is greater than the runup, Weggel's equations yield no overtopping while larger runups in the distribution may still overtop the structure. For these relatively high freeboards, the run-up distribution is broken into 999 elements, instead of 199, to better account for the effect of the higher runups. The overtopping equation for this larger distribution becomes:

$$Q = \frac{1}{999} \sum_{i=1}^{999} Q_i \quad (15)$$

where

$$p = 0.001 * i, i = 1, 2, 3, \dots, 999$$

REFERENCES AND BIBLIOGRAPHY

- Ahrens, J. P. 1977. "Prediction of Irregular Wave Overtopping," CERC CETA 77-7, US Army Engineer Waterways Experiment Station, Vicksburg, MS.
- Ahrens, J. P., and Burke, C. E. 1987. Unpublished report of modifications to method cited in above reference.
- Ahrens, J. P., and McCartney B. L. 1975. "Wave Period Effect on the Stability of Riprap," *Proceedings of Civil Engineering in the Oceans/III*, American Society of Civil Engineers, pp. 1019-1034.
- Ahrens, J. P., and Titus, M. F. 1985. "Wave Runup Formulas for Smooth Slopes," *Journal of Waterway, Port, Coastal and Ocean Engineering*, American Society of Civil Engineers, Vol. 111, No. 1, pp. 128-133.
- Battjes, J. A. 1974. "Surf Similarity," *Proceedings of the 14th Coastal Engineering Conference*, Copenhagen, Denmark.
- Dean, R. G. 1974. "Evaluation and Development of Water Wave Theories for Engineering Applications," Vols. 1-2, CERC Special Report No. 1, US Army Engineer Waterways Experiment Station, Vicksburg, MS.
- Douglass, S. L. 1986. "Review and Comparison of Methods for Estimating Irregular Wave Overtopping Rates," Technical Report CERC-86-12, US Army Engineer Waterways Experiment Station, Vicksburg, MS, pp. 6-14.
- Goda, Y. 1983. "A Unified Nonlinearity Parameter of Water Waves," *Report of the Port and Harbour Research Institute*, Vol. 22, No. 3, pp. 3-30.
- Saville, T., Jr. 1955. "Laboratory Data on Wave Run-Up and Overtopping on Shore Structures," TM No. 64, US Army Corps of Engineers, Beach Erosion Board, Washington, DC.
- Saville, T., Jr., and Caldwell, J. M. 1953. "Experimental Study of Wave Overtopping on Shore Structures," *Proceedings, Minnesota International Hydraulics Convention*, Minneapolis, MN.
- Seelig, W. N. 1980. "Two-Dimensional Tests of Wave Transmission and Reflection Characteristics of Laboratory Breakwaters," CERC TR 80-1, US Army Engineer Waterways Experiment Station, Vicksburg, MS.
- Shore Protection Manual*. 1984. 4th ed., 2 Vols., US Army Engineer Waterways Experiment Station, Coastal Engineering Research Center, US Government Printing Office, Washington, DC, Chapter 7, pp. 43-58.
- Smith, O. P. 1986. "Cost-Effective Optimization of Rubble-Mound Breakwater Cross Sections," Technical Report CERC-86-2, US Army Engineer Waterways Experiment Station, Vicksburg, MS, pp. 45-53.
- Weggel, J. R. 1972. "Maximum Breaker Height," *Journal of Waterways, Harbors and Coastal Engineering Division*, American Society of Civil Engineers, Vol. 98, No. WW4, pp. 529-548.
- Weggel, J. R. 1976. "Wave Overtopping Equation," *Proceedings of the 15th Coastal Engineering Conference*, American Society of Civil Engineers, Honolulu, HI, pp. 2737-2755.

WAVE TRANSMISSION ON IMPERMEABLE STRUCTURES

TABLE OF CONTENTS

Description	5-3-1
Introduction	5-3-1
General Assumptions and Limitations	5-3-1
Wave Transmission by Overtopping	5-3-2
Transmission Coefficient for Sloped Structures with Freeboard	5-3-2
Transmission Coefficient for Vertical or Composite Structures	5-3-3
References and Bibliography	5-3-6

WAVE TRANSMISSION ON IMPERMEABLE STRUCTURES

DESCRIPTION

This application provides estimates of wave runup and transmission on rough and smooth slope structures. It also addresses wave transmission over impermeable vertical walls and composite structures. In all cases, monochromatic waves are specified at the toe of a structure that is assumed to be impermeable. For sloped structures, a method suggested by Ahrens and Titus (1985) and Ahrens and Burke (1987) is used to predict runup, while the method of Cross and Sollitt (1971) as modified by Seelig (1980) is used to predict overtopping. For vertical wall and composite structures, a method proposed by Goda, Takeda, and Moriya (1967) and Goda (1969) is used to predict wave transmission.

INTRODUCTION

The transmission of wave energy beyond protective structures involves a number of complex processes. Some incident wave energy may be reflected by the structure, some wave energy may be dissipated by turbulent interaction with primary armor units (if present), some may be dissipated internally by the finer materials beneath the armor layers of an impermeable structure, and some may be transmitted through or over the structure with resultant wave regeneration. Important factors identifiable in the process include the shape and material composition of the structure, the incident wave environment, as well as the degree of immergence or submergence of the structure.

GENERAL ASSUMPTIONS AND LIMITATIONS

The various relationships for runup and transmission employed in this application are empirically derived from physical model studies originally conducted for specific structures and wave climates. For sloped structures, the run-up methodology is described in the section entitled *Wave Runup and Overtopping on Impermeable Structures* of this *ACES Technical Reference*. For convenience, the pertinent assumptions and limitations are restated below. General assumptions applicable to the various methods can be summarized as:

- Waves are monochromatic, normally incident to the structure, and unbroken in the vicinity of the structure toe.
- Waves are specified at the structure location.
- All structure types are considered to be impermeable.
- For sloped structures the crest of the structure must be above still-water level.
- For vertical and composite structures, partial and complete submersion of the structure is considered.
- Run-up estimates on sloped structures require the assumption of infinite structure height and a simple plane slope.
- The expressions for transmission by overtopping use the actual finite structure height.

As reported in the references, the expressions for runup were primarily determined by empirical curve fitting procedures and consequently do not formally represent "best fit" curves derived by statistical procedures. The exception is the expression for smooth slope runup for nonbreaking wave conditions that was developed using regression analysis.

The methodology for wave transmission was also empirically derived. The transmission predicted by the expression for sloped structures with freeboard was tested over the range of $(0 \leq B/h_s \leq 0.86)$ for smooth impermeable structures, and $(0.88 \leq B/h_s \leq 3.2)$ for rough impermeable breakwaters (Seelig, 1980). Seelig also recommended that the expression be applied in the range $(0.006 \leq d_s/gT^2 \leq 0.03)$. For transmission over vertical or composite structures, the empirical coefficients α and β were determined from laboratory experiments for three breakwater types and wave conditions in the range $(0.14 \leq d_s/L \leq 0.5)$ (Goda, 1969, and Seelig, 1976).

While expressions empirically derived from model data represent a useful and valid technology, engineering judgment should always be applied to the results, particularly when applying the formulas in situations much different from the bounds and character of the original data from which they were derived. Familiarity with the history, techniques, and data bounds of original experimental results should complement the use of sound engineering judgment when applying such procedures.

WAVE TRANSMISSION BY OVERTOPPING

In general, wave transmission at structures is characterized by the following expression:

$$H_T = K_{TO} H_i \quad (1)$$

where

H_T = transmitted wave height

K_{TO} = wave transmission coefficient (overtopping)

H_i = incident wave height

The next two sections discuss the wave transmission coefficient for the simple, idealized impermeable structures.

Transmission Coefficient for Sloped Structures with Freeboard

Wave transmission over a sloped breakwater occurs when runup exceeds the freeboard. Some of the pertinent parameters for the following discussion are shown in Figure 5-3-1 below.

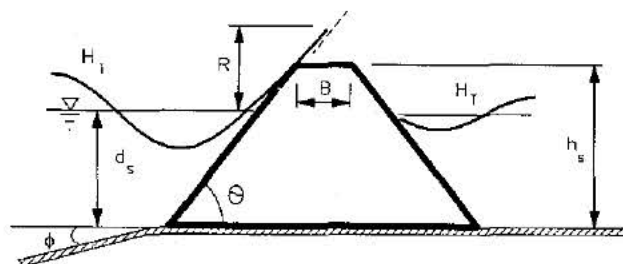


Figure 5-3-1. Transmission over Sloped Structures

The transmission coefficient for sloped structures subject to wave overtopping is estimated by an empirical equation based on the work of Cross and Sollitt (1971) and on 2-D laboratory tests conducted by Seelig (1980).

$$K_{TO} = C \left(1 - \frac{F}{R} \right) \quad (2)$$

where

C = empirical coefficient

$$= 0.51 - 0.11 \frac{B}{h_s} \quad (3)$$

B = crest width of structure

h_s = structure height

$F = h_s - d_s$ = freeboard

d_s = water depth at structure

R = runup

As stated previously, runup is calculated as outlined in the section entitled **Wave Runup and Overtopping on Impermeable Structures** of this *ACES Technical Reference*.

Transmission Coefficient for Vertical or Composite Structures

The transmission coefficient for impermeable vertical-faced structures is estimated by an empirical equation based on the work of Goda, Takeda, and Moriya (1967) and Goda (1969). The equation is presented in Seelig (1976) as:

$$K_{TO} = 0.5 \left\{ 1 - \sin \left[\frac{\pi}{2\alpha} \left(\frac{F}{H_i} + \beta \right) \right] \right\} \quad (4)$$

The empirical coefficients, α and β , were determined from laboratory experiments for three breakwater types for water depth to wavelength ratios of

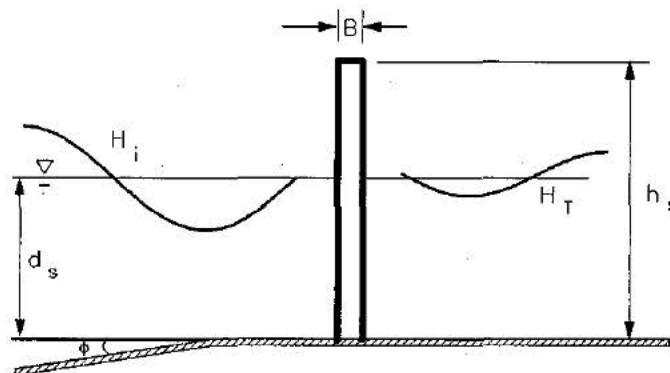
$$0.14 \leq \frac{d_s}{L} \leq 0.5 \quad (5)$$

The breakwater types and definition of terms and symbols are shown in Figure 5-3-2, which is taken from Seelig (1976).

Vertical Thin-Wall Breakwater

$$B \approx 0$$

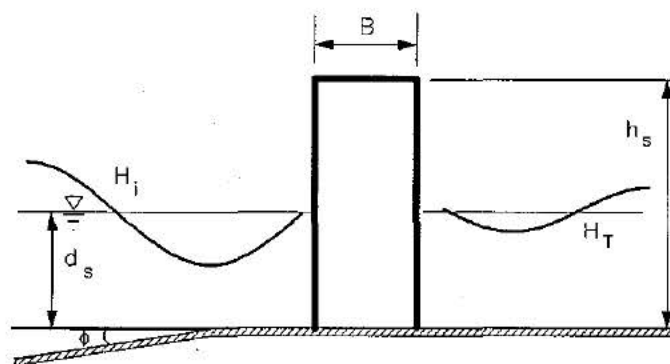
$$\alpha = 1.8 \quad \beta = 0.1$$



Vertical Wall Breakwater

$$B \approx d_s$$

$$\alpha = 2.2 \quad \beta = 0.4$$



Composite Breakwater

$$B \approx d_s$$

$\frac{d_t}{d_s} = 0.3$	$\alpha = 2.2$	$\beta = 0.10$
$\frac{d_t}{d_s} = 0.5$	$\alpha = 2.2$	$\beta = 0.25$
$\frac{d_t}{d_s} = 0.7$	$\alpha = 2.2$	$\beta = 0.35$

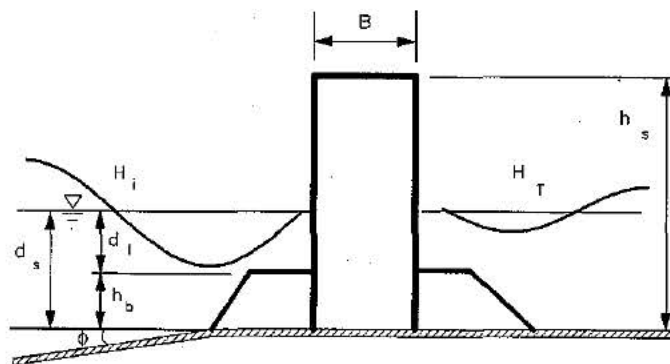


Figure 5-3-2. Transmission over Vertical/Composite Breakwaters (Seelig, 1976)

The range of applicability of K_{T0} is given in Table 5-3-1.

Table 5-3-1 K_{TO} for Vertical and Composite Breakwaters	
K_{TO}	Domain
$K_{TO} = 1.0$	$\frac{F}{H_i} \leq -(\alpha + \beta)$
$K_{TO} = 0.5 \left\{ 1 - \sin \left[\frac{\pi}{2\alpha} \left(\frac{F}{H_i} + \beta \right) \right] \right\}$	$-(\alpha + \beta) < \frac{F}{H_i} < (\alpha - \beta)$
$K_{TO} = 0.0$	$\frac{F}{H_i} \geq (\alpha - \beta)$

β , is defined as

$$\beta = C_1 \beta_1 + C_2 \beta_2 \quad (6)$$

where

$$C_1 = \max \left(0, 1 - \frac{B}{d_s} \right) \quad \text{and} \quad C_2 = \min \left(1, \frac{B}{d_s} \right) \quad (7)$$

Table 5-3-2 presents equations for α and β_1 , and β_2 used to calculate the transmission coefficient for the various breakwater types shown in Figure 5-3-2. These equations were established from analysis of the data in Figure 5-3-2.

Table 5-3-2 α and β_1, β_2 for Vertical and Composite Breakwaters				
Coefficient	Domain - Vertical Breakwaters		Domain - Composite Breakwaters	
	$0 \leq \frac{B}{d_s} < 1.0$	$\frac{B}{d_s} \geq 1.0$	$\frac{d_l}{d_s} \leq 0.3$	$0.3 < \frac{d_l}{d_s} \leq 1.0$
α	$1.8 + 0.4 \left(\frac{B}{d_s} \right)$	2.2	2.2	2.2
β_1	$0.1 + 0.3 \left(\frac{B}{d_s} \right)$	0.4	N/A	N/A
β_2	N/A	N/A	0.1	$0.527 - \frac{0.130}{\left(\frac{d_l}{d_s} \right)}$
d_l = water depth above berm or toe (see Figure 5-3-2)				

REFERENCES AND BIBLIOGRAPHY

- Ahrens, J. P. 1977. "Prediction of Irregular Wave Overtopping," CERC CETA 77-7, US Army Engineer Waterways Experiment Station, Vicksburg, MS.
- Ahrens, J. P., and Burke, C. E. 1987. Unpublished report of modifications to method cited in above reference.
- Ahrens, J. P., and Titus, M. F. 1985. "Wave Runup Formulas for Smooth Slopes," *Journal of Waterway, Port, Coastal and Ocean Engineering*, American Society of Civil Engineers, Vol. 111, No. 1, pp. 128-133.
- Battjes, J. A. 1974. "Surf Similarity," *Proceedings of the 14th Coastal Engineering Conference*, Copenhagen, Denmark.
- Cross, R., and Sollitt, C. 1971. "Wave Transmission by Overtopping," Technical Note No. 15, Massachusetts Institute of Technology, Ralph M. Parsons Laboratory, Boston.
- Douglass, S. L. 1986. "Review and Comparison of Methods for Estimating Irregular Wave Overtopping Rates," Technical Report CERC-86-12, US Army Engineer Waterways Experiment Station, Vicksburg, MS, pp. 6-14.
- Goda, Y. 1969. "Reanalysis of Laboratory Data on Wave Transmission over Breakwaters," *Report of the Port and Harbour Research Institute*, Vol. 8, No. 3.
- Goda, Y. 1983. "A Unified Nonlinearity Parameter of Water Waves," *Report of the Port and Harbour Research Institute*, Vol. 22, No. 3, pp. 3-30.
- Goda, Y., Takeda, H., and Moriya, Y. 1967. "Laboratory Investigation of Wave Transmission over Breakwaters," *Report of the Port and Harbour Research Institute*, No. 13.
- Saville, T., Jr. 1955. "Laboratory Data on Wave Run-Up and Overtopping on Shore Structures," TM No. 64, US Army Corps of Engineers, Beach Erosion Board, Washington, DC.
- Seelig, W. N. 1976. "A Simplified Method for Determining Vertical Breakwater Crest Elevation Considering Wave Height Transmitted by Overtopping," CERC CDM 76-1, US Army Engineer Waterways Experiment Station, Vicksburg, MS.
- Seelig, W. N. 1980. "Two-Dimensional Tests of Wave Transmission and Reflection Characteristics of Laboratory Breakwaters," CERC TR 80-1, US Army Engineer Waterways Experiment Station, Vicksburg, MS.
- Shore Protection Manual*. 1984. 4th ed., 2 Vols., US Army Engineer Waterways Experiment Station, Coastal Engineering Research Center, US Government Printing Office, Washington, DC, Chapter 7, pp. 61-80.
- Smith, O. P. 1986. "Cost-Effective Optimization of Rubble-Mound Breakwater Cross Sections," Technical Report CERC-86-2, US Army Engineer Waterways Experiment Station, Vicksburg, MS, pp. 45-53.
- Weggel, J. R. 1972. "Maximum Breaker Height," *Journal of Waterways, Harbors and Coastal Engineering Division*, American Society of Civil Engineers, Vol. 98, No. WW4, pp. 529-548.

WAVE TRANSMISSION THROUGH PERMEABLE STRUCTURES

TABLE OF CONTENTS

Description	5-4-1
Introduction	5-4-1
General Assumptions and Limitations	5-4-2
Total Wave Transmission	5-4-2
Overtopping Coefficient	5-4-3
Transmission Coefficient	5-4-3
Internal Energy Dissipation	5-4-4
External Energy Dissipation	5-4-8
Synthesis of the Two Preceding Analyses	5-4-12
Hydraulically Equivalent Rectangular Breakwater	5-4-13
References and Bibliography	5-4-16

WAVE TRANSMISSION THROUGH PERMEABLE STRUCTURES

DESCRIPTION

Porous rubble-mound structures consisting of quarry stones of various sizes often offer an attractive solution to the problem of protecting a harbor against wave action. It is important to assess the effectiveness of a given breakwater design by predicting the amount of wave energy transmitted by the structure. This application determines wave transmission coefficients and transmitted wave heights for permeable breakwaters with crest elevations at or above the still-water level. This application can be used with breakwaters armored with stone or artificial armor units. The application uses a method developed for predicting wave transmission by overtopping coefficients using the ratio of breakwater freeboard to wave runup (suggested by Cross and Sollitt, 1971). The wave transmission by overtopping prediction method is then combined with the model of wave reflection and wave transmission through permeable structures of Madsen and White (1976). Seelig (1979,1980) had developed a similar version for mainframe processors.

The material presented here is intended as a brief summary of the methodology. More detailed discussion is presented in Madsen and White (1976) and Seelig (1980).

INTRODUCTION

The transmission of wave energy beyond protective structures involves a number of complex processes. Some incident wave energy may be reflected by the structure, some wave energy may be dissipated by turbulent interaction with primary armor units (if present), some may be dissipated internally by the finer materials beneath the armor layers of a permeable structure, and some may be transmitted through or over the structure with resultant wave regeneration. Important factors identifiable in the process include the shape and material composition of the structure, the incident wave environments, and the degree of immergence or submergence of the structure.

The methodology summarized in the following sections provides an attempt to account for the various processes of wave transmission at an unsubmerged rubble-mound structure subjected to relatively long-period waves. Figure 5-4-1 presents general symbology for the following discussions.

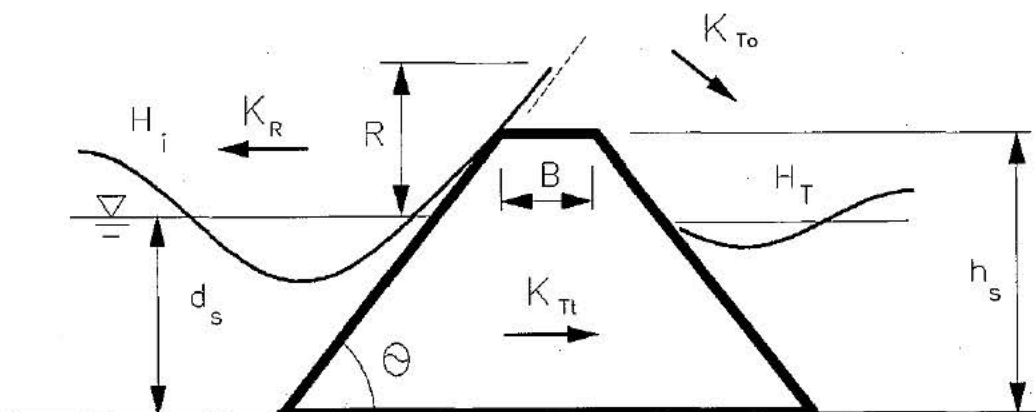


Figure 5-4-1. Wave Transmission over and Through Permeable Breakwaters

GENERAL ASSUMPTIONS AND LIMITATIONS

General assumptions and limitations for the model are:

- Incident waves are periodic, relatively long, and normally incident.
- Fluid motion is adequately described by the linearized governing equations.
- The model can be used only for breakwaters with crests above the still-water line.
- The model can be used for unbroken waves.
- Tests of breakwaters armored with dolos units suggest that the model can be used for artificial armor units.
- Laboratory data showed that the model gives best predictions for shallow-water waves.
- Predictions of transmission coefficients tend to be conservative for transitional or deepwater waves.

TOTAL WAVE TRANSMISSION

A common measure of breakwater performance is that of wave transmission, expressed as a transmission coefficient generally defined as the ratio of the transmitted wave height to the incident wave height.

$$K_T = \frac{H_T}{H_i} \quad (1)$$

where

H_T = transmitted wave height

H_i = incident wave height

There are two basic types of wave transmission considered in this ACES application:

- Wave regeneration caused by overtopping of the structure crest.
- Wave energy transmitted through the permeable materials of the structure.

A total wave transmission coefficient, K_t , is given by

$$K_T = \sqrt{(K_{To})^2 + (K_{Ti})^2} \quad (2)$$

where

K_{To} = overtopping coefficient

K_{Ti} = transmission coefficient

The following sections discuss the formulations for both the overtopping and transmission coefficients.

Overtopping Coefficient

The overtopping transmission coefficient is estimated by an empirical equation based on 2-D laboratory tests (Seelig, 1980).

$$K_{\tau o} = C \left(1 - \frac{F}{R} \right) \quad (3)$$

where

C = empirical coefficient = $0.51 - 0.11(B/h_s)$

$F = h_s - d_s$ = freeboard

h_s = structure height

d_s = water depth

R = wave runup

Wave runup is estimated using the following formula (Ahrens and McCartney, 1975).

$$R = H_i \left(\frac{\alpha \zeta}{1 + b \zeta} \right) \quad (4)$$

where

$\alpha = 0.692$

ζ = surf parameter

$$= \frac{\tan \theta}{\sqrt{\frac{H_i}{L_o}}} \quad (5)$$

θ = angle of seaward face of breakwater

L_o = deepwater wavelength (linear wave theory)

$b = 0.504$

Transmission Coefficient

The coefficient of wave transmission through permeable breakwaters, $K_{\tau t}$, is estimated using the analytical model of Madsen and White (1976). In this model the transmission coefficient is related to a complex function of the following parameters:

- ° Size, porosity, and placement of materials in the breakwater
- ° Breakwater geometry
- ° Seaward slope of the structure
- ° Water depth
- ° Wave height and period
- ° Kinematic viscosity of the water

The Madsen and White model combines an analytical treatment with empirical relationships for the hydraulic characteristics of the porous material and for the friction factor representing energy dissipation on the seaward face of the breakwater. Important assumptions of the model include the following:

- Incident waves are periodic, relatively long, unbroken, and normally incident.
- Fluid motion is adequately described by the linear long-wave equations.

Madsen and White base their analytical solution on the fundamental argument that the problem of reflection from and transmission through a structure may be regarded as one of determining the partition of incident wave energy among reflected, transmitted, and dissipated energy. The analytical model is divided into four analyses.

- Internal energy dissipation - Idealized by considering the problem of the interaction of waves with a homogeneous porous structure of rectangular cross section that is "hydraulically" equivalent to the trapezoidal, multilayered breakwater.
- External energy dissipation - Based upon the associated problem of energy dissipation on a rough impermeable slope.
- Synthesis of the two analyses - Combines the two analyses into a rational procedure for the estimation of reflection and transmission coefficients of trapezoidal, multilayered breakwaters.
- Equivalent breakwater analysis - A simple method to determine characteristics of an idealized homogeneous rectangular breakwater that is hydraulically equivalent to a trapezoidal, multilayered breakwater.

Each of these analyses is briefly discussed in the next four sections.

Internal Energy Dissipation

This section presents a discussion of the treatment of internal energy dissipation within the porous media of the structure. The actual geometry of this portion of the breakwater is replaced by an idealized rectangular crib-style structure of homogeneous material of known properties. The theory also embodies the following additional assumptions:

- The idealized structure is subject to relatively long, normally incident unbroken waves described by linear wave theory.
- The flow resistance within the porous structure is a linear function of velocity.

The theoretical consideration for internal energy dissipation is based upon an analytic solution to simplified long wave equations. The problem domain is depicted in Figure 5-4-2.

Internal energy dissipation is represented by a friction term in the momentum equation only for the subdomain that involves the porous rectangular structure. Within the subdomain representing the structure, a flow resistance of the Dupuit-Forchheimer type (Bear, et al. 1968) is assumed, and an empirical relationship relating flow resistance to stone size, porosity, and fluid viscosity is used to provide a representation of experimentally observed hydraulic properties of porous media. Adopting this empirical formulation of the flow resistance for a porous medium in conjunction with Lorentz' principle of equivalent work leads to a determination of a linearized flow resistance factor in terms of the characteristics of the porous material and the incident wave characteristics.

The resulting analytic solutions to the long-wave equations are manipulated to provide reflection and transmission coefficients for the idealized crib-style breakwater. These coefficients will be used in the synthesis of the separate analyses for energy dissipation and transmission.

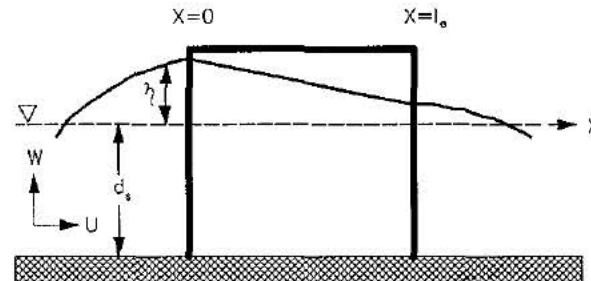


Figure 5-4-2. Wave Transmission Through a Rectangular Porous Breakwater

The equations governing the motion outside and within the structure are

Outside of structure

Within porous structure

$$\left. \frac{\partial \eta}{\partial t} + d_s \left(\frac{\partial U}{\partial x} \right) = 0 \right| \text{continuity} \left| n \frac{\partial \eta}{\partial t} + d_s \left(\frac{\partial U}{\partial x} \right) = 0 \right. \quad (6)$$

$$\left. \frac{\partial U}{\partial t} + g \left(\frac{\partial \eta}{\partial x} \right) = 0 \right| \text{conservation of momentum} \left| \frac{S}{n} \left(\frac{\partial U}{\partial t} \right) + g \left(\frac{\partial \eta}{\partial x} \right) + f \frac{\omega}{n} U = 0 \right. \quad (7)$$

where

η = free surface elevation

d_s = water depth

U = horizontal water particle velocity

g = acceleration due to gravity

S = factor for the effect of unsteady motion (taken as 1)

f = nondimensional friction factor

$\omega = 2\pi/T$ = angular frequency

n = porosity of the porous medium

Since the equations are linear, complex variables may be used. Requiring a periodic solution in terms of radian frequency ω , the following are used:

$$\eta = \zeta(x)e^{i\omega t} \quad (8)$$

$$U = u(x)e^{i\omega t} \quad (9)$$

In these equations $i = \sqrt{-1}$, and the amplitude functions ζ and u are complex functions of x only. Only the real part of the complex solutions for ζ and u constitutes the physical solutions.

General solutions for the governing Partial Differential Equations by region are:

$$\zeta = \alpha_i e^{-ik_o x} + \alpha_r e^{ik_o x} \quad (10)$$

$(x \leq 0)$

$$u = \sqrt{\frac{g}{d_s}} (\alpha_i e^{-ik_o x} - \alpha_r e^{ik_o x}) \quad (11)$$

$$\zeta = \alpha_t e^{-ik_o(x-l_o)} \quad (12)$$

$(x \geq l_o)$

$$u = \sqrt{\frac{g}{d_s}} [\alpha_t e^{-ik_o(x-l_o)}] \quad (13)$$

$$\zeta = \alpha_+ e^{-ikx} + \alpha_- e^{ik(x-l_o)} \quad (14)$$

$(0 \leq x \leq l_o)$

$$u = \sqrt{\frac{g}{d_s}} \frac{n}{\sqrt{s-if}} [\alpha_+ e^{-ikx} - \alpha_- e^{ik(x-l_o)}] \quad (15)$$

where

α_i = complex incident wave amplitude

k_o = wave number

$$= \frac{\omega}{\sqrt{gd_s}} \quad (16)$$

α_r = complex reflected wave amplitude

α_t = complex transmitted wave amplitude

α_+ = complex amplitude of wave propagating in the positive x-direction within the structure

k = complex wave number = $nk_o\sqrt{S-if}$ (17)

α_- = complex amplitude of wave propagating in the negative x-direction within the structure

The general solutions for the motions in the three regions, given Equations 10 through 15, show the problem to involve four unknown quantities. These unknowns are the complex wave amplitudes a_r , a_t , a_+ , and a_- . They may be determined by matching solutions at the common boundaries of the regions and further manipulated to eliminate a_+ and a_- and provide expressions for the complex amplitudes of the transmitted and reflected waves:

$$\frac{\alpha_t}{\alpha_i} = \frac{4\epsilon}{(1+\epsilon)^2 e^{ikl_e} - (1-\epsilon)^2 e^{-ikl_e}} \quad (18)$$

$$\frac{\alpha_r}{\alpha_i} = \frac{(1-\epsilon^2)(e^{ikl_e} - e^{-ikl_e})}{(1+\epsilon)^2 e^{ikl_e} - (1-\epsilon)^2 e^{-ikl_e}} \quad (19)$$

where

$$\epsilon = \frac{\frac{n}{\sqrt{s}}}{\sqrt{\left(1 - \frac{if}{S}\right)}} \quad (20)$$

$$f = \frac{n_r}{k_o l_e} \left\{ \left[1 + \left(1 + \frac{170}{R_d} \right) \frac{16\beta_r}{3\pi} \alpha_t \frac{l_e}{d_s} \right]^{\frac{1}{2}} - 1 \right\} \quad (21)$$

n_r = porosity of reference material = 0.435

l_e = width of idealized breakwater

R_d = particle Reynolds number

$$= \frac{|u_s| d_r}{\nu} \quad (22)$$

$|u_s|$ = horizontal velocity within structure

$$= \alpha_i \sqrt{\frac{g}{d_s}} \left(\frac{1}{1+\lambda} \right) \quad (23)$$

$$\lambda = \frac{k_o l_e f}{2n_r} \quad (24)$$

d_r = 1/2 mean diameter of reference material

ν = kinematic viscosity = 0.0000141

β_r = hydrodynamic characteristic of reference material

$$= 2.7 \left(\frac{1 - n_r}{n_r^3} \right) \frac{1}{d_r} \quad (25)$$

General solutions for the transmission and reflection coefficients for this idealized structure follow directly:

$$T_I = \frac{|\alpha_t|}{\alpha_i} \quad (26)$$

$$R_I = \frac{|\alpha_r|}{\alpha_i} \quad (27)$$

Numerically, T_I , R_I are solved iteratively by first assuming a value for λ and solving for u_s , R_d , f , then solving for a new value of λ , and repeating the procedure until convergence is achieved.

External Energy Dissipation

In the previous section, an analytical solution for the idealized problem of wave transmission through and reflection from rectangular breakwaters was obtained. Since most breakwaters are of trapezoidal, rather than rectangular cross section, a considerable amount of energy may be dissipated on the seaward slope of the breakwater. This external dissipation of energy is not accounted for in the analysis of porous crib-style breakwaters. To account for the external dissipation of energy on the seaward slope of a trapezoidal breakwater, theoretical and empirical relationships are presented for the problem of energy dissipation on a rough, impermeable slope. A theoretical analysis of this problem is based on the following assumptions:

- ° Relatively long, normally incident unbroken waves described by linear wave theory.
- ° Energy dissipation on the rough impermeable slope may be represented as bottom friction.

The problem to be considered is illustrated in Figure 5-4-3.

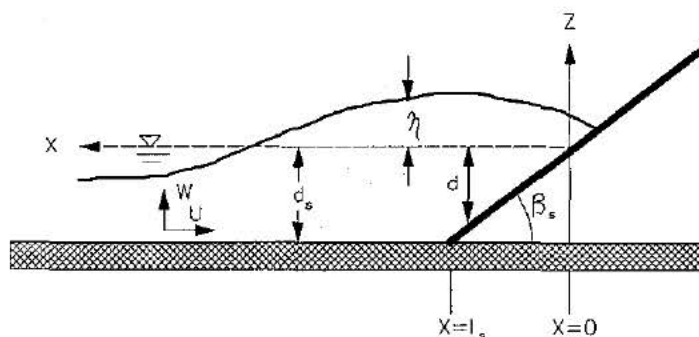


Figure 5-4-3. Wave Runup and Energy Dissipation on Impermeable Slope

The linear long-wave equations for the problem subdomain bounded by the structure slope ($x < l_s$) are given below. These equations also describe the subdomain approaching the structure $x \geq l_s$ with the omission of the friction term in the momentum equation. The orientation of the x -axis has reversed from the previous notation.

<p style="text-align: center;">continuity</p> $\frac{\partial \eta}{\partial t} + \frac{\partial}{\partial x}(dU) = 0$	$\left \right.$	<p style="text-align: center;">conservation of momentum</p> $\frac{\partial U}{\partial t} + g \left(\frac{\partial \eta}{\partial x} \right) + f_b \omega U = 0 \quad (28)$
--	------------------	---

where

- η = surface elevation relative to still water
- d = water depth along sloping breakwater face
- U = horizontal velocity component
- g = acceleration due to gravity
- f_b = linearized bottom friction factor

$$f_b = \frac{\frac{1}{2} f_w |U|}{\omega d} \quad (29)$$

f_w = wave friction factor relating bottom shear stress, τ_b , fluid density, ρ , and velocity

$$\tau_b = \frac{1}{2} \rho f_w |U| U \quad (30)$$

$\omega = \frac{2\pi}{T}$ = radian frequency

Like the previous procedure, the equations are solved by assuming a periodic solution of radian frequency, ω , and introducing complex variables:

$$\eta = \zeta(x)e^{i\omega t} \quad (31)$$

$$U = u(x)e^{i\omega t} \quad (32)$$

General solutions for the governing Partial Differential Equations for the two subdomains are

$$\zeta = \alpha_i e^{ik_o x} + \alpha_r e^{-ik_o x} \quad (33)$$

$(x \geq l_s)$

$$u = -\sqrt{\frac{g}{d_s}} (\alpha_i e^{ik_o x} - \alpha_r e^{-ik_o x}) \quad (34)$$

$$\zeta = AJ_o 2 \left[\frac{\omega^2 (1 - if_b) x}{g \tan \beta_s} \right]^{\frac{1}{2}} \quad (35)$$

$(0 \leq x \leq l_s)$

$$u = -iA \left[\frac{g}{(1 - if_b) x \tan \beta_s} \right]^{\frac{1}{2}} J_1 2 \left[\frac{\omega^2 (1 - if_b) x}{g \tan \beta_s} \right]^{\frac{1}{2}} \quad (36)$$

where

α_i = amplitude of incident wave

$$k_o = \frac{\omega}{\sqrt{gd_s}} \quad (37)$$

d_s = constant water depth seaward of breakwater

α_r = complex amplitude of reflected wave

l_s = submerged horizontal length of the impermeable slope

A = arbitrary constant that is the complex vertical amplitude of the wave motion at the intersection of the still-water level and the slope. The modulus (or magnitude) $|A|$ is treated as an approximate value of the runup on the slope.

J_o = Bessel function of the first kind of order zero

β_s = angle of impermeable slope

J_1 = Bessel function of the first kind of order one

Simultaneous solution at their common boundary ($x = l_s$) yields:

$$\alpha_i e^{ik_o l_s} + \alpha_r e^{-ik_o l_s} = A J_o 2k_o l_s \sqrt{1 - if_b} \quad (38)$$

$$\alpha_i e^{ik_o l_s} - \alpha_r e^{-ik_o l_s} = A \frac{i}{\sqrt{1 - if_b}} J_1 2k_o l_s \sqrt{1 - if_b} \quad (39)$$

The above complex solutions may be manipulated to produce expressions for reflection and runup on rough impermeable slopes:

$$\frac{\alpha_r}{\alpha_i} = \left(\frac{J_o 2k_o l_s \sqrt{1 - if_b} - \frac{i}{\sqrt{1 - if_b}} 2J_1 k_o l_s \sqrt{1 - if_b}}{J_o 2k_o l_s \sqrt{1 - if_b} + \frac{i}{\sqrt{1 - if_b}} 2J_1 k_o l_s \sqrt{1 - if_b}} \right) e^{i2k_o l_s} \quad (40)$$

$$\frac{A}{2\alpha_i} = \frac{e^{ik_o l_s}}{J_o 2k_o l_s \sqrt{1 - if_b} + \frac{i}{\sqrt{1 - if_b}} 2J_1 k_o l_s \sqrt{1 - if_b}} \quad (41)$$

Expressions for a reflection coefficient and nondimensional run-up amplitude follow directly:

$$R_{II} = \frac{|\alpha_r|}{\alpha_i} \quad (42)$$

$$R_u = \frac{|A|}{2\alpha_i} \quad (43)$$

The important parameters in determining the reflected wave amplitude and the run-up amplitude are the submerged horizontal length of the slope relative to incident wavelength, l_s/L and the linearized friction factor, f_b . Since the linearized friction factor appears in the form $\sqrt{1 - if_b}$, it is expedient to introduce the friction angle ϕ defined by

$$\tan 2\phi = f_b \quad (44)$$

since

$$\sqrt{1 - if_b} = (1 + \tan^2 2\phi)^{\frac{1}{4}} e^{-i\phi} \quad (45)$$

The expression for the friction angle ϕ , is

$$\tan 2\phi = f_w \frac{|A|}{d_s} \frac{1}{\tan \beta_s} F_s \quad (46)$$

where

f_w = wave friction factor (empirically determined)

$$= 0.29 \left(\frac{d}{d_s} \right)^{-0.5} \left(\frac{d \tan \beta_s}{|A|} \right)^{0.7} \quad (47)$$

d = average stone diameter

F_s = slope friction constant

$$= \frac{4}{3\pi} \frac{\int_0^1 \left(\frac{J_1(2\psi\sqrt{y})}{\psi\sqrt{y}} \right)^3 dy}{\int_0^1 y \left(\frac{J_1(2\psi\sqrt{y})}{\psi\sqrt{y}} \right)^2 dy} \quad (48)$$

$$\psi = k_o l_s \sqrt{1 - i \tan 2\phi} \quad (49)$$

$$y = \frac{x}{l_s} \quad (50)$$

These equations are solved iteratively by first assuming a value of ϕ , next evaluating R_u and F_s , then calculating a new ϕ , and repeating the procedure until convergence is achieved.

Synthesis of the Two Preceding Analyses

This section discusses the synthesis of the results of the two preceding analyses. The procedure provides approximate values for wave reflection and transmission for trapezoidal multilayered rubble-mound breakwaters.

For most trapezoidal, multilayered breakwaters, the stone size in the layer under the armor layer of the seaward slope is small relative to the material of the armor layer. As a first approximation, the structure may therefore be treated as having an impermeable rough slope. Thus, with incident wave characteristics, rubble-mound armor, and seaward structure slope, the procedure developed in the section entitled **External Energy Dissipation** may be used to approximately account for the energy dissipation on the seaward slope. The remaining wave energy may be expressed as the energy associated with a progressive wave of the following amplitude:

$$\alpha_I = R_{II} \alpha_i \quad (51)$$

where

α_I = wave amplitude representing remaining energy after dissipation on the seaward slope of the breakwater

R_{II} = reflection coefficient of a rough impermeable sloped structure (from external energy dissipation analysis)

α_i = amplitude of incident wave

This remaining energy (represented by wave amplitude α_i) is partitioned among the reflected, transmitted, and internally dissipated energy of a hydraulically equivalent homogeneous rectangular breakwater for which a reflection coefficient R_i and transmission coefficient T_i have been determined as shown in the section entitled **Internal Energy Dissipation**. A rational method for obtaining a homogeneous rectangular breakwater that is hydraulically equivalent to a trapezoidal, multilayered breakwater is developed in the next section entitled **Hydraulically Equivalent Rectangular Breakwater**.

Having now accounted for the external as well as the internal energy dissipation, the amplitude of the reflected wave is found to be

$$|\alpha_r| = R_i \alpha_i = R_i R_{ii} \alpha_i \quad (52)$$

The transmitted wave amplitude is

$$|\alpha_t| = T_i \alpha_i = T_i R_{ii} \alpha_i \quad (53)$$

Therefore, the approximate values of the reflection R and transmission coefficients K_{Ti} of a trapezoidal, multilayered breakwater are

$$R = \frac{|\alpha_r|}{\alpha_i} = R_i R_{ii} \quad (54)$$

$$K_{Ti} = \frac{|\alpha_t|}{\alpha_i} = T_i R_{ii} \quad (55)$$

Hydraulically Equivalent Rectangular Breakwater

This section will present a method for determining an idealized homogeneous rectangular breakwater that is hydraulically equivalent to a trapezoidal, multilayered breakwater.

A hydraulically equivalent breakwater is taken as a homogeneous rectangular breakwater that yields the same discharge as would an actual trapezoidal, multilayered breakwater *with its top layer of stones on the seaward slope removed*. This definition of the equivalent breakwater is illustrated schematically in Figure 5-4-4. Typical realistic breakwaters consist of several different porous materials that are identified by their stone size, d_n , and their hydraulic characteristics, β_n . The idealized homogeneous rectangular breakwater consists of a reference material of stone size, d_r , and hydraulic characteristics, β_r . The reference material is considered representative of the porous materials of the multilayered breakwater.

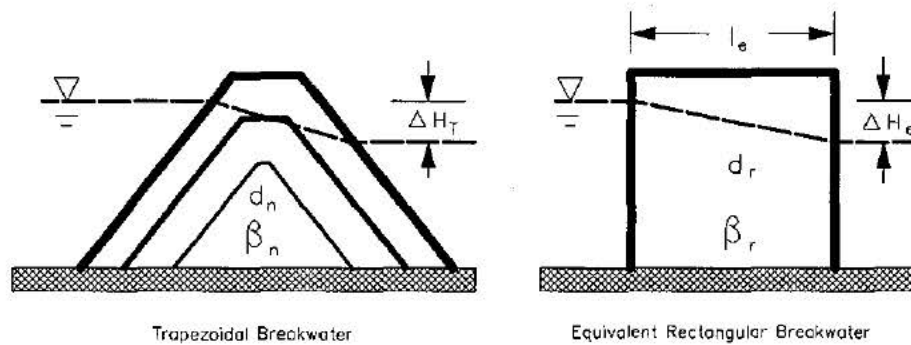


Figure 5-4-4. A Multilayered Trapezoidal Breakwater and Its Idealized Homogeneous Rectangular Equivalent

The flow through the structure is assumed to be one-dimensional (1-D), and the discharge per unit length of the equivalent rectangular breakwater is

$$Q_{\text{equivalent structure}} = \sqrt{\left(\frac{g \Delta H_e}{\beta_r}\right)} \frac{d_s}{\sqrt{l_e}} \quad (56)$$

where

g = acceleration due to gravity

ΔH_e = head difference

β_r = hydrodynamic characteristic of reference breakwater

d_s = water depth

l_e = width of the equivalent breakwater

To evaluate the discharge per unit length of the multilayered trapezoidal breakwater, the structure is segmented into horizontal slices. The slices may be selected arbitrarily; however, it is expeditious to place them at material boundaries or at elevations where slopes change. A typical horizontal slice of height, Δh_j , is shown in Figure 5-4-5. Each slice consists of segments of different porous materials with individual hydraulic characteristics, β_n , and lengths, l_n .

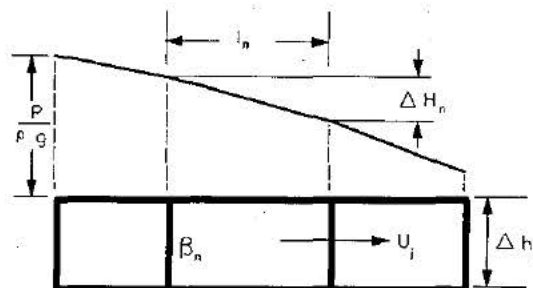


Figure 5-4-5. Illustrative Slice of a Multilayered Trapezoidal Breakwater Section

By summing contributions from all horizontal slices of the trapezoidal breakwater, the total discharge is

$$Q_{\frac{\text{trapezoidal}}{\text{breakwater}}} = \sqrt{\left(\frac{g \Delta H_T}{\beta_r}\right)} d_s \sum_j \left[\frac{1}{\sqrt{\sum_n \left(\frac{\beta_n}{\beta_r} l_n\right)}} \left(\frac{\Delta h_j}{d_s}\right) \right] \quad (57)$$

It is required that the discharges per unit length for the rectangular and trapezoidal breakwaters be identical:

$$Q_{\frac{\text{equivalent}}{\text{structure}}} = Q_{\frac{\text{trapezoidal}}{\text{breakwater}}} \quad (58)$$

The above relationship is reordered to solve for l_e , the equivalent rectangular breakwater.

$$l_e = \left\{ \sum_j \left[\frac{1}{\sqrt{\sum_n \left(\frac{\beta_n}{\beta_r} l_n\right)}} \left(\frac{\Delta h_j}{d_s}\right) \right] \right\}^{-2} \left(\frac{\Delta H_e}{\Delta H_T} \right) \quad (59)$$

where

\sum_j = summation over number of layers in the breakwater

\sum_n = summation over number of materials in the breakwater

$$\beta_n = \beta_o \left(\frac{1 - n_n}{n_n^3} \right) \frac{1}{d_n} \quad (60)$$

$$\beta_o = 2.7$$

d_n = mean diameter of individual material

$$\beta_r = \beta_o \left(\frac{1 - n_r}{n_r^3} \right) \frac{1}{d_r} \quad (61)$$

$$n_r = 0.435$$

d_r = mean diameter of reference material

The equation for l_e shows that the width of the equivalent breakwater may be determined from knowledge of the configuration of the trapezoidal, multilayered breakwater and the corresponding head differences, ΔH_e and ΔH_T .

Runup on the seaward face of both the equivalent and trapezoidal breakwater is taken as a representative value of the head difference.

$$\Delta H_e = (1 + R_I) \alpha_I = (1 + R_I) R_{II} \alpha_I \quad (62)$$

$$\Delta H_T = R_u H_i = 2 R_u \alpha_i \quad (63)$$

where

$$H_i = 2\alpha_i = \text{incident wave height}$$

$$\frac{\Delta H_e}{\Delta H_T} = \frac{(1 + R_I) R_{II}}{2 R_u} \quad (64)$$

The head difference ratio is a function of the reflection coefficient R_I of the equivalent breakwater, which cannot be determined till the width of the equivalent breakwater l_e is known (i.e., an iterative procedure).

REFERENCES AND BIBLIOGRAPHY

- Ahrens, J. P., and McCartney B. L. 1975. "Wave Period Effect on the Stability of Riprap," *Proceedings of Civil Engineering in the Oceans/III*, American Society of Civil Engineers, pp. 1019-1034.
- Bear, J., et al. 1968. *Physical Principles of Water Percolation and Seepage*, United Nations Educational, Scientific and Cultural Organization.
- Cross, R., and Sollitt, C. 1971. "Wave Transmission by Overtopping," Technical Note No. 15, Ralph M. Parsons Laboratory, Massachusetts Institute of Technology, Boston.
- Madsen, O. S., and White, S. M. 1976. "Reflection and Transmission Characteristics of Porous Rubble-Mound Breakwaters," CERC MR 76-5, US Army Engineer Waterways Experiment Station, Vicksburg, MS.
- Morris, A. H. 1981. "NSWC/DL Library of Mathematics Subroutines," NSWC-TR-81-410, Naval Surface Weapons Center, Dahlgren, VA.
- Seelig, W. N. 1979. "Estimation of Wave Transmission Coefficients for Permeable Breakwaters," CERC CETA 79-6, US Army Engineer Waterways Experiment Station, Vicksburg, MS.
- Seelig, W. N. 1980. "Two-Dimensional Tests of Wave Transmission and Reflection Characteristics of Laboratory Breakwaters," CERC TR 80-1, US Army Engineer Waterways Experiment Station, Vicksburg, MS.

LONGSHORE SEDIMENT TRANSPORT

TABLE OF CONTENTS

Description	6-1-1
Introduction	6-1-1
General Assumptions and Limitations	6-1-2
General Energy Flux Equation	6-1-2
Energy Flux Equation (Breaking Wave Conditions)	6-1-3
Energy Flux Equation (Deepwater Wave Conditions)	6-1-4
Estimating Potential Sand Transport Rates Using WIS-CEDRS Data	6-1-5
Wave Transformation Procedure	6-1-6
Coastal Engineering Data Retrieval System	6-1-6
References and Bibliography	6-1-7

LONGSHORE SEDIMENT TRANSPORT

DESCRIPTION

This application provides estimates of the *potential* longshore transport rate under the action of waves. The method used is based on the empirical relationship between the longshore component of wave energy flux entering the surf zone and the immersed weight of sand moved (Galvin, 1979). Three methods are available to the user depending on whether available input data are breaker wave height and direction, deepwater wave height and direction, or using a Wave Information Study (WIS) hindcast data file created by the Coastal Engineering Data Retrieval System (CEDRS). The material presented herein can be found in Chapter 4 of the *Shore Protection Manual* (1984) and in Gravens (1988).

INTRODUCTION

The longshore transport rate, Q , is the volumetric rate of movement of sand parallel to the shoreline. Much longshore transport occurs in or near the surf zone and is caused by the approach of waves at an angle to the shoreline. Q is expressed in terms of sand volume per unit time (such as cubic yards per year or cubic meters per year). The method used to calculate the longshore transport in this ACES application is based on the assumption that longshore transport rate Q is dependent upon the longshore component of wave energy flux P_{ls} entering the surf zone (Equation 4-49 of the SPM (1984)).

$$Q = \frac{K}{(\rho_s - \rho)g\alpha} P_{ls} \quad (\text{unit volume per sec}) \quad (1)$$

where

K = dimensionless empirical coefficient (based on field measurements)

= 0.39

ρ_s = density of sand

ρ = density of water

g = acceleration due to gravity

α = ratio of the volume of solids to total volume, accounting for sand porosity

= 0.6

GENERAL ASSUMPTIONS AND LIMITATIONS

General assumptions and limitations used to derive the longshore energy flux in the surf zone are:

- Conservation of energy flux in shoaling waves.
- Linear wave theory.
- Evaluating the energy flux relation at the breaker position.
- Breaker characteristics described by solitary wave theory.
- Straight bathymetric contours parallel to the shoreline.

Judgment is required in using the empirical relationship between longshore transport rate and the energy flux factor (Equation 1). The accuracy of Q found using the energy flux factor can be estimated to be ± 50 percent (SPM, 1984).

GENERAL ENERGY FLUX EQUATION

The energy flux per unit length of wave crest or, equivalently, the rate at which wave energy is transmitted across a plane of unit width perpendicular to the direction of wave advance is

$$P = E C_g \quad (2)$$

where

E = wave energy density

C_g = wave group speed

The wave energy density is calculated by:

$$E = \frac{\rho g H^2}{8} \quad (3)$$

where

ρ = mass density of water

g = acceleration of gravity

H = wave height

If the wave crests make an angle α with the shoreline, the energy flux in the direction of wave advance *per unit length of beach* is

$$P \cos \alpha = \frac{\rho g H^2}{8} C_g \cos \alpha \quad (4)$$

The longshore component of wave energy flux is

$$P_l = P \cos \alpha \sin \alpha = \frac{\rho g H^2}{8} C_g \cos \alpha \sin \alpha \quad (5)$$

By use of the identity

$$\cos \alpha \sin \alpha = \frac{1}{2} \sin 2\alpha \quad (6)$$

the general equation for P_l becomes

$$P_l = \frac{\rho g}{16} H^2 C_g \sin 2\alpha \quad (7)$$

Up to this point, all results have been for small-amplitude linear wave theory. However, the assumed relation between longshore transport and energy flux in the surf zone requires that P_l be evaluated at the breaker line, where small-amplitude theory is less valid. To indicate approximations for waves entering the surf zone, the symbol P_{ls} will be used in place of P_l . This approximation is called the energy flux factor P_{ls} in the SPM (1984), and like P_l , it is measured in units of energy per second per unit length of shoreline. The next two sections derive approximate formulas for computing the longshore energy flux factor P_{ls} entering the surf zone based on known breaking or deepwater significant wave conditions.

Energy Flux Equation (Breaking Wave Conditions)

If the breaker values of the wave characteristics (H_{sb} significant breaker height and α_b angle of approach) are applied to Equation 7, the energy flux factor results.

$$P_{ls} = \frac{\rho g}{16} H_{sb}^2 C_{gb} \sin 2\alpha_b \quad (8)$$

From linear wave theory

$$C_{gb} = n C_b \quad (9)$$

where

$$n \approx 1.0 \text{ (in shallow water)}$$

$$C_b = \text{wave phase speed at breaking}$$

Group velocity equals wave speed at breaking, and breaking speed is given by solitary wave theory according to the approximation (Galvin and Schweppe, 1980):

$$C_b = 8.02 \sqrt{H_b} \quad (10)$$

Substituting Equation 10 into Equation 8 and simplifying yields the longshore energy flux factor for breaking wave conditions (Equation 4-44 of the SPM (1984)).

$$P_{ls} = 0.0884 \rho g^{\frac{3}{2}} H_{sb}^{\frac{5}{2}} \sin 2\alpha_b \quad (11)$$

Energy Flux Equation (Deepwater Wave Conditions)

Using deepwater values of wave characteristics (H_{s0} significant wave height and α_0 angle of approach), Equation 7 becomes:

$$P_{ls} = \frac{\rho g}{16} H_{s0}^2 C_{gb} \sin 2\alpha_0 \quad (12)$$

Again, from linear wave theory:

$$C_{gb} = n C_b \quad (13)$$

where

$$n \approx \frac{1}{2} \text{ (in deep water)}$$

Again, using solitary wave theory for breaker characteristics (Galvin and Schweppe, 1980):

$$C_b = 8.02 \sqrt{H_b} \quad (14)$$

Local wave height H_b can be related to deepwater height H_0 by refraction and shoaling coefficients, where the coefficients are evaluated at the breaker position.

$$\sqrt{H_b} = \sqrt{K_r K_s H_0} \quad (15)$$

where

K_r = refraction coefficient

$$\sqrt{K_r} = \left(\frac{\cos \alpha_0}{\cos \alpha_b} \right)^{\frac{1}{4}} \quad (16)$$

K_s = shoaling coefficient (approximated by the breaker height index) = 1.3 (Galvin and Schweppe, 1980)

In Equation 16, $\cos \alpha_b$ equals 1.0 to a good approximation. For example, if α_b has a high value of 20° , then $(\cos 20^\circ)^{1/4} = 0.98$.

Substituting the above variables into Equation 11 for P_{ls} and simplifying yields the longshore energy flux factor entering the surf zone using deepwater wave conditions (Equation 4-45 of the SPM (1984)).

$$P_{ls} = 0.05 \rho g^{\frac{3}{2}} H_{s0}^{\frac{5}{2}} (\cos \alpha_0)^{\frac{1}{4}} \sin 2\alpha_0 \quad (17)$$

Estimating Potential Sand Transport Rates Using WIS-CEDRS Data

The following paragraphs describe the procedure that is used in this ACES application for calculating potential longshore transport rates using WIS hindcast wave estimates as provided in a specially formatted data file by the CEDRS (see section titled *Coastal Engineering Data Retrieval System*).

The potential longshore sand transport rate using WIS-CEDRS data is calculated using Equations 1 and 11 which require the breaking wave height and incident angle with respect to the shoreline. WIS-CEDRS hindcast estimates, however, are given for water depths greater than or equal to 10 meters (Jensen, 1983). Therefore, a transformation of the WIS-CEDRS hindcast wave estimates to breaking conditions is necessary. Refraction and shoaling of incident waves provided by WIS-CEDRS is accomplished using linear wave theory and numerically solving Snell's law for wave direction and the equation of conservation of wave energy flux for wave height. The governing equations are given below (Coastal Engineering Technical Note-II-19, 1989). The subscripts 0 and b denote values in deep water and at breaking, respectively.

Wave direction is obtained through Snell's law

$$\frac{\sin(\alpha_0)}{L_0} = \frac{\sin(\alpha_b)}{L_b} \quad (18)$$

where

α_0 = deepwater wave approach angle (extracted from the CEDRS data file)

α_b = wave breaker angle

L = wavelength

$$= \frac{gT^2}{2\pi} \tanh\left(\frac{2\pi d}{L}\right) \quad (19)$$

T = wave period (extracted from the CEDRS data file)

The wave height is obtained by invoking the conservation of wave energy flux directed onshore

$$E_0 C_{g0} \cos(\alpha_0) = E_b C_{gb} \cos(\alpha_b) \quad (20)$$

where

$E_{0/b}$ = wave energy

$$= \frac{1}{8} \rho g H_{0/b}^2$$

H_0 = deepwater wave height (extracted from the CEDRS data file)

H_b = breaking wave height

C_g = wave group speed

$$= \frac{L}{2T} \left[1 + \frac{\frac{4\pi d}{L}}{\sinh \frac{4\pi d}{L}} \right]$$

The breaking wave height is linearly related to the depth at breaking as

$$H_b = \gamma d_b \quad (21)$$

where

$$\begin{aligned} \gamma &= \text{wave breaking index} \\ &= 0.78 \end{aligned}$$

Wave Transformation Procedure

The first step in the wave transformation procedure (Gravens, 1988) is to calculate the wavelength (Equation 19) at the location (denoted by subscript 0) where the wave height, incident angle, period, and water depth are known. These parameters are read by this ACES application directly from the *formatted* WIS-CEDRS data file. Equation 19 is solved by using a Newton-Raphson iteration.

The second step is to determine wave height, water depth, and incident angle at breaking (denoted by subscript b in Equations 18 and 20). Equation 18 is first solved for $\cos \alpha_b$ and substituted together with Equation 21 into the right-hand side of Equation 20. This yields an expression for the conservation of wave energy flux in terms of the known wave characteristics (left-hand side of Equation 20) and the unknown wave characteristics at breaking (right-hand side of Equation 20). Equation 19 evaluated at breaking gives another expression in terms of the wavelength and water depth at breaking. A Newton-Raphson type solution can be used to iterate for the two unknown variables of wavelength and water depth at breaking.

Having determined the wavelength and depth at breaking, breaking wave height is calculated using Equation 21, and the breaking wave angle is calculated using Equation 18. The potential longshore sand transport rate is then estimated using Equations 1 and 11.

Coastal Engineering Data Retrieval System

The CEDRS (available only to Corps of Engineers offices) is an interactive microcomputer resident database system, distinct and separate from ACES, which provides both hindcast and measured wind and wave data for use in the field of coastal engineering. The general goal of CEDRS is to assemble, archive, and make available regional databases containing data applicable to requirements of individual coastal Districts of the Corps of Engineers. The CEDRS databases contain both measured data from several sources and computer model generated hindcast data. The CEDRS system resides completely on an auxiliary hard disk furnished for each regional database. For more information regarding the system, forward inquiries to:

Coastal Engineering Research Center
US Army Engineer Waterways Experiment Station
ATTN: CEWES-CR-O
3909 Halls Ferry Road
Vicksburg, MS 39180-6199

The CEDRS data file that is used by this ACES application provides percent occurrence tables of waves in height and period ranges for specified direction bands at numerous stations on all US coasts. Values in the tables represent the percentage of a 20- or 32-year period during

which waves occur from specified azimuth ranges for the indicated height and period ranges (see reports in the *References and Bibliography* section dealing with Wave information Studies of US Coastlines for more information).

REFERENCES AND BIBLIOGRAPHY

- Coastal Engineering Technical Note II-19. 1989. "Estimating Potential Longshore Sand Transport Rates Using WIS Data," US Army Engineer Waterways Experiment Station, Vicksburg, MS.
- Galvin, C. J. 1979. "Relation Between Immersed Weight and Volume Rates of Longshore Transport," CERC TP 79-1, US Army Engineer Waterways Experiment Station, Vicksburg, MS.
- Galvin, C. J., and Schweppe, C. R. 1980. "The SPM Energy Flux Method for Predicting Longshore Transport Rate," CERC TP 80-4, US Army Engineer Waterways Experiment Station, Vicksburg, MS.
- Gravens, M. B. 1988. "Use of Hindcast Wave Data for Estimation of Longshore Sediment Transport," *Proceedings of the Symposium on Coastal Water Resources*, American Water Resources Association, Wilmington, NC, pp. 63-72.
- Shore Protection Manual*. 1984. 4th ed., 2 Vols., US Army Engineer Waterways Experiment Station, Coastal Engineering Research Center, US Government Printing Office, Washington, DC, Chapter 4, pp. 89-107.
- Vitale, P. 1980. "A Guide for Estimating Longshore Transport Rate Using Four SPM Methods," CERC CETA 80-6, US Army Engineer Waterways Experiment Station, Vicksburg, MS.

Wave Information Studies of US Coastlines

- Corson, W. D., Able, C. E., Brooks, R. M., Farrar, P. D., Groves, B. J., Payne, J. B., McAneny, D. S., and Tracy, B. A. 1987. "Pacific Coast Hindcast Phase II Wave Information," Wave Information Studies of US Coastlines, WIS Report 16, US Army Engineer Waterways Experiment Station, Vicksburg, MS.
- Driver, D. B., Reinhard, R. D., and Hubertz, J. M. 1991. "Hindcast Wave Information for the Great Lakes: Lake Erie," Wave Information Studies of US Coastlines, WIS Report 22, US Army Engineer Waterways Experiment Station, Vicksburg, MS.
- Driver, D. B., Reinhard, R. D., and Hubertz, J. M. 1992. "Hindcast Wave Information for the Great Lakes: Lake Superior," Wave Information Studies of US Coastlines, WIS Report 23, US Army Engineer Waterways Experiment Station, Vicksburg, MS.
- Hubertz, J. M., and Brooks, R. M. 1989. "Gulf of Mexico Hindcast Wave Information," Wave Information Studies of US Coastlines, WIS Report 18, US Army Engineer Waterways Experiment Station, Vicksburg, MS.
- Hubertz, J. M., Driver, D. B., and Reinhard, R. D. 1991. "Hindcast Wave Information for the Great Lakes: Lake Michigan," Wave Information Studies of US Coastlines, WIS Report 24, US Army Engineer Waterways Experiment Station, Vicksburg, MS.
- Jensen, R. E. 1983. "Atlantic Coast Hindcast, Shallow-Water Significant Wave Information," Wave Information Studies of US Coastlines, WIS Report 9, US Army Engineer Waterways Experiment Station, Vicksburg, MS.
- Reinhard, R. D., Driver, D. B., and Hubertz, J. M. 1991. "Hindcast Wave Information for the Great Lakes: Lake Huron," Wave Information Studies of US Coastlines, WIS Report 26, US Army Engineer Waterways Experiment Station, Vicksburg, MS.

Reinhard, R. D., Driver, D. B., and Hubertz, J. M. 1991. "Hindcast Wave Information for the Great Lakes: Lake Ontario," Wave Information Studies of US Coastlines, WIS Report 25, US Army Engineer Waterways Experiment Station, Vicksburg, MS.

NUMERICAL SIMULATION OF TIME-DEPENDENT BEACH AND DUNE EROSION

TABLE OF CONTENTS

Description	6-2-1
Introduction	6-2-1
General Assumptions and Limitations	6-2-1
Theoretical Development of the Model	6-2-2
Numerical Solution	6-2-4
Initial Boundary Conditions	6-2-6
Model Capabilities	6-2-7
References and Bibliography	6-2-8

NUMERICAL SIMULATION OF TIME-DEPENDENT BEACH AND DUNE EROSION

DESCRIPTION

This application is a numerical beach and dune erosion model that predicts the evolution of an equilibrium beach profile from variations in water level and breaking wave height as occur during a storm. The model is one-dimensional (only onshore-offshore sediment transport is represented). It is based on the theory that an equilibrium profile results from uniform wave energy dissipation per unit volume of water in the surf zone. The general characteristics of the model are based on a model described by Kriebel (1982, 1984a, 1984b, 1986). Because of the complexity of this methodology and the input requirements, familiarization with the above references is strongly recommended.

INTRODUCTION

The model described herein, called XSHORE, is a 1-D model in that only cross-shore sediment transport is represented. This implies that the effect of longshore transport is negligible as, for example, if the gradient of longshore transport were near zero. The model is based on the theory that the equilibrium shape of a beach profile is related to uniform wave energy dissipation per unit volume of water in the surf zone under breaking waves (Dean, 1977).

GENERAL ASSUMPTIONS AND LIMITATIONS

General assumptions and limitations adopted in developing the beach and dune erosion numerical model are:

- ° An equilibrium beach profile can be attained if a beach is exposed to constant wave and water level conditions for a sufficiently long time.
- ° Longshore sediment transport is neglected, and beach and dune erosion results solely from cross-shore transport.
- ° The model is restricted to calculating beach and dune erosion; i.e., recovery (accretive) processes are not well represented.
- ° Cross-shore sediment transport is caused by breaking of short-period waves.
- ° Wave transformation in the nearshore is approximated using the assumptions of straight and parallel bathymetric contours and linear wave theory.
- ° Surf zone wave heights are assumed to be proportional to the local water depth.
- ° Wave runup and setup can be neglected.
- ° Waves are considered normally incident inside the surf zone.
- ° Median grain size (sand-size material) is constant along the profile.

THEORETICAL DEVELOPMENT OF THE MODEL

The development of the model begins by assuming that the nearshore profile can be described by a monotonic function of depth, h , which increases in the seaward direction, x , across the actively modified portion of the profile according to the relationship (Bruun, 1954; Dean, 1977)

$$h = Ax^{\frac{2}{3}} \quad (1)$$

where A is a profile shape coefficient that has been shown to be correlated with median grain size (Moore, 1982). The coefficient A governs the steepness of the subaqueous beach profile and has been related to a unique value of the wave energy dissipation per unit volume, D_{eq} , which exists everywhere in the surf zone if the profile is in equilibrium (Dean, 1977).

Based on these concepts and using shallow-water linear wave theory, the cross-shore sediment transport rate, Q , is expressed in terms of the excess energy dissipation per unit volume of water across the surf zone as

$$Q = K(D - D_{eq}) \quad (2)$$

where

K = empirically determined sand transport rate coefficient

D, D_{eq} = actual and equilibrium energy dissipation per unit volume of water under given local wave and water level conditions

Moore (1982) determined a design curve for K by simulating the large-scale laboratory tests of Saville (1957) (see Kraus and Larson, 1988) using a numerical model based on Equation 2. Profile evolution was best reproduced for the value of

$$K = 1.144 \times 10^{-3} \text{ ft}^4/\text{lb} \quad \text{or} \quad 2.2 \times 10^{-6} \text{ m}^4/\text{N}$$

In differential form, wave energy dissipation per unit volume of water in the surf zone may be written as

$$D = \frac{1}{h} \frac{\partial P}{\partial x} \quad (3)$$

where

P = wave energy flux

This wave energy flux is given by

$$P = E C_g \quad (4)$$

where

E = total wave energy in one wavelength per unit crest width

C_g = wave group speed

The total wave energy is given by

$$E = \frac{1}{8} \rho g H^2 \quad (5)$$

where

ρ = fluid density

g = acceleration of gravity

H = wave height

The quantity C_g is the wave group speed and in shallow water is given by

$$C_g = (gh)^{\frac{1}{2}} \quad (6)$$

Substituting the wave energy E and group speed C_g into Equation 4 produces the following relationship:

$$P = \frac{1}{8} \rho g H^2 (gh)^{\frac{1}{2}} \quad (7)$$

Breaking wave heights are assumed to be proportional to local water depth and given by

$$H = \gamma h \quad (8)$$

where γ is a dimensionless breaking wave constant, equal to 0.78 in the model. Wave energy flux in the surf zone can now be written as a function of total water depth.

$$P = \frac{1}{8} \rho g^{\frac{3}{2}} \gamma^2 h^{\frac{5}{2}} \quad (9)$$

By differentiating Equation 9 according to Equation 3, an expression for energy dissipation per unit volume of water can be derived.

$$D = \frac{5}{16} \rho g^{\frac{3}{2}} \gamma^2 h^{\frac{1}{2}} \frac{\partial h}{\partial x} \quad (10)$$

Assuming a profile shape in equilibrium (which implies $D = D_{eq}$) with uniform energy dissipation per unit volume of water, integrating Equation 10 provides a relationship between water depth, h , and distance offshore, x .

$$h = \left[\frac{24}{5} \left(\frac{D_{eq}}{\rho \gamma^2 g^{\frac{3}{2}}} \right) \right]^{\frac{2}{3}} x^{\frac{2}{3}} \quad (11)$$

Using the equilibrium profile shape given by Equation 11, Equation 10 can be solved for equilibrium energy dissipation, D_{eq} , within the surf zone.

$$D_{eq} = \frac{5}{24} \rho \gamma^2 g^{\frac{3}{2}} A^{\frac{3}{2}} \quad (12)$$

NUMERICAL SOLUTION

In the present model, time-dependent profile response is determined by an explicit finite difference solution of the equation for continuity of sand in the onshore-offshore direction.

$$\frac{\partial h}{\partial t} = \frac{\partial Q}{\partial x} \quad (13)$$

The surf zone is represented by a series of cells in which the incremental change in cross-shore distance from a baseline, Δx , is uniform, and h is the total water depth. Figure 6-2-1 is a schematic representation of the surf zone showing sediment transport over a horizontal grid of uniform width Δx .

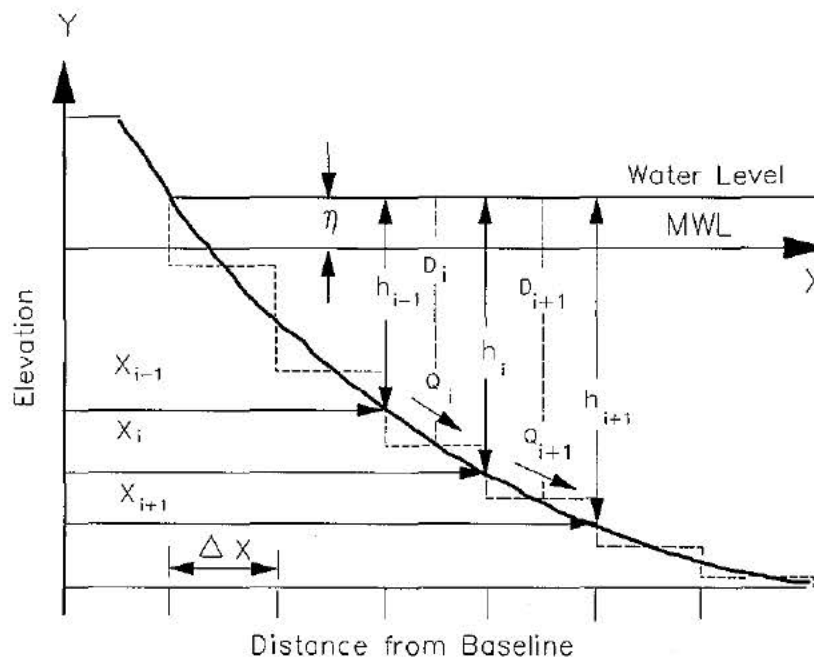


Figure 6-2-1. Numerical Representation of the Beach Profile

Since water level can fluctuate with respect to storm surge and tide, then

$$h_i = \eta_i - d_i \quad (14)$$

η_i = water surface elevation due to storm surge and tide

d_i = bottom elevation

Both η_i and d_i are defined at h_i and are relative to mean water level (MWL). Wave setup in the surf zone and wave runup on the beach face are not represented.

Since D and Q vary with water depth and local bottom slope, the rate of change at each discrete cell differs from adjacent cells. Therefore, Equation 13 can be written as

$$\frac{\Delta h_i}{\Delta t} = \frac{Q_{i+1} - Q_i}{\Delta x} \quad (15)$$

From Equation 2

$$Q_i = K(D_i - D_{eq}) \quad (16)$$

$$Q_{i+1} = K(D_{i+1} - D_{eq}) \quad (17)$$

where

D_i = energy dissipation per unit volume of water at i

D_{i+1} = energy dissipation per unit volume of water at $i+1$

Substituting Equations 16 and 17 into Equation 15

$$\frac{\Delta h_i}{\Delta t} = \frac{K(D_{i+1} - D_{eq}) - K(D_i - D_{eq})}{\Delta x} \quad (18)$$

Since $\Delta h_i = h'_i - h_i$ at an internal grid point and D_{eq} is constant across the surf zone

$$h'_i = h_i + \frac{K \Delta t}{\Delta x} (D_{i+1} - D_i) \quad (19)$$

where

h'_i = water depth at the succeeding time step

From this expression, if D_{i+1} is greater than D_i over time Δt , there will be a net increase in water depth at the succeeding time step.

As a wave breaks over a sloping bottom, the energy dissipated in a distance Δx may be expressed as the difference between the energy flux P entering and exiting a control volume defined by Δx and the water depth, where P_i and P_{i+1} are defined at h_i and h_{i+1} . Therefore,

$$D_{i+1} = \frac{P_{i+1} - P_i}{h_{i+\frac{1}{2}} \Delta x} \quad (20)$$

Combining Equations 9 and 20, the energy dissipation per unit volume of water in the cell between grid points i and $i+1$ is

$$D_{i+1} = \alpha \left[\frac{h_{i+1}^{\frac{5}{2}} - h_i^{\frac{5}{2}}}{0.5(h_{i+1} + h_i)\Delta x} \right] \quad (21)$$

where

$$\alpha = \frac{\rho g^{\frac{3}{2}} \gamma^2}{8} \quad (22)$$

Substituting Equation 21 into the finite difference form of the continuity Equation 19 yields

$$h_i' = h_i + \frac{2\alpha K \Delta t}{(\Delta x)^2} \left[\frac{(h_{i+1}^{2.5} - h_i^{2.5})}{(h_{i+1} + h_i)} - \frac{(h_i^{2.5} - h_{i-1}^{2.5})}{(h_i + h_{i-1})} \right] \quad (23)$$

where

h_i' = calculated water depth at position x_i for the succeeding time step

INITIAL BOUNDARY CONDITIONS

Figure 6-2-2 is a schematic representation of the macro-morphologic features of a beach-dune system, illustrating initial parameters required for constructing an idealized beach profile.

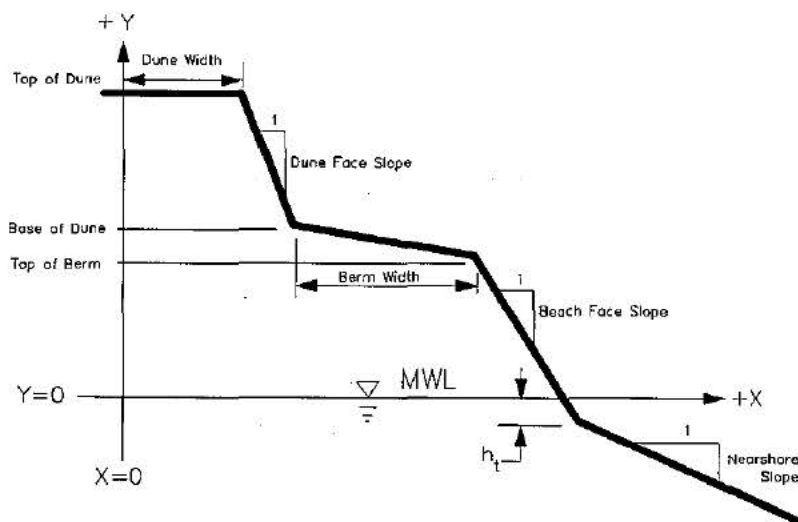


Figure 6-2-2. Idealized Berm, Dune, and Offshore System

A linearly sloping beach face is assumed to intersect an equilibrium profile at a depth, h_t , such that there is a continuous decrease in depth in the offshore direction. This parameter is calculated in the model knowing the beach face slope and the equilibrium profile shape factor, A , which has been shown to be a function of median grain diameter (D_{50}) (Moore, 1982). Once this depth has been defined, erosion of the subaerial beach is assumed to respond geometrically, as determined solely from continuity, from h_t to the top of the berm or top of the dune, depending on profile geometry and water level elevation. When actual profile data are supplied, the user defines the initial landward boundary condition, and all other geometrical parameters are calculated internally.

The offshore boundary condition for the profile response portion of the model is defined at the depth of wave breaking, shoreward of which refraction is assumed to be negligible. The region between the point of wave breaking and h_t is governed by energy dissipation and may be thought of as the dynamic zone. Beyond the breaking depth, energy dissipation is assumed negligible, and sediment transport is defined as zero. Seaward of wave breaking, wave refraction and shoaling are calculated from data input supplied by the user (significant wave height, peak period, and wave angle relative to the shoreline).

MODEL CAPABILITIES

The preceding discussion summarizes the basic equations and conditions used for simulating beach and dune erosion caused by varying water levels and wave heights, as occur during a storm. The present model differs from that of Kriebel (1982) in two significant ways:

- A horizontal grid is used (Δx constant) rather than a vertical grid (Δy constant).
- An explicit finite difference calculation scheme is used rather than an implicit scheme.

Model characteristics that have been implemented in XSHORE, include:

- Capability for generating an idealized beach profile (see schematization shown in Figure 6-2-2) according to criteria provided by the user (e.g. dune width, dune height, dune slope, height at base of dune, berm width, berm height, beach slope, nearshore slope) or use of actual profile data to be entered as x,y pairs.
- Use of time-dependent water level data (tide and/or storm surge) as recorded by tide gages or from predicted tidal variations.
- Use of a time series of wave height, peak period, and wave angle data representing the primary forcing parameters used to operate the model.
- A limitation on the maximum run time of 5 days, since most storm events (periods of assumed dominant erosion through cross-shore sand transport) have a duration less than this period of time.

The smallest time step for data entry and output is 1 hr. Summary statistics include change in shoreline position at the 0, +5, +10, +15 ft contours and associated adjustments in sand volume (yd^3/ft) above mean water level for integer multiples of 1 hr. Simulated profile change data are also written to an ASCII file at the chosen time interval for the user to view with an available graphics software package.

REFERENCES AND BIBLIOGRAPHY

- Birkemeier, W. 1984. "A User's Guide to ISRP: The Interactive Survey Reduction Program," Instruction Report CERC-84-1, US Army Engineer Waterways Experiment Station, Vicksburg, MS.
- Bruun, P. 1954. "Coast Erosion and the Development of Beach Profiles," Technical Memorandum No. 44, Beach Erosion Board, US Army Engineer Waterways Experiment Station, Vicksburg, MS.
- Dean, R. G. 1977. "Equilibrium Beach Profiles: U.S. Atlantic and Gulf Coasts," Ocean Engineering Report No. 12, Department of Civil Engineering, University of Delaware, Newark, DE.
- Kraus, N. C., and Larson, M. 1988. "Beach Profile Change Measured in the Tank for Large Waves, 1956-1957 and 1962," Technical Report CERC-88-6, US Army Engineer Waterways Experiment Station, Vicksburg, MS.
- Kriebel, D. L. 1982. "Beach and Dune Response to Hurricanes," M. S. Thesis, Department of Civil Engineering, University of Delaware, Newark, NJ.
- Kriebel, D. L. 1984a. "Beach Erosion Model (EBEACH) Users Manual, Volume I: Description of Computer Model," Beach and Shores Technical and Design Memorandum No. 84-5-I, Division of Beaches and Shores, Florida Department of Natural Resources, Tallahassee, FL.
- Kriebel, D. L. 1984b. "Beach Erosion Model (EBEACH) Users Manual, Volume II: Theory and Background," Beach and Shores Technical and Design Memorandum No. 84-5-II, Division of Beaches and Shores, Florida Department of Natural Resources, Tallahassee, FL.
- Kriebel, D. L. 1986. "Verification Study of a Dune Erosion Model," *Shore and Beach*, Vol. 54, No. 3, pp. 13-21.
- Moore, B. 1982. "Beach Profile Evolution in Response to Changes in Water Level and Wave Height," M.S. Thesis, Department of Civil Engineering, University of Delaware, Newark, DE.
- Saville, T. 1957. "Scale Effects in Two-Dimensional Beach Studies," *Transactions 7th Meeting of International Association of Hydraulic Research, Lisbon, Portugal*, Vol. 10, pp. A3-1 through A3-10.

CALCULATION OF COMPOSITE GRAIN-SIZE DISTRIBUTIONS

TABLE OF CONTENTS

Description	6-3-1
Introduction	6-3-1
Sediment Analysis	6-3-1
Composite Surface Samples	6-3-2
Composite Core Samples	6-3-3
Soil Classification	6-3-3
Statistical Analysis of Sediment Data	6-3-4
Folk's Graphical Method	6-3-4
Method of Moments	6-3-6
References and Bibliography	6-3-7

CALCULATION OF COMPOSITE GRAIN-SIZE DISTRIBUTIONS

DESCRIPTION

The major concern in the design of a sediment sampling plan for beach-fill purposes is determining the composite grain-size characteristics of both the native beach and the potential borrow site. This application calculates a composite grain-size distribution that reflects textural variability of the samples collected at the native beach or the potential borrow area.

INTRODUCTION

Sediment of a similar grain size (particle diameter) to that of the project, or native beach, is used to construct a beach fill. Particle diameters smaller than that of the native beach will eventually be transported (winnowed) and lost from the project site. Sediment containing finer particle diameters can still be used for construction by placing an overage amount with the assumption that, after the winnowing process is complete, the volume of material remaining is equal to the design volume. This overage is known as the overfill ratio or fill factor.

The fill factor is computed by comparing the grain-size distributions (mean and standard deviation) of the native and borrow sediments (see the ACES application, **Beach Nourishment Overfill Ratio and Volume**). Since only one grain-size distribution (GSD) is used to characterize each population, several (5 to 100) individual sediment samples are mathematically combined into one to form a composite sample. Obviously, the number of samples and the spatial and temporal distribution are critical in determining the composite so that each population is properly represented.

SEDIMENT ANALYSIS

Both native beach and borrow sediments should be analyzed using standard sieving techniques. The sieving process mechanically separates a sediment sample containing an infinite number of particle diameters into finite particle size classes. Table A-4 in Appendix A is a list of standard size classes and corresponding sieve mesh sizes. Statistical parameters such as the median, mean, standard deviation, kurtosis, and skewness can be mathematically computed using data from the GSD.

In this application the individual sediment weight retained on each sieve has been normalized so that the *sum* of the individual sediment weights retained on all sieves equals 100. Stated mathematically, normalized sediment weight for each ϕ size is:

$$w_{\phi \text{ normalized}} = w_{\phi} \frac{100}{\sum w} \quad (1)$$

where

$w_{\phi \text{ normalized}}$ = normalized sediment weight for a specific ϕ

w_{ϕ} = sediment weight on each sieve

$\sum w$ = total weight of sample

Composite Surface Samples

The sediment characteristics of the native beach can vary considerably.

- ° Across the beach profile through varied energy zones.
- ° Along the beach.
- ° At depths within the active profile.
- ° Between seasons.

The native beach composite must reflect these components. A typical plan would call for surficial sediment samples to be taken at regular vertical elevation intervals across the beach profile such as +12, +9, +6, +3, 0, -3, etc., offshore to the point of profile closure. Depending upon the longshore variability, this plan would be repeated along 1 to 4 transects for every mile of the project. To capture the seasonal variation, the beach would be sampled 2 to 3 times a year during the winter storm erosion and summer accretion periods. As an alternative, shallow cores could be taken along profile transects that would represent the spatial and temporal variations captured by the surface samples.

Surface samples are combined into one composite *average* GSD by summing the weights retained on each sieve interval and then dividing by the number of samples. Stated mathematically, the composite sediment weight for a given size is

$$w_{\phi \text{ composite}} = \frac{w_{\phi s_1} + w_{\phi s_2} + w_{\phi s_3} + \dots + w_{\phi s_n}}{n} \quad (2)$$

where

$w_{\phi \text{ composite}}$ = composite weight for a specific sieve

$w_{\phi s_n}$ = sediment weight retained on a specific sieve for each sample

n = number of samples

Composite Core Samples

Cores are usually used to sample potential borrow sites and in some instances the native beach. Cores are brought back to the laboratory to be split, photographed, subsampled, and sieved using standard sieving techniques. Cores are typically subsampled based upon unique lithologic units. A 20-ft core may contain five or more unique units. Some units may be only inches in length, whereas others may be several feet in length.

The composite GSD of each lithologic unit is mathematically weighted proportionally based on its length relative to the core length. For example, if a unit is 1-ft in length from a 10-ft core, each sieve weight for the entire GSD is multiplied by 0.1 (1/10). This proportional weighting is done for all samples in the core resulting in a composite GSD for each core. This scheme is repeated for all cores that are to be included in the core composite. After all individual core composites are created, the entire GSD (consisting of individual sieve weights) for each core is summed and divided by the number of cores. This final step is identical to the procedure in which surface samples are combined into one composite.

A slight variation of the previously described procedure occurs when the user specifies the core composite by an upper and lower elevation limit. For example, a core is a total of 10 ft in length and contains two lithologic units, one 2 ft in length and the other 8 ft in length. The 2-ft unit represents a lithologic unit from an elevation of +11 to +9 ft, and the 8-ft unit represents a lithologic unit from an elevation of +9 to +1 ft. If for example, the user specifies a composite from an elevation of +10 to 0 ft, 1 ft of the 2-ft unit is above the requested upper elevation limit (+10 ft) and 1 ft below the limit. Proportionally, this unit represents 10 percent (1/10) of the core within the requested elevation limits and is thereby weighted accordingly; i.e. the GSD is multiplied by 0.1. The 8-ft unit represents 80 percent (8/10) of the core within the elevation limits; thereby its GSD is multiplied by 0.8. Since no sample was present for the +1 to 0 elevation, the weighting scheme accounts for only 90 (10 + 80) percent of the entire core. This procedure is done for all cores located within the elevation limits.

SOIL CLASSIFICATION

A grade scale commonly used for classifying sediments is the phi (ϕ) scale devised by Krumbein (1934, 1938). The phi scale is a geometric scale to the power of 2 with individual size classes defined as "twice as large or half as large" as some other class (Table A-4, Appendix A). The phi transformation is given by:

$$\phi = -\log_2 d \quad \text{or} \quad 2^{-(\phi)} = d \quad (3)$$

where

d = grain-size particle diameter in millimeters

The advantages of the phi scale are

- The distribution of particle sizes can be plotted on arithmetic graph paper, obviating the necessity of logarithmic graph paper; thus the graphical method of computing sediment statistics is simplified.

- ° Particle diameters for each size class become whole numbers instead of fractions of millimeters.

The disadvantages of the phi scale are

- ° Frequent unfamiliarity on the part of users.
- ° No intuitive relation to numerical results of sieve analysis.
- ° Progression of numerical scales is counter-intuitive (larger value means smaller grain size).

Sediments are classified as GRAVEL, COARSE SAND, MEDIUM SAND, FINE SAND, SILT, and CLAY to indicate the dominant particle size diameter of the sample. The two size schemes used today by coastal engineers are the Unified and Wentworth Soils classifications. These classifications assign similar but different size ranges to each category (Table A-4, Appendix A).

STATISTICAL ANALYSIS OF SEDIMENT DATA

There are two basic methods of obtaining statistical parameters of a GSD. The first method is known as the **Folk Graphic Method**, which was developed before the advent of advanced computers. The Folk method involves plotting a cumulative curve of the sample and determining the particle diameter that corresponds with certain cumulative percentages, i.e. 5, 16, 25, 50, 75, 84, and 95. The second method of obtaining statistical parameters is called the **Method of Moments**. It is a computational (not graphic) method using every size class, and it provides a more accurate measure than the graphic method, which relies on only a few selected percentages.

Folk's Graphical Method

Median (M_d)

The graphic median is the size class in which half of the particles by weight are coarser than the median and half are finer.

Mean (μ)

The mean is probably the best statistical parameter for determining the overall particle size and is given by:

$$\mu = \frac{(\phi_{16} + \phi_{50} + \phi_{84})}{3} \quad (4)$$

Standard Deviation (σ)

The inclusive graphic standard deviation is a measure of sorting and is given by:

$$\sigma = \frac{\phi_{84} - \phi_{16}}{4} + \frac{\phi_{95} - \phi_5}{6.6} \quad (5)$$

Most beach sands have a standard deviation ranging from 0.5 to 2.0.

Skewness (S_k)

The inclusive graphic skewness is a measure of asymmetry and is given by:

$$S_k = \frac{\phi_{16} + \phi_{84} - 2(\phi_{50})}{2(\phi_{84} - \phi_{16})} + \frac{\phi_5 + \phi_{95} - 2(\phi_{50})}{2(\phi_{95} - \phi_5)} \quad (6)$$

A positive value indicates the sediment has an excess amount of fines, whereas a negative value indicates an excess amount of coarse material. The mathematical limits of skewness are -1.0 to +1.0.

Kurtosis (K)

The graphic kurtosis is a measure of the ratio between the sorting of the *tails* (ends) of the curve and the sorting of the central portion. When the central portion is better sorted (values greater than 1.5), the curve is said to be peaked or leptokurtic. If the tails are better sorted than the central portion, the curve is said to be flat-peaked or platykurtic (values between 0.0 and 1.1). Kurtosis is given by:

$$K = \frac{\phi_{95} - \phi_5}{2.44(\phi_{75} - \phi_{25})} \quad (7)$$

Method of Moments

First Moment

By definition, the first moment equals the mean \bar{X} and is expressed as:

$$\bar{X} = \frac{\sum f m_{\phi}}{100} \quad (8)$$

where

f = frequency in percentage for each size class

m_{ϕ} = midpoint of each ϕ size class

Second Moment

The second moment is a measure of the dispersion about the mean and is expressed as:

$$\frac{\sum f (m_{\phi} - \bar{X})^2}{100} \quad (9)$$

The second moment represents the numerical value of the standard deviation; therefore, the standard deviation is expressed as:

$$\sigma = \sqrt{\frac{\sum f (m_{\phi} - \bar{X})^2}{100}} \quad (10)$$

Third Moment

The third moment (known as the *mean cubed deviation*) is the measure of symmetry about the mean and is expressed as:

$$\frac{\sum f (m_{\phi} - \bar{X})^3}{100} \quad (11)$$

Skewness is computed by dividing the *mean cubed deviation* by the cube of the standard deviation and is expressed as:

$$S_k = \frac{\sum f(m_\phi - \bar{X})^3}{100 \sigma^3} \quad (12)$$

Fourth Moment

The fourth moment is the distribution about the mean and is expressed as:

$$\frac{\sum f(m_\phi - \bar{X})^4}{100} \quad (13)$$

Kurtosis is derived by dividing the fourth moment by the standard deviation raised to the fourth power:

$$S_k = \frac{\sum f(m_\phi - \bar{X})^4}{100 \sigma^4} \quad (14)$$

REFERENCES AND BIBLIOGRAPHY

- Folk, R. L. 1974. *Petrology of Sedimentary Rocks*, Hemphill Publishing Company, Austin, TX, pp. 183.
- Friedman, G. M., and Sanders, J. E. 1978. *Principles of Sedimentology*, John Wiley & Sons, New York, NY, Chapter 3.
- Hobson, R. D. 1977. "Review of Design Elements for Beach Fill Evaluation," Technical Paper 77-6, US Army Engineer Waterways Experiment Station, Vicksburg, MS.
- James, W. R. 1974. "Beach Fill Stability and Borrow Material Texture," *Proceedings of the 14th International Conference on Coastal Engineering*, American Society of Civil Engineers, pp. 1334-1349.
- James, W. R. 1975. "Techniques in Evaluating Suitability of Borrow Material for Beach Nourishment," Technical Memorandum No. 60, US Army Engineer Waterways Experiment Station, Vicksburg, MS.
- Krumbein, W. C. 1934. "Size Frequency Distribution of Sediments," *Journal of Sedimentary Petrology*, Vol. 4, pp. 65-77.
- Krumbein, W. C. 1938. "Size Frequency Distributions of Sediments and the Normal Phi Curve," *Journal of Sedimentary Petrology*, Vol. 18, pp. 84-90.

- Krumbein, W. C. 1957. "A Method for Specification of Sand for Beach Fills," Technical Memorandum No. 102, Beach Erosion Board, US Army Engineer Waterways Experiment Station, Vicksburg, MS.
- Moussa, T. M. 1977. "Phi Mean and Phi Standard Deviation of Grain-Size Distribution in Sediments: Method of Moments," *Journal of Sedimentary Petrology*, Vol. 47, No. 3, pp. 1295-1298.
- Shore Protection Manual*. 1984. 4th ed., 2 Vols., US Army Engineer Waterways Experiment Station, Coastal Engineering Research Center, US Government Printing Office, Washington, DC, Chapter 5, pp. 6-24.

BEACH NOURISHMENT OVERFILL RATIO AND VOLUME

TABLE OF CONTENTS

Description	6-4-1
Introduction	6-4-1
General Assumptions and Limitations	6-4-1
Soil Classification	6-4-2
Grain-Size Distributions	6-4-3
Phi Mean and Phi Sorting	6-4-3
Comparison Parameters	6-4-3
Beach-Fill Models	6-4-4
Overfill Ratio	6-4-5
Renourishment Factor	6-4-6
References and Bibliography	6-4-6

BEACH NOURISHMENT OVERFILL RATIO AND VOLUME

DESCRIPTION

The methodologies represented in this ACES application provide two approaches to the planning and design of nourishment projects. The first approach is the calculation of the *overfill ratio*, which is defined as the volume of actual borrow material required to produce a unit volume of usable fill. The second approach is the calculation of a *renourishment factor*, which is germane to the long-term maintenance of a project, and addresses the basic question of how often renourishment will be required if a particular borrow source is selected that is texturally different from the native beach sand.

INTRODUCTION

Beaches can effectively dissipate wave energy and are classified as shore protection structures of adjacent uplands when maintained at proper dimensions. Existing beaches are part of the natural coastal system, and their wave dissipation usually occurs without creating adverse environmental effects. Since most beach erosion problems occur when there is a deficiency in the natural supply of sand, the placement of borrow material on the shore should be considered as one shore stabilization measure.

An important question arises in these situations with respect to the volume of material taken from the borrow zone that will be effectively lost from the project during and following placement due to sorting processes. The design engineer is required to estimate the proportion of a proposed borrow material that will serve a useful function in a specific project requiring beach fill.

Quantitative methods for evaluating the suitability of borrow material as beach fill are those that give overfill ratios or factors or renourishment factors. Overfill ratios apply when the beach in the project area is expected to be stable if composed of sand of certain characteristics, or will be stabilized with engineering structures. Renourishment factors apply where the beach is undergoing erosion and the project requires periodic nourishment for beach stabilization. The methods described can be found in James (1975) and the SPM (1984).

GENERAL ASSUMPTIONS AND LIMITATIONS

The overfill ratio and renourishment factor described herein are not physically related. Each value results from unique models of predicted beach-fill behavior that are dissimilar, although both use the comparison of native and borrow sand texture as input. The overfill ratio is calculated on the assumption that some portion of the borrow material is absolutely stable and hence a finite proportion of the original material will remain on the beach indefinitely. The renourishment factor is calculated on the opposing assumption that no material is absolutely stable, but that a finer material is less stable than coarse material, and hence a coarse beach fill will require renourishment less frequently than a fine one. The models address the different problems in determining nourishment requirements when fill that is dissimilar to native sediments is to be used (overfill ratio) and in predicting how quickly a particular fill will erode (renourishment factor). For design

purposes, the overfill ratio, R_A , should be applied to adjust both initial and renourishment volumes. The renourishment factor, R_J , should be considered an independent evaluation of when renourishment will be required.

It is recommended that selection of borrow material be based on all available historical information on the project area. Computations such as those performed by this ACES application provide useful supplemental inputs for planning and designing, but should not be regarded as accurate predictors. Engineering judgment and experience must accompany design application.

The procedures described herein require enough core borings and samples in the borrow zone, on the beach, and in the nearshore zones to adequately describe the size distribution of borrow and beach material. Size analyses of the borings and samples are used to compute composite size distributions for the two types of materials. These composite distributions are compared to determine the suitability of the borrow material. The concept of *composite* material properties is discussed in Krumbein (1957) and Hobson (1977).

SOIL CLASSIFICATION

A grade scale most commonly used for classifying sediments is the phi (ϕ) scale devised by Krumbein (1934, 1938). The phi scale is a geometric scale to the power of 2 with individual size classes defined as "twice as large or half as large" as some other class (Table A-4, Appendix A). The phi transformation is given by:

$$\phi = -\log_2 d \quad \text{or} \quad 2^{-(\phi)} = d \quad (1)$$

where

d = grain-size particle diameter in millimeters

The advantages of the phi scale are

- ° The distribution of particle sizes can be plotted on arithmetic graph paper, obviating the necessity of logarithmic graph paper; thus the graphical method of computing sediment statistics is simplified.
- ° Particle diameters for each size class become whole numbers instead of fractions of millimeters.

The disadvantages of the phi scale are

- ° Frequent unfamiliarity on the part of users.
- ° No intuitive relation to numerical results of sieve analysis.
- ° Progression of numerical scales is counter-intuitive (larger value means smaller grain size).

Sediments are classified as GRAVEL, COARSE SAND, MEDIUM SAND, FINE SAND, SILT, and CLAY to indicate the dominant particle size diameter of the sample. The two size schemes used today by coastal engineers are the Unified and Wentworth Soils classifications. These classifications assign similar but different size ranges to each category (Table A-4, Appendix A).

GRAIN-SIZE DISTRIBUTIONS

The first stage in specifying beach-fill material is analysis of the sampling material from the existing beach to determine grain-size characteristics (*grain-size distribution*) that will be used as a basis for specification of the fill.

There are two basic methods of obtaining statistical parameters of a *grain-size distribution*. The first is known as the Folk Graphic Method, which was developed before the advent of advanced computers. The Folk method involves plotting a cumulative curve of the sample and determining the particle diameter that corresponds with certain cumulative percentages, i.e. 5, 16, 25, 50, 75, 84, and 95. The second method of obtaining statistical parameters is called the Method of Moments. It is a computational (not graphic) method using every size class, and it provides a more accurate measure than the graphic method, which relies on only a few selected percentages. These two methods are described in more detail in the ACES application titled **Calculation of Composite Grain-Size Distributions**.

Phi Mean and Phi Sorting

Grain-size distributions are usually characterized by two parameters.

- ° The phi mean, M_ϕ , which is a measure of the location of the central tendency of the *grain-size distribution*.
- ° The phi sorting or phi standard deviation, σ_ϕ , which is a measure of the gradation or scale of the spread of the grain size about the phi mean. A low value ($< 0.5 \phi$) indicates that the *grain-size distribution* contains only a narrow range of sizes; it is *well sorted* or *poorly graded*. Conversely, a high value of phi sorting ($> 1.0 \phi$) indicates the presence of a wide range of grain sizes. Material of this type is *poorly sorted* or *well graded*.

Comparison Parameters

It is convenient to define two statistical parameters used to compare the *grain-size distributions* of native and borrow materials. The first parameter, δ , is the phi mean difference and is defined as a scaled difference between borrow and native phi means:

$$\delta = \frac{M_{\phi b} - M_{\phi n}}{\sigma_{\phi n}} \quad (2)$$

where

$-_b$ = subscript b refers to borrow material

$-_n$ = subscript n refers to natural sand on beach

M_{ϕ} = the phi mean

$$= \frac{(\phi_{84} + \phi_{16})}{2} \quad (3)$$

ϕ_{84} = 84th percentile in phi units

ϕ_{16} = 16th percentile in phi units

σ_{ϕ} = standard deviation

$$= \frac{(\phi_{84} - \phi_{16})}{2} \quad (4)$$

The phi mean difference has positive values where borrow materials are, on the average, finer than native materials, and negative values where borrow materials have a phi mean coarser than that of the native materials.

The second comparison parameter, σ , is the phi sorting ratio (phi standard deviation) and is defined as phi sorting of the borrow material over phi sorting of the native material:

$$\sigma = \frac{\sigma_{\phi b}}{\sigma_{\phi n}} \quad (5)$$

Borrow materials more poorly sorted than native materials have values of σ greater than unity; where borrow materials are well sorted in comparison with native materials, σ is less than unity.

BEACH-FILL MODELS

Two basic types of mathematical models have been proposed to handle beach-fill problems. The first model (Overfill Ratio) enables calculation of a fill factor that is an estimate of the volume of a specific fill material needed to create a unit volume of *stable* native beach material. In most cases, fill factors exceed one, indicating that the particular borrow material is less than ideal and that winnowing processes will selectively remove unsuitable parts from the fill until it becomes

compatible with existing beach sediments. The second model (Renourishment Factor) enables calculation of a factor that is used to estimate how often placement of a particular fill will be required to maintain specific beach dimensions. A more detailed and formalized discussion of the two methods can be found in James (1975) and the SPM (1984).

Overfill Ratio

There are four possible combinations that result from a comparison of the composite grain-size distribution statistical parameters (mean and standard deviation) of native material and borrow material. These are listed in Table 6-4-1.

Table 6-4-1. Relationships of Phi Means and Phi Standard Deviations		
Category	Phi Means	Phi Standard Deviations
I	$M_{\phi b} > M_{\phi n}$ Borrow is finer than native material	$\sigma_{\phi b} > \sigma_{\phi n}$ Borrow material is more poorly sorted than native material
II	$M_{\phi b} < M_{\phi n}$ Borrow is coarser than native material	
III	$M_{\phi b} < M_{\phi n}$ Borrow is coarser than native material	$\sigma_{\phi b} < \sigma_{\phi n}$ Borrow material is better sorted than native material
IV	$M_{\phi b} > M_{\phi n}$ Borrow is finer than native material	

The overfill ratio is given by:

$$\frac{1}{R_A} = 1 - F\left(\frac{\theta_2 - \delta}{\sigma}\right) + F\left(\frac{\theta_1 - \delta}{\sigma}\right) + \left[\frac{F(\theta_2) - F(\theta_1)}{\sigma}\right] \exp\left\{\frac{1}{2}\left[\theta_1^2 - \left(\frac{\theta_1 - \delta}{\sigma}\right)^2\right]\right\} \quad (6)$$

where

F = integral of the standard normal curve

Case	θ_1	θ_2
I and II	$\text{Max}\left\{-1, \frac{-\delta}{\sigma^2 - 1}\right\}$	∞
III and IV	-1	$\text{Max}\left\{-1, 1 + \frac{2\delta}{1 - \sigma^2}\right\}$

Renourishment Factor

The renourishment factor (R_J) is a dynamic approach to answering how beach processes can be expected to modify specific fill sediments. It is an estimate of how often renourishment will be needed and helps evaluate the long-term performance of different fill materials with regard to suitability, maintenance, and expense. The conceptual approach is that the active beach system can be viewed as a compartment which receives sediments through longshore transport and from gradual erosion of the inactive *reservoir* of sediments that form the backshore. The compartment loses sediments by longshore and offshore transport beyond its boundaries. In this scheme, a fill is viewed essentially as an increase to the backshore reservoir. Sediment particle residence time in the compartment is longer for coarse-grained sediments than for fine; thus, a comparison between *composite size distributions* of native and borrow sediments can be used to predict the lifetime of a fill. The scheme thus becomes a "bookkeeping" problem of monitoring material going in and out of the system by using mass-balance equations that are similar to the more familiar sediment budget calculations.

To determine periodic renourishment requirements, James (1975) defines a renourishment factor, R_J , which is the ratio of the rate at which borrow material will erode to the rate at which natural beach material is eroding. The renourishment factor is given as:

$$R_J = \exp \left[\Delta \left(\frac{M_{\phi b} - M_{\phi n}}{\sigma_{\phi n}} \right) - \frac{\Delta^2}{2} \left(\frac{\sigma_{\phi b}^2}{\sigma_{\phi n}^2} - 1 \right) \right] \quad (7)$$

where

Δ = winnowing function = 1.0 (recommended value)

A renourishment factor of one-third implies that the borrow material is three times as stable as the native, or that renourishment with this borrow material would be required one-third as often as renourishment with nativelylike sediments. However, an R_J of 3 indicates the borrow is one-third as stable, and if used as beach fill, will require renourishment three times as often as the nativelylike sediments.

REFERENCES AND BIBLIOGRAPHY

- Hobson, R. D. 1977. "Review of Design Elements for Beach Fill Evaluation," Technical Paper 77-6, US Army Engineer Waterways Experiment Station, Vicksburg, MS.
- James, W. R. 1974. "Beach Fill Stability and Borrow Material Texture," *Proceedings of the 14th International Conference on Coastal Engineering*, American Society of Civil Engineers, pp.1334-1349.
- James, W. R. 1975. "Techniques in Evaluating Suitability of Borrow Material for Beach Nourishment," Technical Memorandum No. 60, US Army Engineer Waterways Experiment Station, Vicksburg, MS.
- Krumbein, W. C. 1934. "Size Frequency Distribution of Sediments," *Journal of Sedimentary Petrology*, Vol. 4, pp. 65-77.
- Krumbein, W. C. 1938. "Size Frequency Distributions of Sediments and the Normal Phi Curve," *Journal of Sedimentary Petrology*, Vol. 18, pp. 84-90.

Krumbein, W. C. 1957. "A Method for Specification of Sand for Beach Fills," Technical Memorandum No. 102, Beach Erosion Board, US Army Engineer Waterways Experiment Station, Vicksburg, MS.

Shore Protection Manual. 1984. 4th ed., 2 Vols., US Army Engineer Waterways Experiment Station, Coastal Engineering Research Center, US Government Printing Office, Washington, DC, Chapter 5, pp. 6-24.

A SPATIALLY INTEGRATED NUMERICAL MODEL FOR INLET HYDRAULICS

TABLE OF CONTENTS

Description	7-1-1
Introduction	7-1-1
General Assumptions and Limitations	7-1-2
Numerical Model	7-1-2
Momentum Equation	7-1-2
Continuity Equation	7-1-7
Solution Method	7-1-7
References and Bibliography	7-1-8

A SPATIALLY INTEGRATED NUMERICAL MODEL FOR INLET HYDRAULICS

DESCRIPTION

This application is a numerical model that estimates coastal inlet velocities, discharges, and bay levels as functions of time for a given time-dependent sea level fluctuation. Inlet hydraulics are predicted in this model by simultaneously solving the time-dependent momentum equation for flow in the inlet and the continuity equation relating the bay and sea levels to inlet discharge. The model is designed for cases where the bay water level fluctuates uniformly throughout the bay and the volume of water stored in the inlet between high and low water is negligible compared with the tidal prism of water that moves through the inlet and is stored in the bay. The model has been previously described by Seelig (1977) and Seelig, Harris, and Herchenroder (1977).

INTRODUCTION

Quick, inexpensive estimates of inlet velocities and bay water surface levels associated with tidal or storm event sea level fluctuations are needed in planning the design, construction, and maintenance of coastal inlets. Field data are often unavailable or incomplete. In addition, hydraulic characteristics for proposed inlets are unavailable and must be predicted. The numerical model described herein will predict bay levels, inlet velocities, and discharge as a function of time given the geometry of the system and the water level fluctuations in the sea.

An inlet-bay system typically consists of a *sea* (ocean or lake) connected to a *bay* by one or more *inlets*. Possible system configurations considered in this version of the model include:

- ° 1-Sea - 1-Inlet - 1-Bay System
- ° 1-Sea - 2-Inlet - 1-Bay System
- ° 2-Sea Boundary Conditions - 2-Inlet - 1-Bay System

Figure 7-1-1 depicts a conceptual two-sea, two-inlet, and one-bay system.

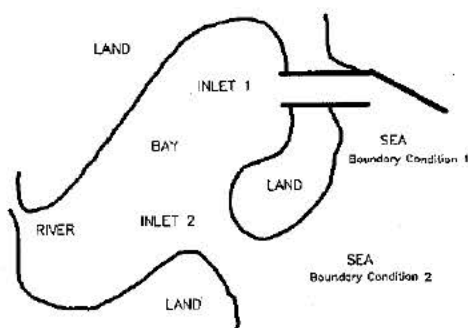


Figure 7-1-1. Conceptual 2-Sea, 2-Inlet, and 1-Bay System

Seaward boundary conditions for the model are specified as water level fluctuations associated with astronomical tides, storm surges, seiches, and tsunamis.

GENERAL ASSUMPTIONS AND LIMITATIONS

General assumptions and limitations for the model include:

- Sea level is specified as a function of time.
- Bay water level remains horizontal.
- The bay is connected to the sea by one or two inlets.
- Bay water surface area is a function of bay water level.
- The water level slope in the inlet is assumed to be linearly related to the friction loss along the inlet between the sea and the bay levels.
- There is a water level drop along the inlet that is proportional to the unrecovered velocity head lost through turbulent eddy diffusion in the bay (flood flow) or sea (ebb flow).
- Storage of water in the inlet is negligible.
- Wind stress on the inlet and bay surface is negligible.
- Water has constant properties throughout the inlet and bay.
- Radiation stress and Coriolis effects are neglected.
- The bay and inlet must contain water throughout the water level cycle.
- The simulation begins with a sea level of zero and zero current.

NUMERICAL MODEL

This model is based upon an area-averaged, one-dimensional momentum equation for the inlet and a continuity equation for the bay.

Momentum Equation

The model is primarily based upon the 1-D momentum equation through the inlet (Harris and Bodine, 1977):

$$\frac{\partial \bar{u}}{\partial t} + \frac{1}{2} \frac{\partial}{\partial x} \bar{u}^2 + g \frac{\partial h}{\partial x} + \frac{1}{A_c} \int_{y_1}^{y_2} (\tau_{zx})_z dy = 0 \quad (1)$$

where

\bar{u} = cross-sectional mean water velocity in the inlet (positive for flood flow, negative for ebb flow)

t = time

x = distance along the main axis of inlet

g = gravitational acceleration

h = water level above datum

A_c = inlet cross-section flow area at x

$(\tau_{zx})_z$ = bottom stress tensor component in the direction of the main axis of the inlet

The first term in the above equation is the temporal acceleration, the second term is the advective acceleration, the third term is the slope of the water surface along the inlet, and the fourth term represents bottom friction. The equation is integrated over the problem domain (length of the inlet between the sea and the bay), with x_s and x_b as the respective limits:

$$\int_{x_s}^{x_b} \frac{\partial \bar{u}}{\partial t} dx + \int_{x_s}^{x_b} \frac{1}{2} \frac{\partial \bar{u}^2}{\partial x} dx + \int_{x_s}^{x_b} g \frac{\partial h}{\partial x} dx + \int_{x_s}^{x_b} \frac{1}{A_c} \int_{y_1}^{y_2} (\tau_{zx})_z dy dx = 0 \quad (2)$$

Carrying out some of the integrations and rearranging, this equation becomes:

$$\frac{\partial}{\partial t} \int_{x_s}^{x_b} \bar{u} dx + \frac{1}{2} (\bar{u}_b^2 - \bar{u}_s^2) + g(h_b - h_s) + \int_{x_s}^{x_b} \frac{1}{A_c} \int_{y_1}^{y_2} (\tau_{zx})_z dy dx = 0 \quad (3)$$

where

h_b, h_s = water levels at the bay and seaward boundaries

From continuity the cross-sectional mean inlet water velocity is equal to the inlet discharge, Q , divided by the inlet cross-sectional area, A_c .

$$\bar{u} = \frac{Q}{A_c} \quad (4)$$

Substituting Equation 4 into 3 and using the product rule for integration, the temporal acceleration of Equation 3 can be expanded to:

$$\int_{x_s}^{x_b} \frac{\partial \left(\frac{Q}{A_c} \right)}{\partial t} dx = \frac{\partial Q}{\partial t} \int_{x_s}^{x_b} \frac{dx}{A_c} + Q \frac{\partial}{\partial t} \left(\int_{x_s}^{x_b} \frac{dx}{A_c} \right) \quad (5)$$

where the second term:

$$Q \frac{\partial}{\partial t} \left(\int_{x_s}^{x_b} \frac{dx}{A_c} \right) = 0$$

since channel storage is neglected.

Substitution of Equation 4 into 3 yields the following expression for the sum of the advective and slope surface terms:

$$\frac{1}{2} \left(\frac{1}{A_b^2} - \frac{1}{A_s^2} \right) Q^2 + g(h_b - h_s) \quad (6)$$

where

A_b, A_s = cross-sectional areas of the inlet at the bay and seaward boundaries

The bottom friction term of Equation 3 is evaluated by using Manning's equation:

$$(\tau_{zx})_z = \frac{gn^2}{kd^{\frac{1}{3}}} |u| u \quad (7)$$

where

n = Manning's coefficient of friction

$$= C1 - C2 \quad d$$

4ft < d < 30ft	C1	d < 4ft
0.037770		0.055
0.000667		0.005

d = water depth

k = conversion factor to adapt Manning's equation to the applicable system of units

u = water velocity in the inlet

The bottom stress is approximated by determining the water velocity, u , at a number of locations throughout the inlet. The inlet is discretized into a flow net or grid consisting of channels (j) and cross sections (i). The major axis of each channel is drawn approximately perpendicular to the flow (Figure 7-1-2). Inlet cross sections are indexed from $i = 1$ (seaward boundary) to $i = IS$ (last cross section at the bay end of the inlet). Channels are indexed $j = 1 \dots IC$ from left to right across the inlet from a seaward perspective. A typical grid cell, denoted as cell (i, j) , consists of that part of the channel j situated between cross sections i and $i+1$. The water velocity in the cell, u_{ij} , is assumed to be at the center of cell (i, j) and to act parallel to the axis of channel j .

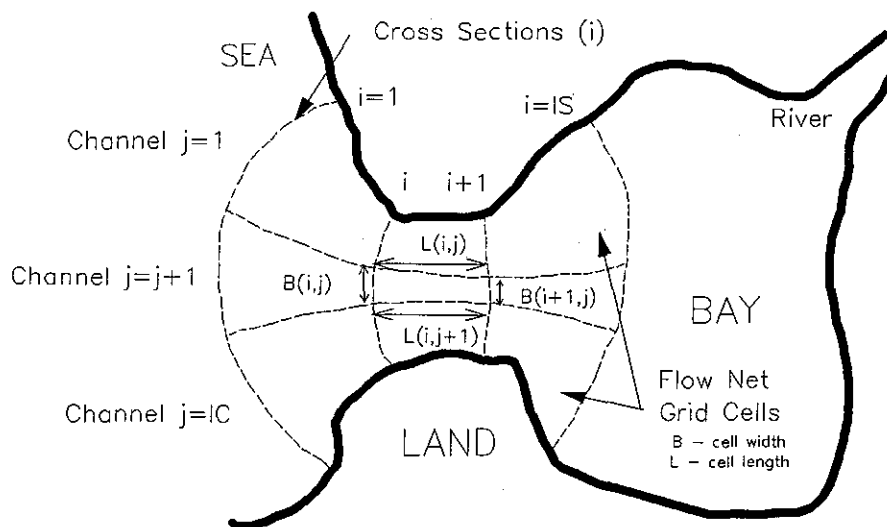


Figure 7-1-2. Inlet Grid System

A weighting function W_j is used to determine the fraction of the total inlet flow Q which passes through a channel at an instant in time.

$$Q_{ij} = W_j Q \quad (8)$$

where

$$Q_{ij} = \text{discharge in cell } (i,j)$$

The weighting function provides a systematic method of distributing flow throughout the inlet for use in evaluating the bottom stress. Major assumptions in developing the weighting function include:

- ° Flow is parallel to the streamlines of the flow net.
- ° Discharge is distributed in each channel of the inlet to minimize total friction within the solution domain.

The weighting function per channel is defined as:

$$W_j = \frac{C_j}{\sum_{i=1}^{IC} C_i} \quad (9)$$

where

$$C_j = \frac{A_j^2 d_j^{\frac{1}{3}}}{n_j^2 Q^2 B_j L_j} \quad (10)$$

A_j = channel cross-sectional area

d_j = water depth of the channel

n_j = Manning's coefficient of friction

Q = inlet discharge

B_j = channel width

L_j = channel length

The mean water velocity in a cell u_{ij} is assumed equal to the discharge in the cell divided by the mean cross-sectional area of the cell perpendicular to flow:

$$u_{ij} = W_j \frac{Q}{A_{ij}} \quad (11)$$

where

A_{ij} = cross-sectional area of the cell perpendicular to flow

The total bottom friction term for Equation 3 is evaluated by using Equations 7 and 11 and integrating across the cross sections and through the inlet to yield:

$$F = \sum_{i=1}^{IS-1} \frac{1}{\sum_{j=1}^{IC} A_{ij}} \sum_{j=1}^{IC} \frac{g n_{ij}^2 |W_j Q| W_j Q B_{ij} L_{ij}}{k d_{ij}^{\frac{1}{3}} A_{ij}^2} \quad (12)$$

where

n_{ij} = Manning's coefficient for a cell

B_{ij} = mean cell width

L_{ij} = mean cell length

d_{ij} = mean instantaneous water depth in a cell

All of the parameters are defined at the center of the cell.

For convenience, let I_g be a geometry integral defined as:

$$I_g = \frac{1}{\int_{x_s}^{x_b} \frac{dx}{A_c}} = \frac{1}{\sum_{i=1}^{IS-1} \left(\frac{\sum_{j=1}^{IC} \frac{L_{ij}}{IC}}{\sum_{j=1}^{IC} A_{ij}} \right)} \quad (13)$$

Substituting Equations 5, 6, and 12 into Equation 3 and multiplying by I_g results in a convenient form for the spatially integrated momentum equation:

$$\frac{dQ}{dt} = -\frac{I_g}{2} \left(\frac{1}{A_b^2} - \frac{1}{A_s^2} \right) Q^2 - g I_g (h_b - h_s) - I_g F \quad (14)$$

In this version of the model, the convective acceleration (first term to the right of the equals sign in Equation 14) is expressed in terms of the empirical loss coefficients. A simple approach (Seelig, Harris, and Herchenroder, 1977) is taken to approximately consider this loss and further simplify the momentum equation. The assumptions are:

- A controlling cross section (throat) exists for the inlet where the cross-sectional area is minimum and losses are effectively encountered.
- Water velocity far from the controlling cross section of the inlet is small.
- The loss can be approximated by multiplying the convective term by a combined empirical ebb- and flood-loss coefficient, C_d (Keulegan, 1967) evaluated at the controlling cross section.

The spatially integrated 1-D momentum equation for flow in the inlet then is:

$$\frac{dQ}{dt} = -\frac{I_g}{2} C_D \frac{Q |Q|}{(A_{min})^2} - g I_g (h_b - h_s) - I_g F \quad (15)$$

where

A_{min} = minimum inlet cross-sectional area (at the throat)

Continuity Equation

The rate of change of water level in the bay is related to inlet discharge plus discharge into the bay from other sources by a simple mass continuity equation:

$$\frac{dh_b}{dt} = \frac{Q_T}{A_{bay}} + \frac{Q_{inflow}}{A_{bay}} \quad (16)$$

where

Q_T = total inlet discharge

$$= \sum_{m=1}^2 Q_m$$

Q_m = discharge of the m^{th} inlet (limited to two inlets)

A_{bay} = instantaneous surface area of the bay

$$= A_0 (1 + \beta h_b)$$

Q_{inflow} = discharge into bay from sources other than the inlet(s)
(such as rivers, bayous, pumped inflows, etc.)

A_0 = initial surface area of the bay

β = bay variation parameter

Solution Method

Equations 15 and 16 comprise a set of simultaneous differential equations. There are several methods for solving these differential equations. The numerical technique used here is a fourth order Runge-Kutta-Gill method. Advantages of this method are that it is self-starting, extremely stable, can handle a long time step, has wide application, and converges quickly. The details of the method are not presented here. The original scheme adopted by Seelig, Harris, and Herchenroder (1977) was a modification of routines published by International Business Machines (1970).

REFERENCES AND BIBLIOGRAPHY

- Harris, D. L., and Bodine, B. R. 1977. "Comparison of Numerical and Physical Models, Masonboro Inlet, North Carolina," CERC GITI Report 6, US Army Engineer Waterways Experiment Station, Vicksburg, MS.
- International Business Machines. 1970. "System/360 Scientific Subroutine Package, Version II Programmer's Manual," White Plains, NY.
- Keulegan, G. H. 1967. "Tidal Flow in Entrances, Water-Level Fluctuations of Basins in Communication with Seas," Technical Bulletin No. 14, Committee on Tidal Hydraulics, US Army Corps of Engineers, Vicksburg, MS.
- Masch, F. D., Brandes, R. J., and Reagan, J. D. 1977. "Numerical Simulation of Hydrodynamics (WRE)," Appendix 2, CERC GITI Report 6, US Army Engineer Waterways Experiment Station, Vicksburg, MS.
- Seelig, W. N. 1977. "A Simple Computer Model for Evaluating Coastal Inlet Hydraulics," CERC CETA 77-1, US Army Engineer Waterways Experiment Station, Vicksburg, MS.
- Seelig, W. N., Harris, D. L., and Herchenroder, B. E. 1977. "A Spatially Integrated Numerical Model of Inlet Hydraulics," CERC GITI Report 14, US Army Engineer Waterways Experiment Station, Vicksburg, MS.

MISCELLANEOUS ROUTINES

TABLE OF CONTENTS

Introduction	8-1-1
Wave Steepness	8-1-1
Monochromatic Wave Breaking	8-1-1
Nearshore Region	8-1-1
Structure Vicinity	8-1-2
References and Bibliography	8-1-3

MISCELLANEOUS ROUTINES

INTRODUCTION

This section of the reference manual contains descriptions of miscellaneous routines in the ACES package that support several methodologies throughout the software. The nature of these routines is to provide checks associated with wave stability to assure compliance with limiting assumptions shared by several methodologies.

WAVE STEEPNESS

The maximum height of a wave is limited by a maximum wave steepness for which the wave form can remain stable. Waves reaching the limiting steepness will begin to break and dissipate a portion of their energy. A simple formula for approximating a limiting wave steepness in uniform finite depths was proposed by Miche (1944):

$$\frac{H}{L} = 0.142 \tanh(kd) \quad (1)$$

where

H = wave height

L = wavelength

k = wave number = $2\pi/L$

d = still-water depth

MONOCHROMATIC WAVE BREAKING

A number of methodologies assume unbroken monochromatic wave conditions. Wave breaking is a significant yet complex phenomenon difficult to measure or accurately predict. No one theory or empirical expression adequately addresses the variability of observed data, yet some estimate of the process is required for design purposes. The following sections discuss the breaker criteria adopted for nearshore regions as well as at structure locations within ACES.

Nearshore Region

For situations where the nearshore slope is considered flat ($m = 0$), breaker height H_b is estimated using the expression (McCowan, 1894):

$$H_b = 0.78d \quad (2)$$

where

d = water depth

The above expression is also used when nearshore slope is unknown.

More recent estimates for breaker parameters in the nearshore region include the effects of wave steepness (H_o/L_o) and beach slope (m). Expressions for either breaker height or breaker index ($\gamma_b = H_b/d_b$) as functions of ($H_o/L_o, m$) have been given by Iversen (1952), Weggel (1972), Singamsetti and Wind (1980), and Sunamura (1981). Smith (1986) summarized additional data available from seven other independent investigations. Testing of the expressions of the above investigators against these additional data resulted in a selection for the expressions used in ACES. It is reemphasized that these expressions provide only rough estimates for design purposes.

For cases where a finite nearshore slope is known ($m > 0$), the breaker height is estimated as (Singamsetti and Wind, 1980):

$$H_b = H_o \left[0.575 m^{0.031} \left(\frac{H_o}{L_o} \right)^{-0.254} \right] \quad (3)$$

where

H_o = deepwater wave height

$m = \tan \phi$ = nearshore slope

L_o = deepwater wavelength

and the breaker depth, d_b , is estimated as (Weggel, 1972):

$$d_b = \frac{H_b}{b - \alpha \frac{H_b}{T^2}} \quad (4)$$

where

$$b = \frac{1}{0.64(1 + e^{-19.5m})}$$

$$\alpha = 1.36(1 - e^{-19m})$$

T = wave period

Structure Vicinity

The maximum breaker height to which a structure might be subjected is estimated as (Weggel, 1972):

$$H_b = \frac{d_s}{m\alpha(18.5m - 8)} \left[P - \sqrt{P^2 - \frac{4mb\alpha}{(d_s/T^2)}(9.25m - 4)} \right] \quad (5)$$

where

d_s = water depth at the structure

APPENDICES

The following pages contain the miscellaneous material referenced in the main body of the Technical Reference. Appendix A consists of various tables of coefficients.

APPENDIX A - TABLES

TABLE OF CONTENTS

Table A-1: K_D Values for Use in Determining Armor Unit Weight	A-1
Table A-2: Layer Coefficient and Porosity for Various Armor Units	A-2
Table A-3: Rough Slope Run-up Coefficients	A-2
Table A-4: Grain-Size Scales (Soil Classification)	A-3
Table A-5: Major Tidal Constituents	A-4
References and Bibliography	A-5

APPENDIX A - TABLES

Table A-1

K _D Values for Use in Determining Armor Unit Weight (Source: EM 1110-2-2904)							
Armor Units	n ⁽²⁾	Placement	Structure Trunk ⁽⁷⁾		Structure Head		
			Breaking Wave	Nonbreaking Wave	Breaking Wave	Nonbreaking Wave	Slope cot θ
Quarrrystone							
Smooth rounded	2	Random	1.2 ⁽¹⁾	2.4	1.1 ⁽¹⁾	1.9	1.5-3.0 ⁽⁸⁾
Smooth rounded	>3	Random	1.6 ⁽¹⁾	3.2 ⁽¹⁾	1.4 ⁽¹⁾	2.3 ⁽¹⁾	1.5-3.0 ⁽⁸⁾
Rough angular	1	Random ⁽³⁾	--- ⁽³⁾	2.9 ⁽¹⁾	--- ⁽³⁾	2.3 ⁽¹⁾	1.5-3.0 ⁽⁸⁾
Rough angular	2	Random	2.0	4.0	1.9 ⁽¹⁾ 1.6 ⁽¹⁾ 1.3	3.2 2.8 2.3	1.5 2.0 3.0
Rough angular	>3	Random	2.2 ⁽¹⁾	4.5 ⁽¹⁾	2.1 ⁽¹⁾	4.2 ⁽¹⁾	1.5-3.0 ⁽⁸⁾
Rough angular	2	Special ⁽⁴⁾	5.8	7.0	5.3 ⁽¹⁾	6.4	1.5-3.0 ⁽⁸⁾
Parallelepiped ⁽⁹⁾	2	Special	7.0 - 20.0	8.5 - 24.0 ⁽¹⁾	---	---	1.0-3.0
Tetrapod and Quadripod	2	Random	7.0	8.0	5.0 ⁽¹⁾ 4.5 ⁽¹⁾ 3.5 ⁽¹⁾	6.0 5.5 4.0	1.5 2.0 3.0
Tribar	2	Random	9.0 ⁽¹⁾	10.0	8.3 ⁽¹⁾ 7.8 ⁽¹⁾ 6.0	9.0 8.5 6.5	1.5 2.0 3.0
Dolos	2	Random	15.0 ⁽⁶⁾	31.0 ⁽⁶⁾	8.0 ⁽¹⁾ 7.0	16.0 ⁽¹⁾ 14.0 ⁽¹⁾	2.0 ⁽⁵⁾ 3.0
Modified cube	2	Random	6.5 ⁽¹⁾	7.5	---	5.0 ⁽¹⁾	1.5-3.0 ⁽⁸⁾
Hexapod	2	Random	8.0 ⁽¹⁾	9.5	5.0 ⁽¹⁾	7.0 ⁽¹⁾	1.5-3.0 ⁽⁸⁾
Toskane	2	Random	11.0 ⁽¹⁾	22.0	---	---	1.5-3.0 ⁽⁸⁾
Tribar	1	Uniform	12.0	15.0	7.5 ⁽¹⁾	9.5 ⁽¹⁾	1.5-3.0 ⁽⁸⁾
Quarrrystone - graded angular riprap	-	Random	2.2	2.5	---	---	---
<p>(1) CAUTION: These K_D values are unsupported and are provided only for preliminary design.</p> <p>(2) n is the number of units comprising the thickness of the armor layer.</p> <p>(3) The use of single layer of quarrrystone armor units is not recommended for structures subject to breaking waves, and only under special conditions for structures subject to nonbreaking waves. When it is used, the stone should be carefully placed.</p> <p>(4) Special placement with long axis of stone placed perpendicular to structure face.</p> <p>(5) Stability of dolosse on slopes steeper than 1 on 2 should be substantiated by site-specific tests.</p> <p>(6) Refers to no-damage criteria (<5 percent displacement, rocking, etc.); if no rocking (<2 percent) is desired, reduce K_D 50 percent (Zwamborn and Van Niekerk, 1982).</p> <p>(7) Applicable to slopes ranging from 1 on 1.5 to 1 on 5.</p> <p>(8) Until more information is available, the use of K_D should be limited to slopes ranging from 1 on 1.5 to 1 on 3. Some armor units tested on a structure head indicate a K_D-slope dependence.</p> <p>(9) Parallelepiped-shaped stone: long slab-like stone with long dimension approximately three times the shortest dimension (Markle and Davidson, 1979).</p>							

Table A-2

Layer Coefficient and Porosity for Various Armor Units (Source: SPM)				
Armor Unit	n	Placement	Layer Coefficient	Porosity %
Quarrystone (smooth)	2	Random	1.02	38
Quarrystone (rough)	2	Random	1.00	37
Quarrystone (rough)	>3	Random	1.00	40
Quarrystone (parallelepiped)	2	Special	-	27
Cube (modified)	2	Random	1.10	47
Tetrapod	2	Random	1.04	50
Quadripod	2	Random	0.95	49
Hexipod	2	Random	1.15	47
Tribar	2	Random	1.02	54
Dolos	2	Random	0.94	56
Toakane	2	Random	1.03	52
Tribar	1	Uniform	1.13	47
Quarrystone	Graded	Random	-	37

Table A-3

Rough Slope Run-Up Coefficients (Source: Smith, 1986)		
Armor Material	a	b
Riprap	0.956	0.398
Rubble (Permeable - No Core)	0.692	0.504
Rubble (2 Layers - Impermeable Core)	0.775	0.361
Modified Cubes	0.950	0.690
Tetrapods	1.010	0.910
Quadripods	0.590	0.350
Hexapods	0.820	0.630
Tribars	1.810	1.570
Dolosse	0.988	0.703

Table A-4

Grain-Size Scales (Soil Classification)					
Unified Soils Classification		ASTM Mesh	PHI	MM	Wentworth Classification
Cobble			-8.00 -7.00 -6.75 -6.50 -6.25	256.00 128.00 107.60 90.51 78.11	Cobble
Coarse Gravel			-6.00 -5.75 -5.50 -5.25 -5.00 -4.75 -4.50 -4.25	64.00 53.82 45.28 38.06 32.00 28.91 22.83 19.00	Pebble
Fine Gravel			-4.00 -3.75 -3.50 -3.25	16.00 13.45 11.31 9.51	
SAND	Coarse	2.5	-3.00	8.00	
		3	-2.75	6.73	
		3.5	-2.50	5.66	
		4	-2.25	4.76	
		5	-2.00	4.00	
		6	-1.75	3.36	
	Medium	7	-1.50	2.83	
		8	-1.25	2.38	
		10	-1.00	2.00	
		12	-0.75	1.69	
		14	-0.50	1.41	
		16	-0.25	1.19	
		18	0.00	1.00	
		20	0.25	0.84	
		25	0.50	0.71	
		30	0.75	0.59	
		35	1.00	0.50	
		Fine	40	1.25	0.42
	45		1.50	0.35	
	50		1.75	0.30	
	60		2.00	0.25	
	70		2.25	0.21	
	80		2.50	0.177	
	100		2.75	0.149	
120	3.00		0.125		
140	3.25		0.105		
170	3.50		0.088		
200	3.75		0.074		
230	4.00		0.0625		
Silt	270	4.25	0.0526		
	325	4.50	0.0442		
	400	4.75	0.0372		
		5.00	0.0313		
		6.00	0.0158		
		7.00	0.0078		
Clay		8.00	0.0039		
		9.00	0.0020		
		10.00	0.0009		
		12.00	0.0002		
					GRAVEL
					SAND
					MUD

REPORT DOCUMENTATION PAGE			Form Approved OMB No. 0704-0188	
Public reporting burden for this collection of information is estimated to average 1 hour per response, including the time for reviewing instructions, searching existing data sources, gathering and maintaining the data needed, and completing and reviewing the collection of information. Send comments regarding this burden estimate or any other aspect of this collection of information, including suggestions for reducing this burden, to Washington Headquarters Services, Directorate for Information Operations and Reports, 1215 Jefferson Davis Highway, Suite 1204, Arlington, VA 22202-4302, and to the Office of Management and Budget, Paperwork Reduction Project (0704-0188), Washington, DC 20503.				
1. AGENCY USE ONLY (Leave blank)	2. REPORT DATE September 1992	3. REPORT TYPE AND DATES COVERED Final report		
4. TITLE AND SUBTITLE Automated Coastal Engineering System: Technical Reference		5. FUNDING NUMBERS		
6. AUTHOR(S) David A. Leenknecht, Andre Szuwalski, Ann R. Sherlock		8. PERFORMING ORGANIZATION REPORT NUMBER		
7. PERFORMING ORGANIZATION NAME(S) AND ADDRESS(ES) USAE Waterways Experiment Station Coastal Engineering Research Center 3909 Halls Ferry Road Vicksburg, MS 39180-6199		9. SPONSORING/MONITORING AGENCY NAME(S) AND ADDRESS(ES) US Army Corps of Engineers Washington, DC 20314-1000		
11. SUPPLEMENTARY NOTES Available from National Technical Information Service, 5285 Port Royal Road, Springfield, VA 22161.		10. SPONSORING/MONITORING AGENCY REPORT NUMBER		
12a. DISTRIBUTION/AVAILABILITY STATEMENT Approved for public release; distribution is unlimited.		12b. DISTRIBUTION CODE		
13. ABSTRACT (Maximum 200 words) The Automated Coastal Engineering System (ACES) is an interactive computer-based design and analysis system in the field of coastal engineering. The general goal of the ACES is to provide state-of-the-art computer-based tools that will increase the accuracy, reliability, and cost-effectiveness of Corps coastal engineering endeavors. Reflecting the nature of coastal engineering, methodologies (called "applications" in this guide) contained in this release of the ACES are richly diverse in sophistication and origin. The contents range from simple algebraic expressions, both theoretical and empirical in origin, to numerically intense algorithms spawned by the increasing power and affordability of computers. Historically, the methods range from classical theory describing wave motion, to expressions resulting from tests of structures in wave flumes, and to recent numerical models describing the exchange of energy from the atmosphere to the sea surface. (Continued)				
14. SUBJECT TERMS ACES Automated Coastal Engineering System		15. NUMBER OF PAGES 218		
		16. PRICE CODE		
17. SECURITY CLASSIFICATION OF REPORT UNCLASSIFIED	18. SECURITY CLASSIFICATION OF THIS PAGE UNCLASSIFIED	19. SECURITY CLASSIFICATION OF ABSTRACT	20. LIMITATION OF ABSTRACT	

19. (Concluded).

In a general procedural sense, much has been taken from previous individual programs on both mainframes and microcomputers. The ACES is designed for a current base of PC-AT (including compatibles) class of personal computers resident at many Corps coastal offices. While expected to migrate to more powerful hardware technologies, this current generation of ACES is designed for the above environment and is written in FORTRAN 77.

The documentation set for the ACES comprises two manuals: User's Guide and Technical Reference. The User's Guide contains instructions for using the individual applications within the ACES software package. The Technical Reference contains theory and discussion of the various methodologies contained in the ACES.